

DOCTORAMENTO
MEDICINA DENTÁRIA

**Innovative calcium phosphate
bioactive and nanostructured
coatings for enhanced
osseointegration of dental implants**

Eduardo Fernando Antunes Santiago

D

2022



Eduardo Fernando Antunes Santiago

Innovative calcium phosphate
bioactive and nanostructured coatings for
enhanced osseointegration of dental implants



Tese apresentada à Faculdade de Medicina Dentária da Universidade do Porto
para obtenção do grau de Doutor em Medicina Dentária

Dezembro 2022

Orientação

Professor Doutor **Pedro de Sousa Gomes**

F.M.D. - U.P.

Coorientação

Professora Doutora **Maria Helena Raposo Fernandes**

F.M.D. - U.P.

Professora Doutora **Catarina Ferreira dos Santos**

ESTSetubal/IPS e CQE-IST– U.L.

Apoios para a realização da tese - BoneLab – Faculty of Dental Medicine U.P.

i3S Scientific Platform Bioimaging

Fundação para a Ciência e Tecnologia (FCT)

Megagen Portugal Lda e Megagen Korea

Animal and Veterinary Research Center – U.T.A.D.

to infinity and beyond”
Buzz Lightyear

B

Resumo / Abstract

Resumo

As reabilitações orais com implantes dentários são uma abordagem terapêutica previsível, com elevadas taxas de sucesso. A perda de implantes pode ocorrer, apesar de raramente, por falta de osteointegração durante os primeiros meses. A modulação das características da superfície dos implantes é um ponto chave, bem conhecido como fator determinante para o aumento da sobrevivência e do sucesso clínico das reabilitações. Apesar das evoluções realizadas, com bons resultados biológicos, existe ainda margem para melhorar o comportamento clínico dos implantes no que diz respeito à integração nos tecidos e à prevenção da peri-implantite. Assim, este projeto tem como objetivo o desenvolvimento e a caracterização de um revestimento inovador de fosfato de cálcio, bioativo e nanoestruturado, aplicado sobre implantes de titânio com um processo de modificação de superfície de uma só etapa, de forma a induzir uma resposta biológica mais efectiva. Os revestimentos desenvolvidos foram caracterizados relativamente às propriedades físico-químicas e biológicas através de abordagens *in vitro* e *in vivo*, demonstrando um aumento da funcionalidade biológica das superfícies modificadas (Figura 1).

Abstract

Implant-based rehabilitations are a predictable treatment option with high survival rates. Implant failure can occur, although rarely, as insufficient osseointegration occurs within the first few months. Implant surface characteristics are acknowledged as a key point for increased implant survival and success. Despite the enhancement of the biological outcomes of existing developments, there is still a margin to improve the clinical implant behavior in terms of tissue integration and peri-implantitis prevention. This project aims the development and characterization of an innovative bioactive nanostructured calcium phosphate coating, applied to titanium implants through a one-step surface modification process, for enhanced biological response. Developed coatings were thoroughly characterized regarding physic-chemical and biological

properties through *in vitro* and *in vivo* approaches, showcasing enhanced biological functionality (Figure 1).

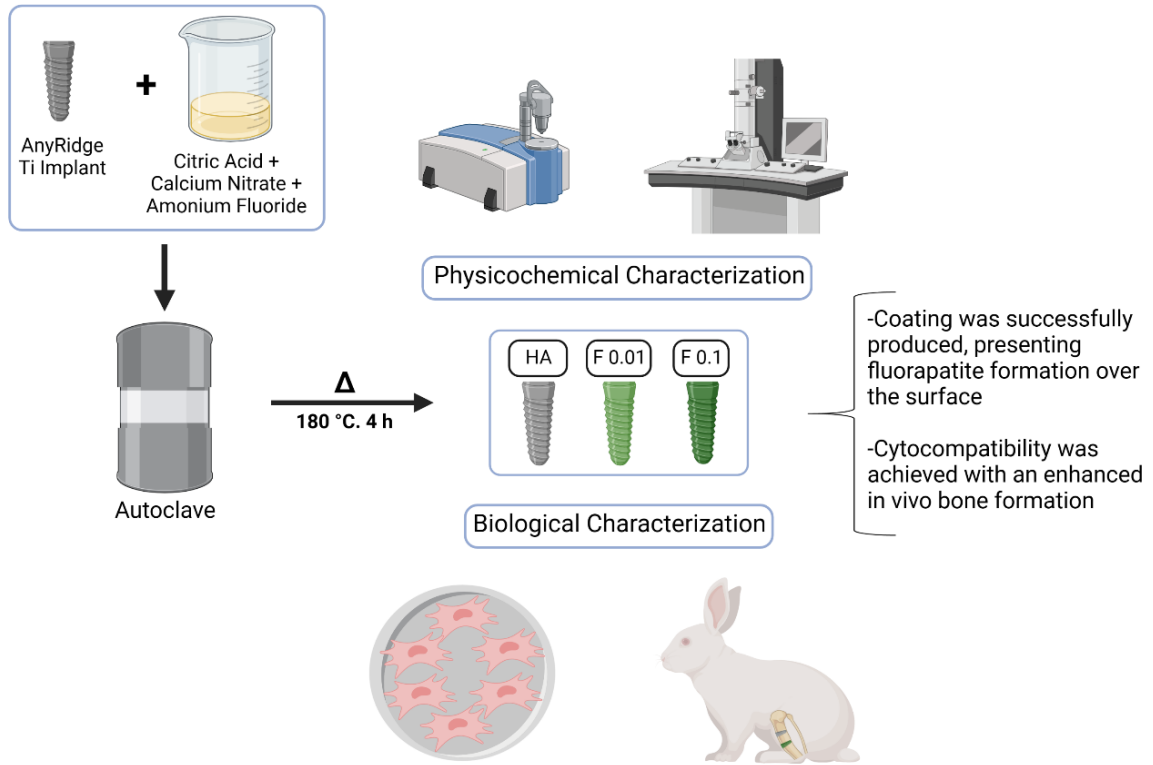


Figure 1 – Graphical overview of the research work.

Agradecimientos

- Ao Professor Doutor Miguel Pinto, por todo o apoio desde há 20 anos para cá.
- Ao Professor Doutor Pedro Gomes, pela amizade sincera e honesta.
- À Professora Doutora Maria Helena Fernandes, por acreditar em mim e no projecto.
- À Professora Doutora Catarina Santos, pelos ensinamentos de uma área que tanto pode complementar a medicina dentária.
- Ao Professor Doutor Bruno Colaço, pelo carinho com que me recebeu e guiou no processo da experimentação in vivo.
- Ao Vitor, pela ajuda, disponibilidade e simpatia com que me presenteou, mesmo sabendo tão pouco sobre mim.
- A todo o pessoal da FMDUP, que com tanto carinho me trata já há tantos anos.
- Ao Professor Doutor José António Pereira, por me fazer sentir parte da família dele.
- À Megagen Portugal e Headquarters, por me facilitarem tanto o processo com o material e imagens cedidas.
- A todos os meus Amigos, que de forma directa ou indirecta contribuíram para a minha confiança e para o meu empenho, com todo o apoio demonstrado.
- Ao meu Padrinho, o Professor Doutor António Faria Gomes, pelo exemplo profissional que foi durante toda a vida, e pelo coração gigante que sempre expôs.
- À minha Mãe... por ser quem me formou a personalidade e me tornou quem sou hoje.
- Ao meu Pai, que sempre foi e será a voz da minha consciência, e o meu parceiro de trabalho mais influente.
- Ao meu Luisinho, que faz com que veja a vida com outros olhos, e de forma tão bonita e simples.
- À minha Sofia... por seres a minha pessoa... amo-te sem fim.

São palavras escassas, que não chegam para transmitir o que sinto por cada um de vocês.

E tantos outros agradecimentos que ficam por escrever, mas que me preenchem o coração.

Membros do Conselho Científico

Presidente - Prof. Doutor Paulo Rui Galvão Ribeiro de Melo

Vice-Presidente - Prof. Doutor Américo dos Santos Afonso

Secretário - Prof. Doutor César Fernando Coelho Leal da Silva

Membros

Prof. Doutor Américo dos Santos Afonso

Prof. Doutora Ana Paula Coelho de Macedo Augusto

Prof. Doutora Ana Paula Mendes Alves Peixoto Norton

Prof. Doutor César Fernando Coelho Leal da Silva

Prof. Doutora Cristina Maria Ferreira Guimarães Pereira Areias

Prof. Doutor Filipe Poças de Almeida Coimbra

Prof. Doutor Germano Neves Pinto da Rocha

Prof. Doutora Inês Alexandra Costa Morais Caldas

Prof. Doutora Irene Graça Azevedo Pina Vaz

Prof. Doutor João Carlos Antunes Sampaio Fernandes

Prof. Doutor Jorge Manuel de Carvalho Dias Lopes

Prof. Doutor José António Ferreira Lobo Pereira

Prof. Doutor José António Macedo de Carvalho Capelas

Prof. Doutor José Carlos Reis Campos

Prof. Doutora Maria Cristina Pinto Coelho Mendonça de Figueiredo Pollmann

Prof. Doutora Maria de Lurdes Ferreira Lobo Pereira

Prof. Doutora Maria Helena Guimarães Figueiral da Silva

Prof. Doutora Maria Helena Raposo Fernandes

Prof. Doutora Maria João Feio Ponces Ramalhão

Prof. Doutor Mário Jorge Rebolho Fernandes da Silva

Prof. Doutor Miguel Fernando da Silva Gonçalves Pinto

Prof. Doutor Pedro de Sousa Gomes

Prof. Doutor Pedro Manuel Vasconcelos Mesquita

Prof. Doutor Ricardo Manuel Casaleiro Lobo de Faria e Almeida

List of Abbreviations

In alphabetical order:

A-MEM – Alpha minimum essential medium

BIC – Bone to implant contact

BMSCs – Human bone marrow-derived stromal cell

BS – Bone surface

BV – Bone volume

BV/TV – Bone volume fraction

EDS – X-ray energy dispersive spectroscopy

F 0,1 – Fluor coating with 0,1 M F

F 0,01 – Fluor coating with 0,01 M F

FBS – Fetal bovine serum

FTIR – ATR – Attenuated total reflectance spectroscopy

HA – Hydroxyapatite

RFU – Relative fluorescence units

SEM – Scanning electron microscopy

SLA - Sandblasted, large grit, acid-etched

TEM – Transmission Electron Microscope

TIS – Intersection surface

TPS - Titanium plasma spray

TS – Total surface

XPS – X-ray photoelectron spectroscopy

Figure Index

Figure 1 – Graphical overview of the research work.	E
Figure 2 - Overall 65+ years population around the world. (from https://ourworldindata.org/age-structure) [3]	2
Figure 3 - Life expectancy in the world from 1955 to the present. (From https://www.worldometers.info/demographics/world-demographics/) [1]	3
Figure 4 – Rehabilitation option - removable dental prosthesis [10].	6
Figure 5 – Rehabilitation option – fixed dental prosthesis [11].	7
Figure 6 - Rehabilitation option - single dental implant with a crown.	7
Figure 7 - Rehabilitation option - multiple dental implant solutions [13].	8
Figure 8 - Dental implant example [13].	9
Figure 9 - Single tooth replacement with implant [13].	9
Figure 10 – Several teeth replaced with implants [13].	10
Figure 11 – Implant-supported overdenture [13].	10
Figure 12 - Ancient findings of teeth replacements [19].	12
Figure 13 - Linkow blade and other evolutions of dental implants [20].	13
Figure 14 - Planning implant placement [13].	15
Figure 15 - Implant with healing abutment [13].	15
Figure 16 - Schematic representation of the socket shield technique [25].	17
Figure 17 - Prosthetic stage over implants [27].	17
Figure 18 - Schematic representation of peri-implantitis consequences within the peri-implantar tissues [11].	18
Figure 19 – Schematic representation of the alveolar bone loss after tooth extraction.	19
Figure 20 – Implant failure evolution scheme [8].	20
Figure 21 – Implant fracture associated with the lack of bone support.	22
Figure 22 – Schematic representation of the comparative establishment of periodontitis vs periimplantitis.	22
Figure 23 – Implant contamination path through the abutment.	23

Figure 24- Schematic representation of osteointegrated implants, peri-implant tissues and natural teeth [13].	24
Figure 25 - Cone beam computed tomography example.	25
Figure 26- Sinus lift and implant placement [54].	27
Figure 27 - Free gingival graft around implants [54].	28
Figure 28 – Anyridge Implant surface treated with S-L-A, followed by the incorporation of calcium ions, creating a CaTiO₃ nanostructure that is expected to enhance osteoblastic activity [13].	31
Figure 29 - Anyridge Implant surface presented in Figure 28, with higher amplification [13].	34
Figure 30 – Representative image of a low magnification scanning electron microscopy of implant surfaces [13].	35
Figure 31 - The structure of hydroxyapatite crystals [102].	45
Figure 32 - The structure of fluorapatite crystals [116].	48
Figure 33 - Used autoclave system for the preparation of the coatings through the hydrothermal method.	52
Figure 34 - Schematic representation of the synthesis of fluorapatite coatings.	53
Figure 35 - Implant coating production schematization.	54
Figure 36 - Physical and chemical characterization schematization.	55
Figure 37 - Implant groups HA, F 0.1, and F 0.01 distribution in tissue culture plates.	55
Figure 38 - Biological characterization schematization – in vitro assays.	56
Figure 39 - New Zealand white rabbits (<i>Oryctolagus cuniculus</i>).	58
Figure 40 - Representation of the implant placement at the proximal tibia.	59
Figure 41 - Implant distribution within the in vivo experimental study.	60
Figure 42 - Operation table featuring the implantology motor and the O₂ administration tube.	61
Figure 43 - Implant Megagen® System surgical Kit and surgical instruments used. ...	61
Figure 44 - Trichotomy for surgery.	62
Figure 45 - Mepivacaine 3% infiltration.	62
Figure 46 - Incision, full thickness flap elevation, and exposed bone surface from the surgical area.	63

Figure 47 - Bone drilling protocol and implant placement examples.	64
Figure 48 - Soft tissue suturing in layers.	64
Figure 49 - Biological characterization schematization – in vivo assays.	65
Figure 50 – Representative SEM images of the surface of the HA coatings obtained by the hydrothermal method (a). Inset corresponds to a high magnification area of the defined region.....	68
Figure 51 – Representative SEM images of the surfaces of the F 0.01 coatings obtained by the hydrothermal method (b). Inset corresponds to a high magnification area of the defined region.	69
Figure 52 – Representative SEM images of the surfaces of the F 0.1 coatings obtained by the hydrothermal method (c).....	70
Figure 53 - Magnified SEM image of F 0.1 (corresponding to the square area in figure 52 (c). Inset shows a representative TEM image of the F 0.1 coating particles, displaying representative measurements.	71
Figure 54 - EDS elemental mapping images for F (e), Ca (f), P (g), O (h), and Ti (i) of the F 0.1 coating surface.....	72
Figure 55 - ATR-FTIR spectra of the F 0.01 and F 0.1 coatings (j).....	73
Figure 56 - XPS of the F 0.1 coating: (k) P 2p, (l) Ca 2p, (m) F 1s (n) C 1s.....	74
Figure 57 - Metabolic activity of human mesenchymal stromal cell cultures established over HA-, F 0.01-, and F 0.1-coated substrates for 21 days.	75
Figure 58 – Representative SEM micrographs of human mesenchymal stromal cell cultures established over HA-, F 0.01-, and F 0.1-coated substrates for 10 days.	76
Figure 59 – Representative SEM micrographs of human mesenchymal stromal cell cultures established over HA-, F 0.01-, and F 0.1-coated substrates for 21 days.	76
Figure 60 – Representative 3D microtomographic reconstruction of implants placed in the proximal tibia, on the 4 weeks’ group.	77
Figure 61 - – Representative microtomographic cross-section of an implant placed in the proximal tibia, on the 4 weeks’ group, disclosing the bone-implant interface.	78
Figure 62 - Bi-dimensional microtomographic reconstructions of HA, F 0.01, and F 0.1 implants, at the 4 weeks’ time point. Bottom images correspond to the inset areas of the top images. Scale bars correspond to 1 mm.	79

Figure 63 - Histomorphometric data of the coated constructs – HA, F 0.01, and F 0.1, at the 4 weeks’ time point. $p < 0.05$; * significant different to control; # significant different to the other experimental group. 80

Figure 64 - Representative three-dimensional microtomographic reconstructions of the coated constructs – HA, F 0.01, and F 0.1, at the 4 weeks’ time point. 81

Figure 65 - Bi-dimensional microtomographic reconstructions of HA, F 0.01, and F 0.1 implants, at the 8 weeks’ time point. Bottom images correspond to the inset areas of the top images. Scale bars correspond to 1 mm. 82

Figure 66 - Histomorphometric data of the coated constructs – HA, F 0.01, and F 0.1, at the 8 weeks time point. $p < 0.05$; * significant different to control. 83

Figure 67 - Representative three-dimensional microtomographic reconstructions of the coated constructs – HA, F 0.01, and F 0.1, at the 8 weeks’ time point. 84

Figure 68 - Fractal growth schematization based on the information of Vidal et al and Wu et al [117, 118]. 90

Table Index

Table 1 - Implant characteristics according to the topographic level [59, 67]	33
Table 2 - Some of the different surface treatments in alphabetical order [72-76].....	37
Table 3 - Advantages in using coating in implant surface	39
Table 4 - Disadvantages of using coated surfaces [79]:	40

Index

<i>Resumo / Abstract</i>	C
Resumo	D
Abstract	D
<i>Agradecimentos</i>	F
<i>Membros do Conselho Científico</i>	H
<i>List of Abbreviations</i>	J
In alphabetical order:	K
<i>Figure Index</i>	L
<i>Table Index</i>	P
<i>Index</i>	Q
<i>I. Introduction</i>	1
1. Population aging	2
2. Process of aging and aging in the oral environment	4
3. Oral rehabilitation options	6
4. Dental implants – an introduction	9
5. Dental implants – a not-so-recent history	12
6. Dental implants workflow	15
7. Advantages of dental implants	19
8. Dental implants success and survival rates	20
9. Osteointegration	24
10. In addition to Implants	27
11. Dental implants' three-dimensional structure and composition	29
12. Modulation of the surface topography – Macro-, micro- and nano- patterns for surface modification	31
13. Innovative surface coatings for dental implants surface	44
<i>II. Objectives</i>	49
	Q

<i>III. Materials and Methods</i>	51
3.1 – Preparation and characterization of fluorapatite-coated titanium implants	52
3.2 – Biological characterization - In vitro response to osteoblastic cells	56
3.3 – Biological characterization - <i>In vivo</i> response to bone implantation	58
3.4 – Statistical analysis	66
<i>IV. Results</i>	67
4.1 – Coating preparation and characterization	68
4.2 – Biological evaluation	74
4 weeks	79
8 weeks	82
<i>V. Discussion</i>	85
5.1 - Dental implants	86
5.2 - Coating methodology - the hydrothermal method	86
5.3 - Fluor and fluorapatite coating	87
5.4 - Coating preparation and characterization	89
<i>VI. Conclusion</i>	100
About the future	102
<i>In memoriam</i>	104
<i>References</i>	105
<i>Attachment I</i>	2
<i>Attachment II</i>	3

I. Introduction

"In every job that must be done, there is an element of fun"
Mary Poppins

1. Population aging

According to worldwide recognized statistics websites <https://www.worldometers.info/> and <https://www.census.gov/>, the world in the final trimester of 2022, after the Covid-19 pandemic, had a population of about 8 billion [1] [2]. From this total number, the population aged 65 or above is about 703 million, which is about 9% (Figure 2) [3].

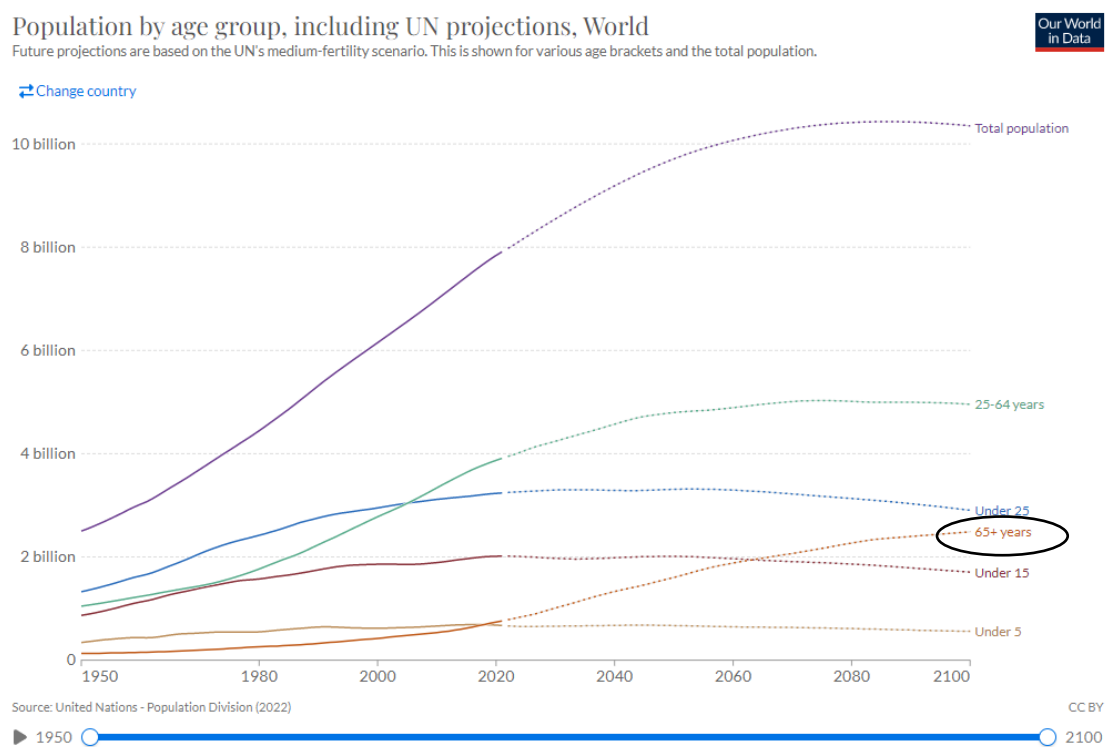


Figure 2 - Overall 65+ years population around the world. (from <https://ourworldindata.org/age-structure>) [3]

In Portugal, from a population of around 10 million, 20.2% are over 65 years old. An aging population that seems to be getting older as the years go by (Figure 3) [1]. Life expectancy was 73 years, in 2020; an increase of 2 years compared with 2010 data, and it appears that the tendency is to continue to increase [1].

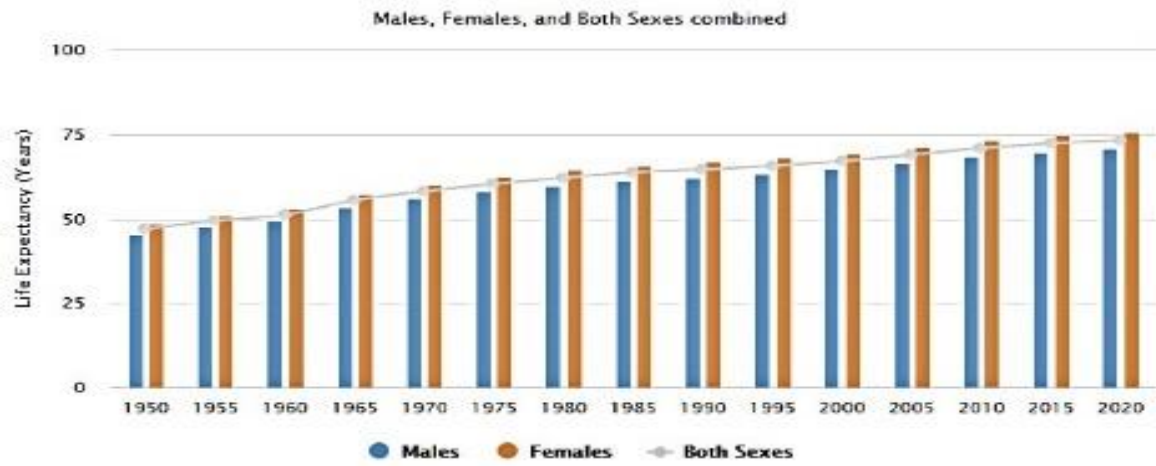


Figure 3 - Life expectancy in the world from 1955 to the present. (From <https://www.worldometers.info/demographics/world-demographics/>) [1]

2. Process of aging and aging in the oral environment

The National Institute of Aging (NIH), from the U.S. Department of Health & Human Sciences, is an organization specialized in studying the aging process [4]. According to this organization, aging involves changes in several processes, such as biological, physiological, environmental, psychological, behavioral, and social. Some of these are benign, such as greying hair, but others result in a decline in the function of the senses and activities of daily life, like chewing and eating. Higher susceptibility to, and increased frequency of disease or disability are also evident. Overall, aging is the major risk factor for a number of chronic diseases in humans [4, 5].

The biology of aging has been studied and has originated explaining theories. The conclusion is that there is no specific factor to explain aging, but it seems that while the passing of time is regular and unmutated, the rate of aging can be changed, and even slowed through behavior and healthy living practices [4]. Aging is not a disease itself but it can be looked upon as a risk factor for many systemic conditions and diseases. These diseases, in turn, either chronic or inherited, may accelerate aging through a decrease in functionality and reduced quality of life [4]. Teeth loss is an example of this [6].

Some discoveries from the National Institute of Aging tell us that any intervention that extends lifespan can also extend health span [4]. Another discovery is that starvation and malnutrition lead to cell-based stress-response defenses [4], and this may be worsened by teeth loss, more common at an increased age [6].

Normal aging and disease may be hard to differentiate. Particularly, in the oral environment, teeth can show enamel wearing, chipping, or fracture lines, and become darker [5]. Also, endodontic structures may be diminished because of secondary dentin formation [5]. These are physiological and functional changes.

Root or coronal caries and periodontal tissue losses, however, represent disease [5]. While periodontal attachment loss in a limited quantity is associated with aging, resulting sometimes in gingival recessions [5], severe periodontitis - characterized by severe tissue destruction, occurs in 10.5-12% with the highest incidence at 35-40 years of age, according to Lamster et al [5].

The mucosal tissue also suffers physiological changes throughout life, such as a reduction in the wound-healing capacity [5]. Environmental factors, like smoking, for example, elevate mucosal pathology risk [5]. Some chronic medications and chronic disorders (e.g., diabetes mellitus type 2) are more frequently found in the elderly and have negative effects like, for example, reduction of salivary gland function [5].

Older adults have another major factor of imperative importance – the masticatory function. If bad nutrition and diet may influence the appearance and evolution of chronic diseases, an adequate masticatory function may allow an easier way of maintaining health [5]. A dentition of only 20 teeth in occlusion is seen as enough for successful oral aging, from biological and social perspectives [5]. Tooth loss can be seen at any age. However, at younger ages, the biological response is increased and more alert than that verified for older individuals. Also, in older adults, tooth decay, wearing, trauma, caries, etc. are more probable, because of a longer exposition of various risk factors throughout the years. Decreased motor skills, also highly influence oral health [7].

Higher life expectancy, as discussed above, also implies that systemic diseases or chronic medications may be present for a longer time, in cases such as diabetes, cardiovascular diseases, etc., and may affect oral health in a negative way. On the other hand, oral infections or chronic oral inflammation may deteriorate systemic conditions, and contribute to a negative evolution, starting a process that may lead to serious complications. There is a mutual influence between oral and systemic conditions [8].

3. Oral rehabilitation options

As masticatory function starts to be less than optimal, and because of its importance in general health and influence on longevity, it should be treated with a long list of options for its maintenance or, better said, rehabilitation. According to the World Health Organization, edentulism reaches incidences between 26% to 54%, throughout the world, with a significant impact on general health [9]. Edentulism promotes impairment, psychological disability, bone atrophy, and/or functional limitation. The social factor is also of major importance, to allow individuals to look their prime and to be accepted by social standards as healthy individuals.

In a tooth loss case, the sooner it is replaced according to protocol timings, the better the conditions will be for the subsequent rehabilitation. If a young adult needs oral rehabilitation, he is more prone to have better physiological conditions and a better biological response to any replacement option decided. If the missing tooth is not replaced by one of the options, generally speaking, several modifications will occur, such as the resorption of alveolar bone. On the other hand, an older body will have a higher probability of presenting systemic conditions and/or medications that can hinder rehabilitation options [8].



Figure 4 – Rehabilitation option - removable dental prosthesis [10].

Several options can be considered for oral rehabilitation (Figure 4, Figure 5, Figure 6, Figure 7), depending on the type of edentulism. There are 2 main groups of

edentulism: partial and complete edentulism. For each, there are removable or fixed options available, each with advantages and disadvantages.

Removable options have a lower cost and can be performed, in most cases, with no associated surgical intervention. These oral prostheses can be made of acrylic, metal, and/or flexible materials. The major disadvantage is the difficulty in tolerating these dentures, especially in cases with advanced maxillary bone resorptions, more frequent in older ages [7].

When the decision is a fixed oral rehabilitation, there are 2 options:

- if there are natural teeth and one wants to use them as support when the adjacent teeth to the space can be improved in terms of resistance, or if we have no bone available for dental implant placement, a dental bridge can be placed (Figure 5);

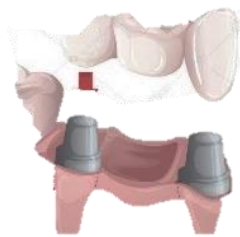


Figure 5 – Rehabilitation option – fixed dental prosthesis [11].

- If natural teeth are not an option for use, dental implants may replace the tooth root, and act as support for a crown, that can be either screwed or cemented. A surgical placement is needed for implantation, but it is normally a low-risk procedure (Figure 6) [7].



Figure 6 - Rehabilitation option - single dental implant with a crown.

If a patient has complete edentulism, the solution may rely on the use of 2, 4, 6, or even more dental implants to guarantee prosthetic support (Figure 7). These are situations that need extra planning so that we can understand the ideal or possible placement for the implants. For correct implantology and prosthetic planning, radiographic/imagiologic complementary exams are imperative, and justifiable, not neglecting the ALARA guidelines [12].

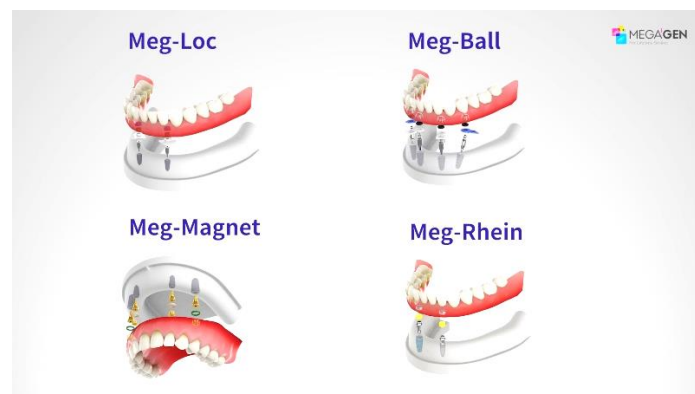


Figure 7 - Rehabilitation option - multiple dental implant solutions [13].

What we see more commonly is that there is an increase in elderly patients requiring complex implant-based rehabilitation, with sensitive clinical conditions and impaired bone quality or quantity, or associated comorbidities [6]. Accordingly, there is a continuous aim for the development of innovative products with the best possible characteristics for optimizing the osteointegration process, and faster treatments, in anatomical locations with complex characteristics, or low-quality bones. Furthermore, if the outcomes are improved in these adverse conditions, they will also be enhanced in more favorable conditions.

4. Dental implants – an introduction

In the past decades, dental implants have become more popular (Figure 8), following the evolution, advancements, and availability of innovative materials that allow them to be more reliable and provide enhanced treatment outcomes for patients. Dental implant-based rehabilitation and placement are standardized and provide many advantages for long-lasting functional rehabilitation of the maxillofacial region. This rehabilitation is a predictable treatment option with high survival rates [14, 15]. Nonetheless, they still have major challenges in treatment planning and execution [16, 17].



Figure 8 - Dental implant example [13].

A dental implant is an engineered piece made to substitute the function of a tooth root (Figure 9), placed in contact with the alveolar bone, and able to support a dental crown, a bridge, a denture, or a facial prosthesis, or even to act as an anchorage for orthodontic therapies, as with mini-implants. For a replacement of a single tooth, it can either have: a) an abutment screwed to the implant so that the dental crown can be cemented; b) an abutment screwed to the implant, allowing for the subsequent screwing of the prosthetic component; or c) it can be a single piece with the abutment fused to the prosthetic component [7].



Figure 9 - Single tooth replacement with implant [13].

When the rehabilitation plan involves several fixed teeth, supported by more than one dental implant, it is called a bridge of fixed denture over implants - replacing the natural teeth function in similar situations. The number of teeth is usually superior to the number of implants supporting the piece, and the interface between the bridge and the implants respects the same principles as in single-tooth rehabilitations. This option may vary from considering the involvement of two teeth to a full arch – fixed full denture (Figure 10) [7].



Figure 10 – Several teeth replaced with implants [13].

Implants may also be used to support removable dentures to restore edentulous arches – overdentures (Figure 11) – for higher support, retention, and stability. In this option, the abutment has a small connector, linked to the opposite analogous in the inner side of the overdenture [7].

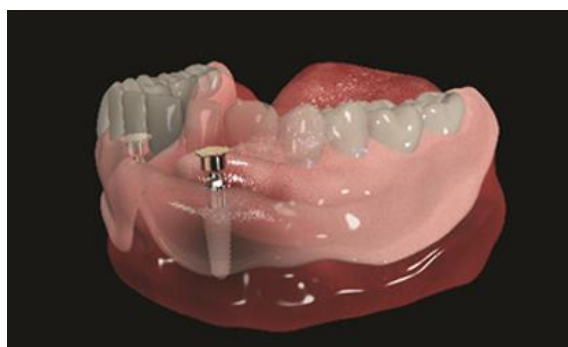


Figure 11 – Implant-supported overdenture [13].

There is also a different type of implant, smaller in size and simpler to place, that has a temporary anchorage function for orthodontic forces. It allows forces to have favorable vectors so that a tooth can be moved in a certain way, which would be a lot more difficult - if not impossible - to achieve with other forms of anchorage. Because implants do not induce bone remodeling processes in their vicinity - they will not move upon fixation, and therefore will provide an enhanced anchorage. Most do not fully osteointegrate and are also easier to remove at the end of the treatment [7].

5. Dental implants – a not-so-recent history

Humans have always understood the need to have good oral health and masticatory function, as well as the need to restore the lost function through scientific advances, techniques, and materials, that seem to exist since ancient times. Dating back thousands of years ago, archaeological evidence of teeth replacement attempts are known (Figure 12), with different methods for stabilization and maintenance [18].

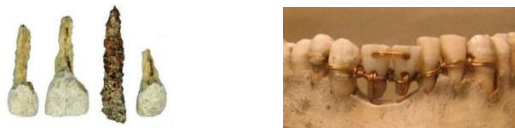


Figure 12 - Ancient findings of teeth replacements [19].

The Ebers papyrus, from 3700 BC, describes for the first time, the diseases related to gums and teeth. Hesi-Re (3000 BC) was considered the first dental healthcare practitioner. Also, thousands of years ago, in China, bamboo pegs were carved and tapped into the bone. In 2.500 BC, back in Egypt, gold ligatures were used to stabilize damaged or loose teeth and ivory teeth were placed in jaws and even transplanted human teeth were collected. In 500 BC Etruscans used animal bones to carve teeth for replacing missing ones, and Phoenicians used gold wire splints in compromised mobile teeth. From 600 AD, a mandible of a young Mayan female adult with seashells directly carved into the mandible bone, replacing the form and function of lower incisors, was discovered, as well as teeth restorations made with turquoise and jade [18].

In the 18th century, Hunter transplanted teeth between humans, and in the 19th century, Maggiolo placed a gold implant tube in a fresh extraction alveolus. These techniques of replacing teeth were the starting point for dental implant-based rehabilitation [18].

In modern times, implant-based therapies date back to the early 20th century. In the first decades, Greenfield started the thought of using an iridioplatinum basket to support a gold crown. In the 30s, Vitallium implants appeared, by Strock [8]. They were

orthopedic screws used primarily in animal experiments, and later in humans, to replace teeth. Adams, in the same decade, patented the cylindrical endosseous implant, and in the following decade, Formiggini and Zepponi developed the dental implant with a post shape. In Sweden, Dahl introduced the subperiosteal implant [8]. Titanium was introduced by Bothe, Beaton, and Davenport in the 40s, and also in a publication in "Surgery, Gynecology and Obstetrics", that showed the intimacy between bone and titanium screws and the difficulty in removing the former from the latter. This phenomenon would later be named osteointegration by Brånemark, in 1951 [8]. In this same year, Leventhal experimented with rabbits and found that titanium could be an ideal metal for bone-related surgery and bone-fixing applications. In the next year, Brånemark continued the experimental studies in rabbits' femurs and found that bone tissue would grow towards titanium, making it extremely hard to remove [8].

The author found a high level of proximity between bone and the implanted titanium, with areas of close adhesion between both. He continued his study with more animal models and human experimentation, further confirming this principle. This was a golden decade for the evolution of implants. It also included Linkow's works, which reported the placement of titanium implants in oral bone with teeth attached to thin and long metal blades, to treat partial and complete edentulism [8].

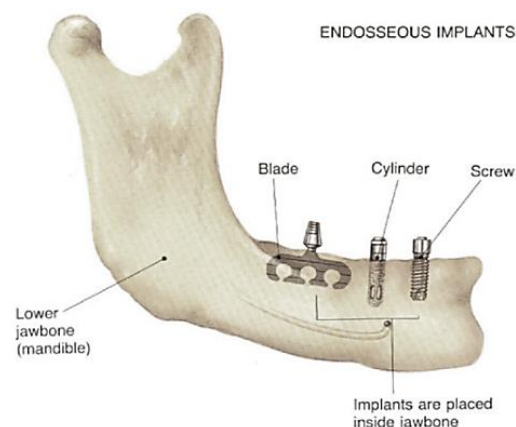


Figure 13 - Linkow blade and other evolutions of dental implants [20].

Later, in 1965, Brånemark treated for the first time, a patient with a titanium implant for full mouth rehabilitation and continued observing the phenomenon of osteointegration. From this time to the present, the implants have been modeled into a root format – slightly conical and normally threaded for easier bone placement, and became a usual and accessible treatment option, even with variable shapes and surface textures (Figure 13) [8].

With the common option of dental implant-based rehabilitation, the high success rates, and its massification as a therapeutic approach, other areas also evolved to try to improve the conditions for implantation and osteointegration [8]. Bone grafting studies evolved rapidly and are now allowing more possibilities for long-term successful oral rehabilitation with dental implants [8].

As an example, more recent treatment modalities like the all-on-4 concept, techniques with reduced surgical and recovery times, placement of zygoma implants, three-dimensional treatment planning, and guided surgery, also make implant-based therapies more approachable to a wider range of patients [21]. Even when bone atrophy is too advanced for conventional dental implants' placement, the subperiosteal technique is starting to be, again, a viable treatment option [21].

6. Dental implants workflow

In a first appointment for collecting the medical history that shows the possibility for oral rehabilitation with implants and aims for the planning of the surgical procedure through imagiologic exams (Figure 14), it is determined if the implant is to be immediately placed after the extraction, if the procedure is delayed for up to 3 months, or if the implant placement is planned for more than 3 months after extraction [21]. Regarding the procedure itself, most authors recommend similar surgical protocols, as following described in brief.

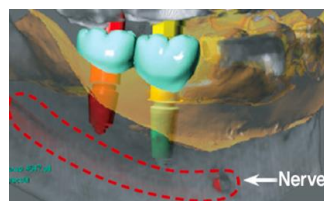


Figure 14 - Planning implant placement [13].

The first surgical step is normally a full-thickness incision and the periosteal detachment or, for flapless surgery, a tissue punch is performed. When bone is exposed, a series of calibrated drills are used under copious irrigation to prepare a receiving bed, starting with pilot drills, and following protocols with wider drills, until a final drill calibrated for the implant size previously determined. The implant is then screwed into place at low speed, manually with a wrench, or with a handpiece, using a precise torque to respect the bone biology, the implant and bone resistance, and the maintenance of the characteristics of the surface of the implant [8].



Figure 15 - Implant with healing abutment [13].

At this time, various options may be followed to attach the prosthesis to the implant: a) a cover screw, if the implant is to be covered by gingiva and a second surgery is planned to expose the head of the implant and place a healing abutment (Figure 15); or an immediate provisional prosthesis if the gingiva is to be adapted around the head of the implant, with immediate loading, early loading in 1-12 weeks, or delayed loading if over 3 months [8].

In the 1970s up to the 1990s, a 2-stage approach was defended, with the thought that it could improve the survival of the implant. Recent studies show that no significant differences regarding general outcomes are found between 1-stage or 2-stage approaches, and it all comes up to soft tissue management, and/or the need for bone regeneration [22].

The osteointegration process requires more or less time, depending on the type of implant, the patient characteristics, and several other aspects also discussed throughout this work. Normally, when immediate loading is not performed, 3-6 months may be necessary for the bone to heal around the implant, before placing the prosthetic part of the rehabilitation. If the implant has sufficient initial stability – no less than 35 Ncm, the prosthesis may be loaded immediately, according to several recent research, which gives more relevance to the density of bone and the number of implants splinted together, than to the healing time [8].

Another option would be to immediately perform implant surgery in the same procedure as the teeth extraction, for bone preservation and time reduction [8]. With this, there is evidence of a small amount of an higher risk of early failure, or associated complications [8]. Some variation of the techniques to improve the outcomes includes root membrane [23], or socket shield [23] (Figure 16), to preserve the level of vestibular bone in mainly the anterior maxilla [24].

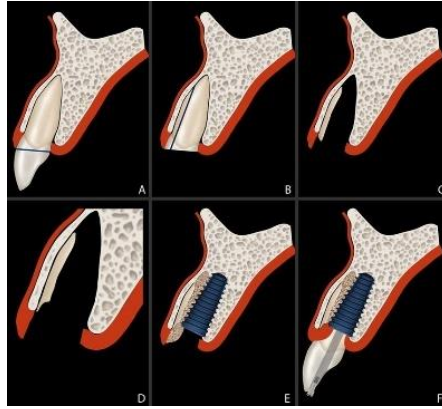


Figure 16 - Schematic representation of the socket shield technique [25].

After osseointegration, implants are ready for the definitive prosthetic stage, for details such as aesthetics, structural resistance, and vertical dimension of occlusion [21]. After impressions to replicate the intra-oral conditions, occlusion registration, and determination of color and shapes, the crown is then manufactured by a laboratory. If an abutment is used, it is screwed to the implant. The interface between implant and abutment can vary, but nowadays platform switching is generally used to get a tighter seal of the gingiva around the head of the implant and abutment, to lessen bacterial invasion [26]. The crown is then screwed or cemented over the abutment (Figure 17), or directly to the implant [21].

If the prosthesis is a removable denture, retention abutments with two parts are used, mounted directly on the implants with a male adaptor or ball, or to a custom-made metal bar, and the respective part of the retention system on the denture [21]. Implants can also hold a fixed denture, by screwing the denture into abutments called multi-units [21].

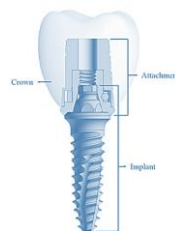


Figure 17 - Prosthetic stage over implants [27].

After the rehabilitation is complete, maintenance is essential so that the long-term prognosis may be elevated. Periodontal probing, anti-plaque actions done either by the professional or by the patient, aim to prevent peri-implantitis (Figure 18), a microbial-triggered immune-inflammatory condition similar to periodontitis, that is associated with the loss of supporting tissues [28, 29]. Peri-implantitis is caused by bacteria, plaque, and oral biofilm because of a lack of maintenance [8]. It starts as an early reversible form called peri-implant mucositis, and evolves if untreated, to irreversible loss of hard and soft tissues around the implant, which can culminate into implant loss [29]. Peri-implantitis treatment is still broadly unpredictable, but attempts may be made to recreate tissues around implants that prevent the pathological condition development, through open-flap debridement together with grafts, among other strategies [29].

Crowns over implants and implants' retained dentures must be functionally controlled, and if needed, adapted. Dental floss, manual and electric toothbrushes, and oral irrigators, with proper hygiene techniques, must be used by patients for adequate tissue maintenance around implants, just as they should for natural dentition. Professional appointments must be spaced according to the risk factors of the patient and evaluated by the dentist [30].



Figure 18 - Schematic representation of peri-implantitis consequences within the peri-implantar tissues [11].

7. Advantages of dental implants

Implants have advantages and disadvantages when compared to other oral rehabilitation options. For example, comparing an option of a single implant to a tooth-supported fixed partial denture, considering the high implant survival rates and the option of not involving natural and possibly healthy teeth, implant-based rehabilitation takes the lead [8]. The main disadvantage of the implant-based approach is the necessity of a surgical procedure, which on the other hand, is seen in most cases as a minor intervention, framed within common oral surgical procedures [8]. Another issue is when a tooth is extracted, and nothing else but the natural course of healing is promoted. In this case, alveolar bone resorption happens through multiple dimensions (Figure 19), and adjacent teeth lean to the edentulous space, increasing the difficulty of subsequent prosthetic rehabilitation [8]. There is a need for careful planning, from the moment of extraction, for a better decision from the start.



Figure 19 – Schematic representation of the alveolar bone loss after tooth extraction.

Other advantages for implant-retained fixed or -supported prosthesis, in full arch cases, when compared to removable dentures, are the major improvements in stability, retention, phonetics, reduced size of the removable prosthesis in the palate and phalanx zones, improvement of function, maintenance of chewing muscles and facial expressions, and lower incidence of soft tissue traumatic ulcers [8]. We can also find advantages in using well-planned implant-based options in bone level and quantity stability, maintenance of occlusal vertical dimension, easier aesthetic tooth positioning, better and stable occlusion, and improvement in psychological health [8].

8. Dental implants success and survival rates

Dental implant-based rehabilitation and placement are becoming progressively standardized, providing many advantages for long-lasting functional rehabilitation of the maxillofacial regions, despite the major challenges in treatment planning and execution [16, 17]. This rehabilitation, as previously discussed, is a predictable treatment option with high survival rates [14, 15]. Notwithstanding, implant failure also occurs, whether rarely, as insufficient osseointegration occurs in 1-2% of cases within the first months, and in around 5% of cases, at medium to long-term periods [31] (Figure 20).

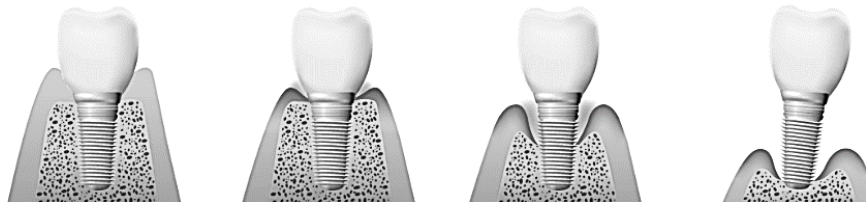


Figure 20 – Implant failure evolution scheme [8].

The implant success rate differs from the survival rate by having stricter criteria of inclusion [8]. Survival rates usually refer to an implant that is present in its function, but with the possibility of aesthetics problems, for example. A success rate indicates that the main standards decided initially when the implant was placed are still being maintained, such as the absence of pain, infection, mobility, gingival bleeding (although controversial), and technical or prosthetic complications, as well as radiographic radiolucency or bone loss over 1.5 mm in a 6-24 week period [32]. Factors such as the skill of the surgeon, quality and quantity of alveolar bone, patient's maintenance capability, and primary stability of the implant, all seem to influence the success rate [8]. In other words, the survival rate of an implant indicates a situation that, even with possible complications, the implant remains in function [32]. However, in a more intricate evaluation, the success rate of dental implants must be in a complication-free situation or associated with easily resolved problems [32]. In a normal healthy situation, survival rates of dental implants at 5 years are around 93-98% [8]. Some literature also

shows a success rate of 52-76% within the 16-20 years follow-up, with complications up to 48% of the situations [33], therefore, proper maintenance is essential to prevent any failure [8].

Several complications can influence the survival and success rates of dental implants [34]. The first ones may occur during surgery or immediately after, with infection, excessive bleeding, tissue damage or necrosis, injury of noble anatomic structures, such as inferior alveolar nerve or maxillary sinus, or lack of primary stability when placing the implant in a site [34]. In a middle-term period, the main issue is the failure to osseointegrate. After 6-24 weeks, the implant stability is confirmed, the soft tissue around is checked and a radiographic control is performed [8]. Comparatively, immediate loading protocols may have a higher rate of failure, because of the proximity in time to surgical trauma or extraction [21]. The most frequent factor for osseointegration failure is either the general health of the patient that contraindicates the implant surgery or behavior-related practices that induce failure through factors such as smoking or improper dental hygiene [8].

In the long-term view, the lack of success of an implant may be linked to the aesthetics, with soft tissue of poor quality, absence of papillae, badly shaped or inadequate color of the rehabilitation, or bone resorption [8]. It can also be associated with biomechanical factors in cantilevers, bruxism, and occlusion forces with an unfavorable distribution [8]. Implants can also fracture (Figure 21) or have problems in the interface with the prosthetic components. Cemented crowns and bridges over implants increase failure risk, by having cement escaping to the interface and becoming a niche for inflammation, leading subsequently to bone loss. For example, when looking at the prosthetic components of implant rehabilitations, rates of success in single crown implants over 5 years are around 96.8%, with screw abutment loosening being the most significant complication in these situations [21]. In fixed complete dentures, the most common complication is veneer fracture, ranging from 13-30% at 5 years; and around 65% at 15 years [21]. In removable dentures, the major issue seems to be the loosening of retention, in about 33% [21].

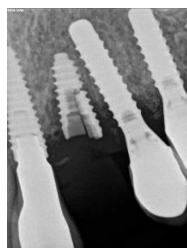


Figure 21 – Implant fracture associated with the lack of bone support.

The failure can also be associated with bone loss or soft tissue loss around the implant by microorganisms-triggered response – periodontitis, leading to periimplantitis (Figure 22), or by periimplantitis alone [8].

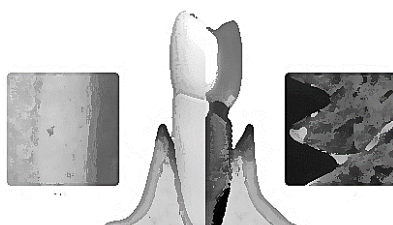


Figure 22 – Schematic representation of the comparative establishment of periodontitis vs periimplantitis.

Periodontitis may itself lead to a lower implant success rate as stated above, associated with an increased marginal bone loss and incidence of peri-implantitis [35]. According to Marrone et al [36], 7.2% of patients with chronic periodontitis had implant failure, while in healthy patients it only seems to occur in around 1.2%. Jiang et al [37] found implant failure at an 8% rate in chronic periodontitis patients, but only 3.3% in healthy patients. Casado et al [38] reported 9.2% implant failure in patients with chronic periodontitis versus 3.6% in healthy ones. Levin et al [39] found 4.2% of implant failure in patients with severe chronic periodontitis, 2.7% in moderate chronic periodontitis, and 1.2% in healthy patients. Karoussis et al [40] and Rocuzzo et al [41] also found similar results.

Periimplantitis is an immune-inflammatory process in tissues around the implant (Figure 23), that can lead to peri-implant pocket formation and bone resorption, and culminate in implant loss [42]. Periimplantitis prevalence ranges between 1-47%,

depending on inclusion parameters for diagnosis [8]. Early inflammation at the implant site and lower jaw placement seem to have a high association risk for late implant failure [42]. In the initial stages, the disease may appear as mucositis, of immune-inflammatory origin in response to an altered biofilm, but without associated tissue destruction [8]. A systematic literature review by Derks & Tomasi in 2015 showed a prevalence of mucositis from around 19 to 65% and periimplantitis from 1-47% [43]. It seems that several factors are in intimate relation with the evolution of disease around implants, and the authors find it necessary for studies to apply consistent case definitions to avoid such a large subjectivity.

The treatment of periimplantitis is very unpredictable, and the best way to deal with it is prevention. Implant survival after surgical treatment of periimplantitis, according to Rocuzzo, in a 10-year follow-up, is 74%, and treatment success was only 20%-42% effective, in different surfaces [44]. This indicates the importance and influence of different implant surface treatments in similar situations [41].



Figure 23 – Implant contamination path through the abutment.

Progressive bone loss around implants may be further caused by factors related to the implants, clinician, patient, treatment protocol, prosthetic overload, quality of care, and maintenance [45]. Mechanical bone-implant interface, and implant success and survival, are majorly influenced by implant surface characteristics and coatings [46]. Different surfaces can be decontaminated when treating existing peri-implant conditions [47], but the main purpose relies on prevention, as discussed above, and also on the development of optimized implant surface coatings for enhanced bone-implant interfaces.

9. Osteointegration

In a simple description, dental implants aim for an osteointegration process consisting in establishing a direct interface between the implant surface and orofacial bone [21]. It is a rigid fixation (Figure 24), clinically asymptomatic, with an alloplastic material, and maintained during functional forces [48]. This process can endure physical loads for decades. If the implant is osteointegrated after the surgical placement, then prosthetic rehabilitation may follow. According to several theories, different healing times are required for osteointegration before the prosthesis is placed over the implant, or an abutment, as previously discussed.



Figure 24- Schematic representation of osteointegrated implants, peri-implant tissues and natural teeth [13].

With the osteointegration phenomenon, demonstrated by Schroeder in the mid-1970s in Switzerland, implant development has come a long way. They started being looked at as directly anchored structures to the bone tissue, while data from a series of factors that were found to greatly influence the osteointegration outcomes were determined by Albrektsson in 1981: namely biocompatibility, implant design, implant surface characteristics, host health, surgical technique used, and applied forces [8].

At the moment of the implant placement, mechanical primary stability is achieved by the intimate contact and friction between the implant's surface and the

bone, which will be absorbed between the 1st and 4th week after placement, and replaced by newly formed tissue [21]. With time, the initial stability will be modified to create a biological connection. This is why osseointegration is a dynamic process from its initial establishment up to the maintenance phases [48].

Risk factors for the success of implant-based rehabilitation treatments also include the patient's general health and associated medication that influence the healing response and bone characteristics [8]. Also, intraoral conditions - such as periodontitis, and surgical-related factors - such as the stress applied to the implant during normal function, are of high importance [48]. For the latter, planning the placement and number of implants is a major factor for success, distributing biomechanical forces between implants, and between implants and the rest of natural teeth if present [48]. Also, insufficient primary stability or high initial implant mobility can lead to failure ([8].

Imageology exams such as Cone Beam Computed Tomography (CBCT) (Figure 25) or similar are needed for a three-dimensional understanding of the ideal placement location of the implants, respecting the bone quality and quantity, preserving noble structures, and following adjacent natural teeth [49].

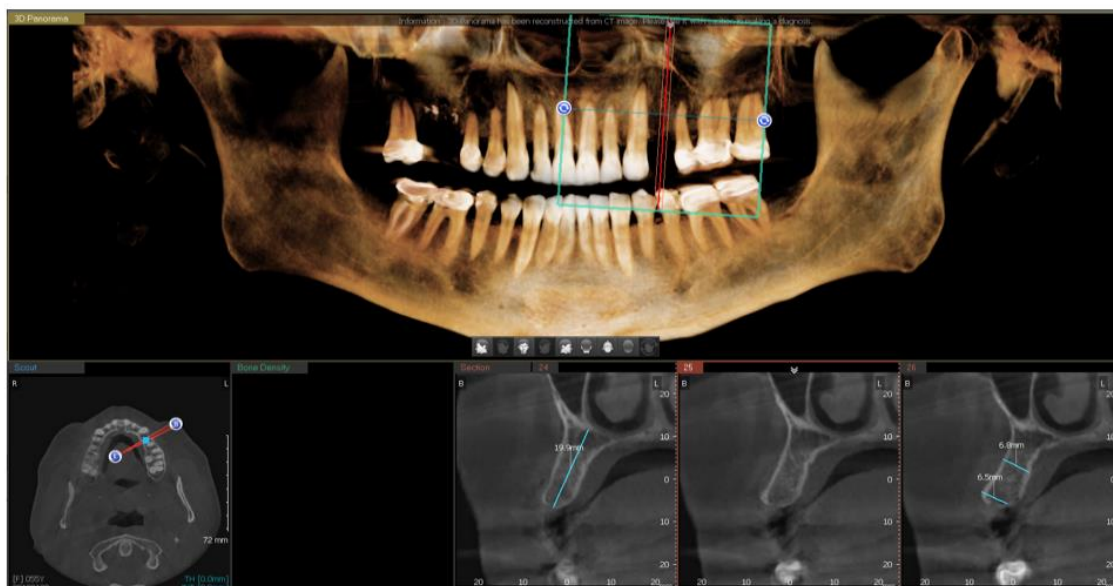


Figure 25 - Cone beam computed tomography example.

In more difficult cases with atrophic maxillaries, it may be necessary to augment the quantity of bone, performing bone grafts either through sinus lift or vertical/horizontal bone augmentation, and gingival grafts for soft tissue management, to aim for the best possible outcomes for an implant-based therapy [8, 50].

For optimal biomechanical performance, the implant must be placed, after planning, in the best bone location available, and in the best position accounting for the prosthesis, so that forces are well distributed either through the prosthesis and the implants [21]. Even so, implants are tested by manufacturers for resistance to long-term forces like masticatory strength, until failure is achieved, to understand the limitations of the materials [51].

Regardless of the type of implant, there is still a significant number of failures, between 2 and 10%, being reported in some literature [52]. Failures of dental implants may be classified as early or later failures. Early failures are due to the inadequacy of the host tissues to establish osteointegration, while late failure occurs when the collapse takes place after osteointegration [53]. Excessive surgical trauma together with impaired healing ability, premature loading leading to relative displacement between the implant and bone (generating wear debris), and infection, are likely to be the most common causes of early implant losses [53]. On the other hand, bacterial plaque accumulation leading to peri-implantitis, and overload, leading to partial or total disruption of the bone/implant interface, are the major etiological agents causing late failures [52]. Furthermore, the implant surface properties may influence the failure pattern, as will be following discussed.

10. In addition to Implants

To achieve a successful implant placement, enough bone tissue and healthy conditions at the chosen receptor site, as well as healthy keratinized soft tissue, are essential for good all-around results [21]. If these conditions are not present, there are several procedures that should be considered prior to, or during the implant placement (Figure 26, Figure 27) [21].

When bone height or width is not enough, bone grafting can be performed to reach a minimum amount of hard tissue for dental implant fixation/osteointegration [21]. Guided bone graft augmentation consists briefly in filling bone defects, using autografts (patients' autologous bone), allografts (bone with human, animal, or synthetic origin), and a resorbable or non-resorbable membrane that may or may not complement the covering of the graft [21]. The purpose is for natural bone to replace or fill the gaps of the grafted bone for a better receptor site for the implant, being continuously remodeled [21]. This grafting can be used for sinus lift approaches, either through the implant prepared site or through a lateral window [21], for horizontal alveolar augmentation to increase width [21], or for vertical alveolar augmentation to increase height [21].

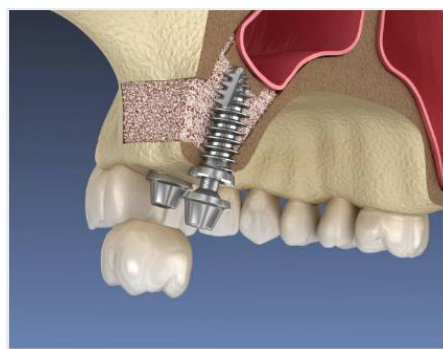


Figure 26- Sinus lift and implant placement [54].

Other surgical techniques such as the lateralization of the inferior alveolar nerve, or the onlay bone grafting with bone collected from extraoral sites are options with a

higher rate of morbidities associated [55]. Orthodontic extrusion is also an option for vertical augmentation [56].

When the soft tissue is also insufficient or with low quality of keratinization, the risk of bacterial invasion is increased, and the prognosis of the implant is reserved [21]. But the necessary “band” of attached gingiva can be achieved with a soft tissue graft, either a lateralized graft, a connective tissue graft, or an epithelium plus connective tissue free graft [21]. If an increased volume is needed for aesthetic reasons, a connective tissue graft can be placed below the epithelium for that purpose [57].



Figure 27 - Free gingival graft around implants [54].

11. Dental implants' three-dimensional structure and composition

Dental implants are presented in various shapes and sizes, from many different manufacturers, allowing professionals to choose from a wide range of options [14]. There are about 1300 implant systems, that vary broadly regarding:

1. Shape - most usually, cylindrical, or tapered - dimension, length, and width;
2. Thread design;
3. Implant-abutment connection;
4. Surface topography, surface chemistry, and wettability.

11.1 Titanium alloy

Of the available systems, the most commonly used dental implant is composed of pure titanium, or a titanium alloy, screw-shaped, and with a macroscopical rough surface [21]. Titanium is a metal with high resistance to corrosion in various media, and with high biocompatibility because it is non-toxic and neither induces major activation of the immunologic response [58]. It has an elastic modulus similar to the bone, allowing for loads to be more evenly distributed throughout the neighboring tissues, precluding bone degradation and displaying a good stress shielding [58]. Titanium is broadly inert biologically and can allow direct cell adhesion, further forming an oxide layer – titanium oxide, that is stable and exerts a protective effect on the internal material, increasing the resistance to corrosion [58]. It can also attract calcium and phosphate ions, and form apatite, enhancing osseointegration [58]. This apatitic layer is, however, very thin and easily destroyed, and for this reason, various attempts to protect and increase it have been made through different approaches [58]. One of the disadvantages of titanium is its grey color, which in some non-ideal cases, could be identified through the mucosa, hindering the esthetics and requiring the use of connective tissue graft as a complement [58]. Also, titanium's low deformity and wear resistance, and high reactivity with impurities can be seen as a drawback of this material [58].

Commercially pure titanium is assorted into four grades – 1 to 4 – according to purity and oxygen content [58, 59]. Grade 1 presents the highest purity and best corrosion resistance but has the lowest mechanical strength. Grade 4 has the biggest strength and is the composition of most titanium implants [58]. To enhance some of the best properties, binary titanium alloys have been developed, because titanium alloys' characteristics are related to their phases/crystalline structures. This is why adding some elements seems to stabilize those particular phases [58]. Also, these combinations could protect the oxide layer, as a coating strategy [58, 59].

As so, titanium-based alloys have taken the frontline of reference biomaterials for orthopedic, maxillofacial, and dental therapeutic applications, aiming for bone healing and/or fixation, given the appropriate mechanical, chemical, and biological properties [60]. These include a high strength-to-weight ratio, high yield, and fatigue resistance, as well as an adequate biological response [61]. By and large, the major limitations of titanium-based materials for bone application rely on the potential feeble osseointegration – particularly in aged and disease-affected individuals – which may culminate into interfacial displacement between the implant and the adjacent bone; and the release of metallic cations with potential local and/or systemic toxicity [62, 63].

So, the titanium alloy's most common composition in implants is the Ti-6Al-4V - the grade 5 titanium alloy, with 6% aluminum and 4% vanadium, characterized by having excellent yield strength, tensile strength, corrosion resistance, and fabricability [58]. Aluminum acts by improving the strength and lowering the weight of the alloy, and vanadium is responsible for improving ductility – resistance to deforming without fracture - and formability [58]. This grade 5 has the disadvantage of low wear resistance and low shear form – stiffness mismatch between bone and implant, which could result in the resorption of bone [58]. Therefore, surface treatments seem necessary to improve this limitation [58].

12. Modulation of the surface topography – Macro-, micro- and nano-patterns for surface modification

Increased osseointegration challenges lead to the requirement for technical improvement of planning, assisting to enhance loading protocols, facilitate osseointegration and ensure long-term bone-implant contact with stable marginal bone [6]. These demands have guided innovative research, modifying the focus on the design and geometry of the implant, to the enhancement of bioactive capabilities of implants' surfaces [64].

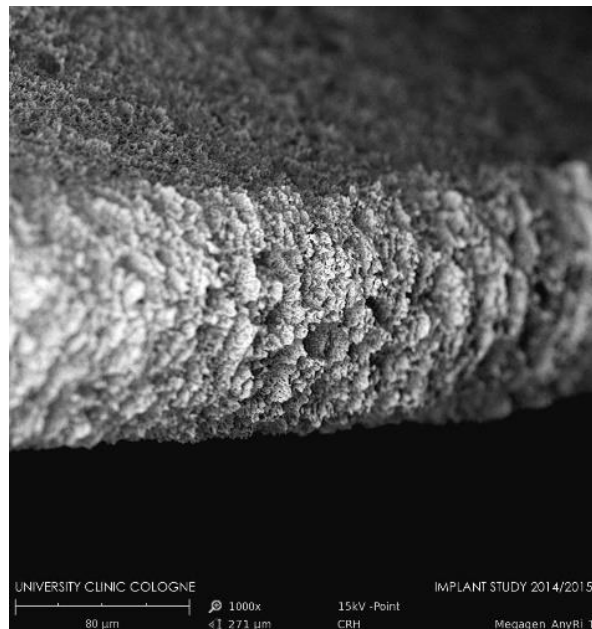


Figure 28 – Anyridge Implant surface treated with S-L-A, followed by the incorporation of calcium ions, creating a CaTiO_3 nanostructure that is expected to enhance osteoblastic activity [13].

Ever since osseointegration is an approached issue, dental implant surfaces seem to have major impacts on attained outcomes. However, only in the 1990s decade, with powerful enough measurement techniques, the recognition of the implant surface importance emerged, and several characterizations were given significance to the modulation of chemical and/or physical surface alterations [65]. Within this frame, implant surface characteristics are a key point for increased implant survival and success. The modification of topography and surface energy (Figure 28, Figure 29)

through additive (e.g., coating) or subtractive (e.g., blasting and etching) techniques enables the modulation of biological response to improve the interaction implant surface-hosts' tissue response, improving osseointegration [31]. Studies have shown the superiority of surface modifications toward histomorphometric outcomes and biomechanical features upon implantation [66]. Furthermore, surface modifications have been developed to minimize bacterial adhesion and colonization, objectively trying to limit peri-implantitis development [66]. Nonetheless, despite achieved enhancements in biological outcomes of established developments, it's still possible to improve clinical implant behavior in tissue integration and peri-implantitis prevention [66].

In Table 1 - Implant characteristics according to the topographic level [59, 67], a schematized display of major characteristics of dental implant classification, based on topography, can be found. Throughout the years, the importance has been focused on achieving biological improvements through the modulation of molecular events, via different levels of topographic domains [59].

Table 1 - Implant characteristics according to the topographic level [59, 67]

Macro Characteristics	<p>Scale: 1-10 mm</p> <p>Important for: initial stability, for the simplification of the surgical technique, among others</p>	<ol style="list-style-type: none"> 1. Coronal part Interface Collar – wide, normal, or narrow Bone level (with/without platform switching) or tissue level 2. Midbody Type of taper Type of threads 3. Apical Apical shape Apex-specific characteristics (ex.: grooves)
Micro Characteristics	<p>Scale: 1-10 μm</p> <p>Achieved by etching, anodisation, and other methods</p> <p>Important for increasing bone-to-implant surface</p>	<ol style="list-style-type: none"> 1. Roughness/porosity <ul style="list-style-type: none"> - Distribution of peaks and valleys along the evaluated profile 2. Vertical parameter <ul style="list-style-type: none"> - Mean height from peak to valley along roughness profile 3. Horizontal parameter <ul style="list-style-type: none"> - Average interpeak distance along the roughness profile
Nano Characteristics	<p>Scale: 1-100 nm</p>	<ol style="list-style-type: none"> 1. Example: Higher surface energy <ul style="list-style-type: none"> - Increases wettability to blood - Increases binding of fibrin and matrix proteins - Allows cell attachment and tissue healing 2. Molecular-sized structures (ex: Fluor incorporation)

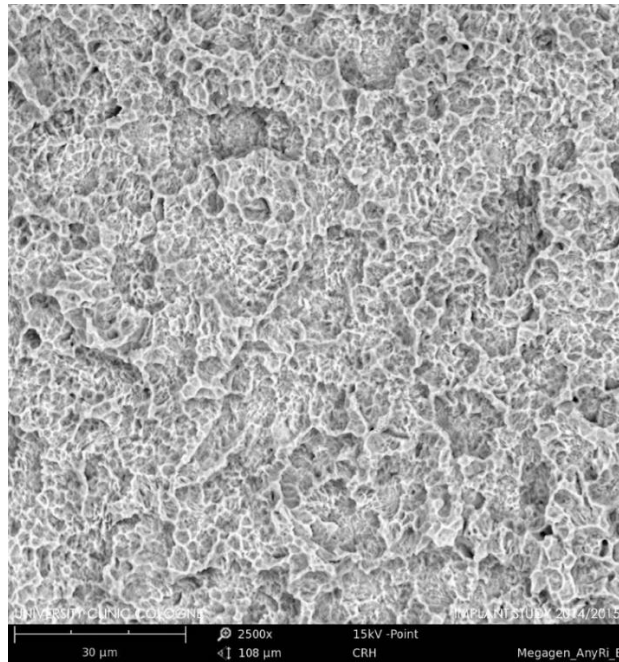


Figure 29 - Anyridge Implant surface presented in Figure 28, with higher amplification [13].

According to Albrektsson, there are 3 dimensions, applied to oral implant surface properties: mechanic, topographic and chemical [68]. Mechanical properties have not yet been exhaustively studied from a clinical point of view [21]. Topographically, Albrektsson demonstrated that a moderately rough surface was the one with the best response, at the time of the assay [68]. Buser et al, in a study about the adhesion strength in the interface of an SLA (i.e., sandblasted, large grit, and acid-etched surface) surface and comparing it with machined surfaces and TPS (i.e., titanium plasma spray), found that the adhesion strength in the interface of titanium implants can be significantly influenced by their superficial characteristics, and the best results of resistance to traction were found with roughed surfaces over machined surfaces [69]. Several other studies have supported the influence of implant surface roughness on the quality of osseointegration [70, 71].

Microscopically (Figure 30), most manufacturers change the implant surface, either through etching, anodic oxidation, or blasting, so that the surface area may increase for bone contact, and osteointegration may bio-actively become more effective [72]. The surface should be defined, and it should be determined which thickness of the most outer part of the implant bulk could be included in the definition. Some authors

define the 100 nm thick peripheral layer as the surface, and, for example, in an implant-coated surface, with, for instance, hydroxyapatite, according to this thickness, the coating would be considered the surface core material [59]. However, this definition is sometimes difficult to maintain, because some coatings' thickness could shuffle the equation [59].



Figure 30 – Representative image of a low magnification scanning electron microscopy of implant surfaces [13].

Dental implant manufacturers try to innovate with unique surface topographies, through mechanical, chemical, electrochemical, and laser treatments, to achieve faster healing and better osseointegration quality, as presented in Table 2 - Some of the different surface treatments in alphabetical order [72-76].

There are three main implant surface modification techniques, according to the classic literature [66]:

1. Mechanical treatment with blasting or machining – implants without coatings are submitted to mechanical treatments, aiming for a direct apposition of bone to the implant. Usually, that is achieved with machined detailing or with roughness augmentation. Machined detailing can vary from threaded surfaces to holes or re-entrances for enhanced bone growth in the detailing. Roughness augmentation is done by hard oxide particles blasting – e.g., Ti oxide, Al oxide, or Si oxide. After the blasting, acid treatment is recommended to remove possible oxide particle inlays and to uniform the blasting-created roughness [72].
2. Acid chemical treatment, anodization, or ionic implantation with the objective of surface cleaning, roughness creation, and surface activation through structural modifications of the oxide layer. These treatments include acid attack, anodization, and nitrification [66].
3. Application of surface coatings – generally to create a bioactive surface, but also for the prevention of ion liberation, minimization of the surface contamination

caused by implant making process, and to further achieve a roughed and porous surface. The hydrothermal method is included in this technique [73, 74].

In Table 2, some surface treatments are presented.

Table 2 - Some of the different surface treatments in alphabetical order [72-76]

Surface treatment technique	Implant System / Type of Surface examples
<p style="text-align: center;">Acid-etching</p> <p><i>Etching with acids to increase surface roughness and area, and for cleaning surfaces</i></p> <p style="text-align: center;"><i>Micro and nanoscale topographies</i></p> <p><i>In exaggerated use – high wrinkles and superficial deformations</i></p>	<p style="text-align: center;"><i>Biomet 3i Osseotite® and Nanotite®</i></p>
<p style="text-align: center;">Alkali-based treatment</p> <p style="text-align: center;"><i>Solutions of NaOH or CaP on surface</i></p> <p><i>Micro and nanoscale layer, alkali-titanate layer – modifies the base material interface</i></p> <p><i>Joined with hydrothermal treatment – hydrophilicity, better for cell and bone adhesion</i></p>	
<p style="text-align: center;">Anodizing</p> <p><i>Electrochemical technique for thickening and roughening the titanium oxide layer</i></p> <p style="text-align: center;"><i>Micro and nano-level topographies</i></p> <p><i>Nanotubes achieved by electrolyte solution, changes in temperature and voltage, cathode and anode surface</i></p> <p style="text-align: center;"><i>Combined with acid etching, blasting, or machined surfaces</i></p> <p><i>Studied for drug delivery systems on implant surfaces</i></p>	<p style="text-align: center;"><i>Nobel Biocare TiUnite®</i></p>
<p style="text-align: center;">Biodegradable coatings</p> <p style="text-align: center;"><i>Preliminary research and needs more investigations</i></p> <p><i>Implantable surfaces with polysaccharides, chitosan, and collagen, among others</i></p> <p style="text-align: center;"><i>Application in already treated surfaces may impair some of the properties</i></p> <p><i>For example – coating with polymer loaded with amoxicillin on Ti surface – diminishes hydrophilicity, but improves biocompatibility and antibacterial properties</i></p>	
<p style="text-align: center;">Bioprinting</p> <p><i>3D-fabrication in Ti, Ti alloys or ZrO₂, with customization of implants for each case</i></p> <p style="text-align: center;"><i>Surface quality still inefficient on micro and nano scales</i></p> <p style="text-align: center;"><i>Still needs more evolution</i></p>	
<p style="text-align: center;">Grit Blasting</p> <p><i>Projection of micro or nano-particles at high speed onto the implant, with titanium dioxide, aluminum dioxide, and/or hydroxyapatite. Hydroxyapatite treatments also include resorbable blast media and microtextured surface treatments</i></p> <p style="text-align: center;"><i>Creates depressions by deforming the base material</i></p> <p style="text-align: center;"><i>Roughness on micro or nano-level</i></p>	<p><i>Dentsply implants Astra Tech TiOblast®,</i></p> <p><i>Zimmer Dental MTX®,</i></p> <p><i>Inclusive® Tapered implants</i></p>

<p style="text-align: center;">Hydrothermal</p> <p><i>Techniques of crystallizing substances from high-temperature aqueous solutions at high vapor pressures;</i></p> <p><i>Can generate nanomaterials that are not stable at elevated temperatures. Nanomaterials with high vapor pressures can be produced by the hydrothermal method with minimum loss of materials</i></p> <p><i>Simpler, and cost-effective method</i></p>	<p style="text-align: center;">Megagen Anyridge Xpeed®</p>
<p style="text-align: center;">Laser treatment</p> <p><i>Laser beam high-intensity pulses onto a layer that coats the metal surface, inducing a honeycomb pattern with pores</i></p> <p style="text-align: center;"><i>Micro and nanoscale</i></p> <p><i>Reproducible morphologies that seem to Increase the viability of osteogenic cells</i></p>	<p style="text-align: center;">BioHorizons® laser-Lok®</p>
<p style="text-align: center;">Machining</p> <p style="text-align: center;"><i>1st process ever to be applied</i></p> <p><i>Involves laths for the implant design and maintains roughness on macro and microscale</i></p> <p style="text-align: center;"><i>Requires 4–6-month healing for rehabilitation</i></p>	
<p style="text-align: center;">Plasma-spraying</p> <p><i>Titanium in powder form injected into a plasma torch at high temperatures in vacuum or low atmospheric pressure environment</i></p> <p style="text-align: center;"><i>Layer adheres by melting and sintering</i></p> <p style="text-align: center;"><i>Micro and nanoscale</i></p> <p><i>Different materials – titanium, gold, silver, and ceramics, can be used</i></p> <p><i>Disadvantage: weak interface implant-coating – extreme surgical care in clinical insertion</i></p>	<p style="text-align: center;">titanium plasma sprayed TPS®</p>
<p style="text-align: center;">Sandblasted and acid-washed / etched</p> <p style="text-align: center;"><i>SLA – most employed and effective surface treatment</i></p> <p><i>After the blasting process, the surface is washed with either a non-etching or etching acids</i></p> <p style="text-align: center;"><i>Osseointegration success/cell adhesion - 1-2 months</i></p> <p style="text-align: center;"><i>Micro and nano level application</i></p> <p style="text-align: center;"><i>Deformations by blasting</i></p> <p style="text-align: center;"><i>Irregularities and cleaning the surface by etching</i></p>	<p style="text-align: center;">Camlog promote®, Dentsply Implants Frialti® and Friadent® plus, Strauman SLA®</p>

It is also important to mention contamination or pollution of the surfaces, which may impact the functional characteristics [59]. CO₂ and nitrogen contaminations from the air are inevitable, but inadequate surface treatments and implant handling can severely originate organic contaminations, indicated by, for example, XPS analysis, showing a thick carbon overcoat on the implant's surface, or the presence of unexpected ions [59]. These contaminations are not intentional and must not be mixed up with treatment surface modifications.

There are numerous advantages in coating the implant surfaces as presented in Table 3, in which we can find some of those advantages, as recently reviewed [69, 77].

Table 3 - Advantages in using coating in implant surface

<i>Faster osseointegration</i>
<i>Immediate function allowed</i>
<i>Soft tissue integration</i>
<i>Higher resistance to traction forces</i>
<i>Higher resistance to shear forces</i>
<i>Increased initial stability</i>
<i>Higher and increased bone-implant contact</i>
<i>Improved results in less dense bone (D3 and D4)</i>

On the other hand, implant surface coating may also bring some disadvantages, to keep in mind, as stated in Table 4 - Disadvantages of using coated surfaces [79]. When placing an implant, there are several challenging conditions, such as wear and degradation by mechanical, chemical, and microbiological processes [72]. Friction, lubrication, and/or wear between interfaces added to the challenging conditions, define the eventual bio-tribocorrosion of implants [72]. Although it is a condition with any implantable metallic devices, it also should be mentioned when approaching dental implant surfaces [72]. It starts with the placement of the implant, with frictional forces, torque, and loading that may damage the surface. The following loading forces under function, with intense and repetitive movements, can induce superficial rupture, and even the saliva, if it has a reduced pH, can contribute to a corroding microenvironment

[72]. Also, metabolites from the inflamed or infected environment can promote biocorrosion, by lowering local pH and promoting the phenomenon [72].

One final topic on implant surface characteristics is the importance of the concentration and levels of minority elements [72]. For example, aluminum can be used in surface treatments, but above certain levels, it becomes cytotoxic [72]. This is also true for other elements such as fluor [78]. This showcases the importance of determining in preliminary studies, the best percentage of new elements added to implant surfaces, aiming for direct contact with living tissues, such as the bone [78].

Table 4 - Disadvantages of using coated surfaces [79]:

The risk of surface damage when placing the implant, especially in denser bones

An increase in surface roughness may favor bacterial contamination of bone

Increase of plaque retention above bone level

Increased treatment difficulty in the event of peri-implantitis

The implant cost increases

Several studies have been presented on this subject, some including prospective analysis, and some retrospective analysis [80-88]. Some prospective clinical studies showed success rates of 99% in the mandible and 100% in the maxilla, when implants with resorbable blast media surface treatment technique were used [80], and around 96.6% for hydroxyapatite-coated implants [81]. A 9-year long study with more than 2.000 implants in 731 patients showed a cumulative survival rate of 98% for hydroxyapatite-coated implants, and MTX implants (i.e., non-coated microtextured surface, Tapered Screw-Vent MTX Texturing (TSVT) - a standard dental implant produced by Zimmer-Biomet) [82]. In 2006, 60 patients with compromising clinical factors treated with MTX implants, reported a 98% of survival rate, with only 4 of 218 implants failing in the first year [83]. Another study, with 550 resorbable blast media surface treatment technique, compared immediate loading and late loading and achieved no significant difference at 5-year follow-up, with survival rates of 98-100% [84]. In 2011, abrasive-blasted, acid-etched implants, resorbable blast media surface treatment, and titanium-dioxide-texture implants were compared, and a cumulative

survival rate was 100% [85]. Retrospective clinical studies in the literature show around 97-98% implant success rate after 8 and 10 years [86, 87]. A 5-year study of implants with 2 types of coating techniques – abrasive-blasted acid-etched and resorbable blast media also showed similar survival rates [88].

Some literature suggests that independently of the surface treatments, outcomes seem to be comparable, and with no benefit of a specific morphological characteristic over other structures, from a clinical point of view [89-91]. However, Matos, in a revision work, concluded that rough surfaces, when compared with smooth ones, present better results, although nanoroughness may present itself as a better solution for the future [92].

It seems that the development of innovative surface technologies will never be too much, aiming at enhancing implant surface-to-bone and soft tissue interactions and healing response improvements [21].

Titanium and titanium alloys seem to present excellent biocompatibility and the local tissues easily tolerate this thanks to the highly active TiO₂ layer, as mentioned above [58]. The micro-rough surface is created by applying a titanium dioxide particulate jet (titanium plasma spray) over the implant's surface so that it creates a topography able to transfer physiologic strengths and stimulate bone formation, which leads to an increased bone-implant contact area, and a better mechanical interface between both [93].

The presence of such a rough surface – for example, TPS 150-400 μm or TiOblast[®]-, works as a three-dimensional surface with increased contact, that stimulates osteogenesis by adhesion. The surface area increase can get up to 600% microscopically, and it increases functional strength support by up to 30% [93]. It also leads to higher resistance of bone-implant traction and shear forces, as well as load transfers [93]. The surface roughness increase can also improve the implant's initial stability, especially when the bone is less dense [93]. One of the main problems that can occur with this type of surface, is the release of ions, and the production of adverse effects in tissues if the interface with the implant is large [58].

Some implants are presented as having hybrid design – such as Osseotite® - because they combine 3 mm polished titanium on the coronal surface to maintain soft tissue health, and a microtextured surface in the rest of the implant surface, with 1-3 µm between peaks and 5-10 µm of depth. This surface, according to some authors, increases the adherence to bone and the percentage of bone contact [94]. The double acid etching with hydrochloric acid and sulfuric acid is a reliable method for obtaining a uniformly rough surface, in which distance may vary from 0.3-1.5 µm between peaks and 1-2 µm in depth. These dimensions created on the implant's surface will be of major importance in the coagulum retention ability per-surgically, and the consequent bone matrix formation [95]. It promotes a strong connection between the coagulum and the implant and increases erythrocyte agglomeration and platelet activation [94]. Park et al study on erythrocytes and platelets interaction with the implant, showed that the quantity of erythrocyte agglomeration on Osseotite® surface was 54% higher than in a machined surface [96].

In 1991, the ITI group evaluated the influence of new titanium surface formats on osseointegration. Several topographies were obtained through different methods and tested. SLA® – Sandblasting, Large grit, Acid etched – the surface was created with silicate jet, forming macroroughness, and followed by acid etching with HCL/H₂SO₄, for microroughness of 2-4 µm. This surface achieved the best bone contact index, reducing osseointegration time for 45 days by increasing local cytokines and growth factors production [97]. Due to its microroughness, the SLA surface provided a higher rate of osseointegration and a loading time decrease of 50%, when compared to plasma-sprayed titanium surface - TPS®. It also reduced the three-month healing time of the TPS® surface to six weeks [97]. Also, an investigation on extra-oral cortical bone, with short healing times – 3-6 weeks – showed that the SLA® surface treatment method produced a higher bone-to-implant contact when compared to titanium plasma-sprayed titanium - TPS® [77]. Buser also studied the SLA® surface adhesion strength in the implants interface in comparison to machined and TPS® surfaces and showed that after 4, 8, and 12 weeks after placement, the machined surface presented the lowest values of adhesion, with significative differences. At 4 weeks, SLA® implants presented the highest values of adhesion [69].

These are examples to show how different modifications on the surface characteristics influence implant's success rate, and the importance of macro and microstructure modifications of a titanium implant.

As mentioned, besides shape, the chemical modification of the surface is an important variable for bone growth on the surface of the implant, because it influences the surface charge density and its hydrophilic characteristics [98]. Hydrophilicity is directly dependent on the surface energy, and it dictates the level of contact of a biomaterial with the tissue cells that come in contact [98]. The increase in the hydrophilic profile promotes a better interaction between the implant's surface and the biologic environment around it [98].

SLActive® surface production is similar to SLA®, however, these are made in a special closed environment with a nitrogen atmosphere, and maintained in an isotonic solution of sodium chloride, that protects the pure surface of the titanium against carbonates and organic components' contamination, naturally present in the air [58]. This preserves the purity of the surface and therefore its reactivity [58]. The hydrophilic characteristic of this surface promotes the direct adsorption of blood proteins, which guarantees that the natural and biological process of bone formation starts as early as possible [58]. The active surface attracts blood proteins and forms a dense layer. Platelets adhere to that layer and a fibrin web is formed. These molecules attract mesenchymal cells, and bone formation starts. Pre-osteoblasts join the implant surface and gradually differentiate into osteoblasts. At this point, a non-mineralized bone matrix is formed. In a final stage of osseointegration, the bone matrix mineralizes assuring secondary stability of the implant in the bone [98].

13. Innovative surface coatings for dental implants surface

To heighten the implants' functionality, coating applications – and specifically those with bioactive ceramic materials such as hydroxyapatite (HA) – have been developed, aiming for improved construct stability, long-term functionality, and decreased corrosion [5]. Bioceramic coatings show an effective osteoconduction and potential osteoinductive ability, translated into enhanced bioactivity with the human bone tissue, as previously discussed [6].

A titanium oxide layer is a very thin layer that promotes osteoblastic actions but is easily destroyed as mentioned above [58]. Some methods can be attempted to protect this layer, by coating the implant's surface, using, for example, electrochemical oxidation, anodic oxidation, or heating under atmospheric pressure [58]. One other alternative is the use of the hydrothermal method, described throughout this work. These methods can thicken the oxide layer, preventing titanium ions leakage and therefore protein denaturation and eventually cells' necrosis [58].

The vast majority of clinically developed bioceramic coating strategies rely on plasma-spraying methodologies. Nevertheless, this coating approach may originate structural and phase discrepancies – elapsing from the high processing temperature – that create a thick (30–100 μm), highly crystalline, non-uniform coating, and consequently, dissimilar surficial resorption and biofunctionality; as well as a reduction in the interfacial coating-substrate strength [74, 93, 99]. An alternative coating methodology – the hydrothermal method – can be used as a simple, scalable, cost-effective, environmentally friendly, and versatile process [73, 74]. In addition, it can produce homogeneous coatings on complex-shaped substrates - such as threaded dental implants, with defined chemical composition and crystallinity similar to that of mineral bone tissue [100].

13.1 Hydroxyapatite and dental implants

In previous reports, it has been established, characterized, and optimized the production of pure phase HA through the hydrothermal method [100]. Hydroxyapatite

(HA) - $(\text{Ca})_{10}(\text{PO}_4)_6(\text{OH})_2$ (Figure 31) – specifically calcium hydroxyapatite, is a compound of defined crystallography. It belongs to the hexagonal system, with special groups $P6_3/m$, characterized by a perpendicular symmetry to three equivalent axes “a” (a_1 , a_2 , a_3), forming 120 degrees in between. The unit cell contains a complete representation of the apatite crystal, which consists of Ca, PO_4 , and OH groups, together [101].

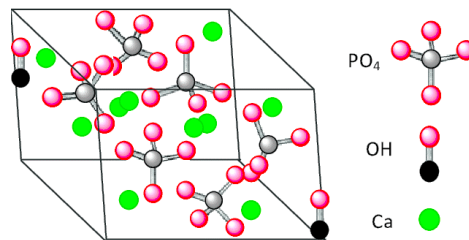


Figure 31 - The structure of hydroxyapatite crystals [102].

The hydroxyapatite connection to bone tissue has shown to be reasonably effective in the long term [101]. However, its mechanic properties and the high implant fatigue do not allow it to be used as an anchor of implants' submitted to loading [101]. In this way, coatings with high mechanical resistance have been made using effort-transferring means such as porous, gaps, grooves, or rough surfaces [101]. Hydroxyapatite can thereover be used as a solid bone-filling material or as a coating for any type of metal, but with these disadvantages in mind [101]. Also, regarding the direct union between bone and hydroxyapatite, the resistance and the interface healing are better than the bone-titanium or bone-TPS interfaces and present less metal corrosion [103]. However, with its exposition, plaque retention may increase, converting the area into a bacterial focus with a higher level of bacterial toxins, due to the surface characteristics and charges [103].

13.2 Calcium Phosphate and dental implants:

Tricalcium phosphate ($\text{Ca}_3(\text{PO}_4)_2$) in dental implant surfaces can also bring some particular characteristics. One example was presented by Biohorizons® in the late 1990s – with the RBT or Resorbable blast texturing [104]. It is composed of biocompatible

calcium phosphate sprayed over the implant's surface, and that dissolves in the manufacturing process “passivation” phase, leaving a rough and pure titanium oxide exposed surface that the manufacturer concludes as ideal [105].

Since the year of its presentation, in 2000, Ti-Unite® surface has titanium oxide enriched with a highly crystalline phosphate. The porous surface structure is characterized by low micrometric dimensions – 1-10µm, and even smaller porous with a 1µm diameter [106]. This surface seems to promote osteoconduction because it allows osteogenic cells that evolve into pre-osteoblasts, to invade the surface. They form cytoplasmatic extensions – pseudopods – that migrate and adhere to the surface, using the porous structures, and fully differentiated into osteoblasts that secrete bone matrix. This promotes a fast and direct bone apposition on the implant's surface [106]. The bone growth inside the porous strengthens the stability of the matrix-to-implant connection [106]. Some other studies demonstrate good connections between the Ti-Unite® surface and epithelial tissues through hemidesmosomes [107]. On a connective tissue level, it can find three main orientations of fibers: parallel to the longitudinal implant axle; circumferential dense fibers; and thin fibers, oriented functionally towards the titanium oxide surface enriched with highly crystalline phosphate [107].

Megagen Xpeed® surface of their pure Grade 4 titanium implants also incorporate calcium ions, after being treated with the S-L-A method, mentioned above. According to the manufacturer, this particularity activates osteoblasts, and promotes cations on implants surface, which promotes PO_4^{3-} ions' adherence. After this, new calcium ions adhere to the new phosphate layer. In this way, the apatite layer is increased, and hydroxyapatite is formed quickly [108].

13.3 Fluor and dental implants

Fluor is also studied as a possible element on implant surfaces. Aiming for improved bioactivity, the addition of fluoride (F^-) to the HA lattice, allowing the formation of fluorapatite (Figure 32) via hydroxyl substitution, can be innovatively assayed [78]. The fluoride substitution has been described to increase the density and reduce the solubility of the bioceramic [109], further improving the biological response

within the bone tissue through the release of fluoride ions capable of increasing osteoblastic proliferation and differentiation [78, 110, 111]. Notwithstanding, fluoride content needs to be precisely balanced within the materials' composition, as a high fluoride release may be cytotoxic to bone cells and ultimately impair the bone healing/regeneration process [110, 112]. Fluor has other demonstrated advantages, including an improvement in bone density [111]. One surface that presents titanium dioxide modified with fluor is OsseoSpeed®. It presents a nanoroughness topography, and the concept of this surface was based on Jan Ellingsen theory that states that modifying the titanium oxide with fluor, and introducing it to the bone, would start a biological modulation process that would culminate in more bone production, and in a faster way [113, 114].

Some laboratory studies reveal that this modification attracts calcium phosphate to its surface, forming crystals. This process of calcium and phosphate adsorption favors new bone formation and therefore, the bone adhesion process, which also tend to be quicker [78, 114].

Fluor is also a part of fluorapatite ($\text{Ca}_5(\text{PO}_4)_3\text{F}$) - calcium fluorophosphate, a hard crystalline solid. It is often combined as a solid solution with hydroxyapatite ($\text{Ca}_5(\text{PO}_4)_3\text{OH}$ or $\text{Ca}_{10}(\text{PO}_4)_6(\text{OH})_2$) in biological matrices [115].

Fluorapatite has a prism like structure, a similar composition to the apatite crystals of dental hard tissues, and can be synthesized by the hydrothermal method [115]. It shows higher biocompatibility and bioactivity than hydroxyapatite, with lower resorption, and it also releases fluor ions, with osteoconductive and antibacterial characteristics [115]. It seems that fluorapatite can be beneficial as a dental implant coating, proven to present enhanced osteoconductive properties, over hydroxyapatite [115].

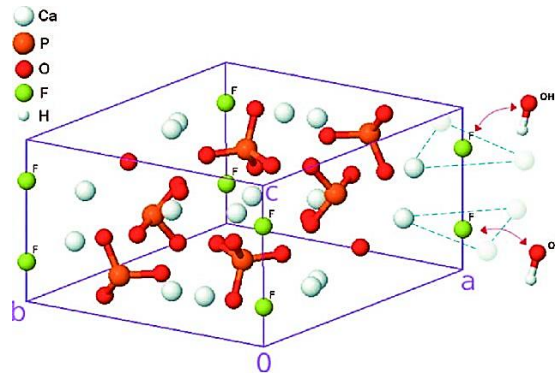


Figure 32 - The structure of fluorapatite crystals [116].

13.4 Citrate groups in coatings' morphology

Citrate ions are reportedly shown to be useful for the production of fluorapatite particles [117]. When citrate and fluor ions are present, fluorapatite is formed [117]. The formation of fluorapatite particles seems to come from a fractal growth, allowed by a large dipolar field along the c axis of fluorapatite structure, that is provided by citrate ions [117]. Citrate groups seem to have an important role in achieving a nanostructure that would allow for a thinner coating with fluorapatite, and also enhance the substitution of OH^- by F^- , and accelerate the crystallization process [118-120]. They are also known to enhance the biomineralization process [118-120]. The presence of citrate species on the produced coatings is expected to synergize with F to improve the osteogenic response.

II. Objectives

"Imagination is the only weapon in the war with reality"
Cheshire Cat, Alice in Wonderland

This project aims at the synthesis, preparation, and characterization of fluorapatite coatings, applied to titanium implants developed using the hydrothermal method with distinct fluoride contents, towards the enhancement of the biological response study, for maximum bone tissue ingrowth.

Comparatively to existent coating applications, the new surface treatments are expected to enhance the biological functionality and allow for a better adaptation to the machined surface of the threaded implant due to the reduced thickness - within the nanorange scale - allowing for an adequate elastic response upon deformation, maintaining a structural homology with the titanium substrate.

Accordingly, the specific objectives of this work are:

1. The use of the hydrothermal method for coating applications, to obtain an innovative implant surface treatment;
2. The characterization of the developed coatings through an *in vitro* study with human osteoblastic cells;
3. The evaluation of the *in vivo* response, as a proof-of-concept study using different groups of clinically relevant coated implants (4mm x 7mm), with distinct fluoride content;
4. The characterization of the developed coatings regarding physic-chemical, and biological properties through *in vitro* and *in vivo* approach.
5. The assessment of the biological response of the constructs evaluated by microtomographic and histomorphometric analysis, at distinct time points.

III. Materials and Methods

*"You must not let anyone define your limits because of where you come from.
Your only limit is your soul."
Gusteau, Ratatouille*

3.1 – Preparation and characterization of fluorapatite-coated titanium implants

3.1.1 – Implants

Commercially pure titanium Grade 4 implants (AnyRidge® 4x7 mm) and discs (10x3mm), kindly donated by MegaGen® (Seoul, Korea), were used as substrates for coating deposition. Implants (for the *in vivo* study) and discs (for the *in vitro* study) were cleaned with acetone and water and placed inside the inner Teflon reactor chamber of the inox steel autoclave until further preparation. One implant per autoclave was placed.



Figure 33 - Used autoclave system for the preparation of the coatings through the hydrothermal method.

- a. - Synthesis of the hydroxyapatite and fluorapatite coatings by the hydrothermal method

Coatings were prepared through the hydrothermal method in an autoclave (Figure 33). The hydroxyapatite and fluorapatite coating solutions were produced following the precipitation method [100], as summarized In Figure 34. Briefly:

- A 0.6 M aqueous solution of citric acid ($C_6H_8O_7 \cdot H_2O$, 99.5%), with a pH of 8.0, was prepared with ammonium solution (NH_4 , 25%).
- Then, a 0.2 M solution of calcium nitrate ($(CaNO_3)_2 \cdot 4H_2O$, 99%) was added to the citric acid solution (solution A).
- Finally, a 0.2 M, 0.1 M, or 0.01 M solution of ammonium hydrogen phosphate ($(NH_4)_2HPO_4$) was added, dropwise, to solution A, together with a 0 M, 0.1 M, or 0.01 M solution of ammonium fluoride, to obtain the hydroxyapatite coating and two coating solutions with different concentrations of F ions.

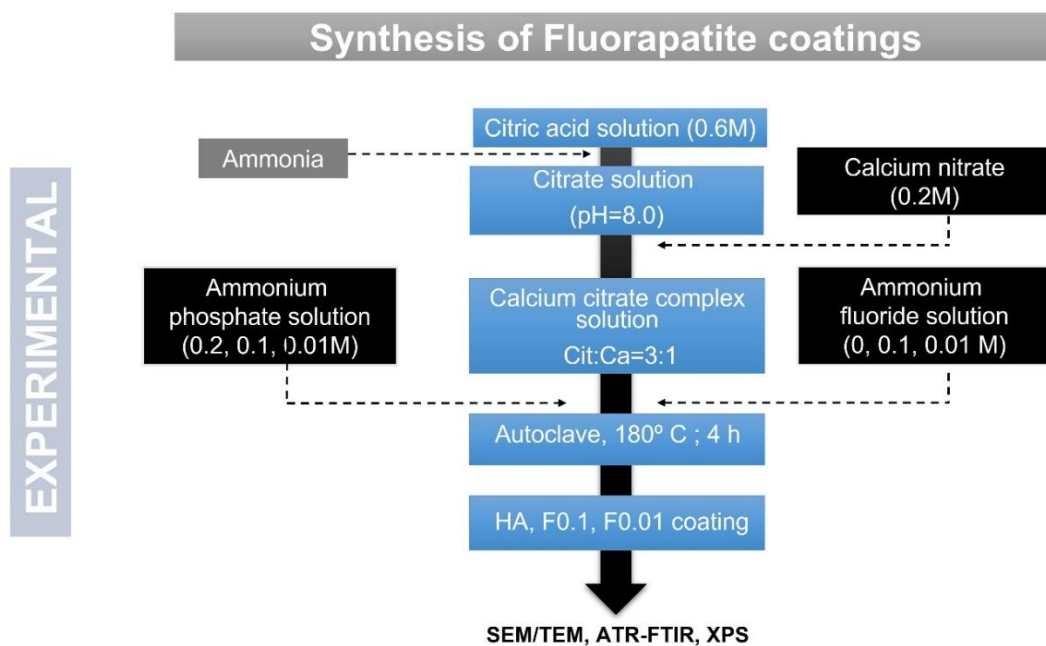


Figure 34 - Schematic representation of the synthesis of fluorapatite coatings.

After this, the autoclave was filled up to 50% of a Teflon reactor volume, and the prepared solutions were immediately transferred to that reactor Teflon vessel and placed in the autoclave. The implants were sitting at the bottom of the autoclave. The sealed autoclave was set up to 180 °C for 4h, the samples were then removed, and so the coated implants were named:

- HA,
- F 0.1, and
- F 0.01, respectively (Figure 35, Figure 37).

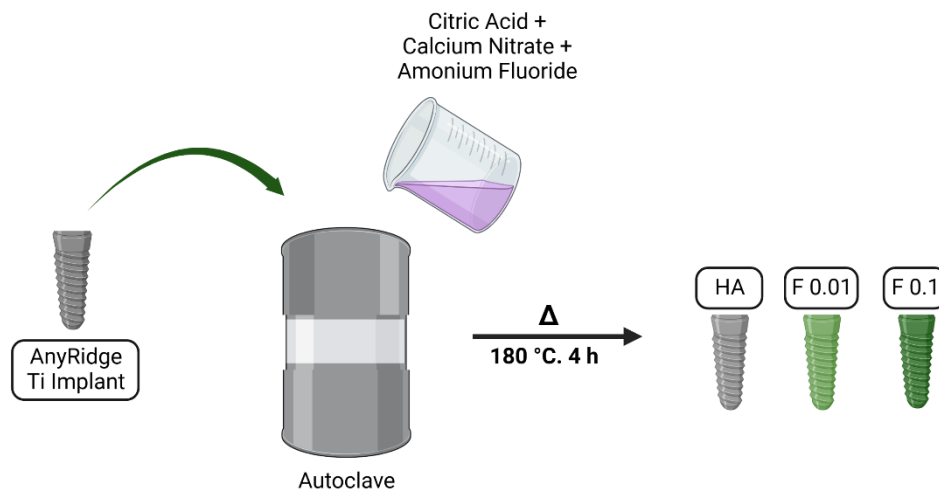


Figure 35 - Implant coating production schematization.

b. - Physical and chemical characterization

The morphology of the developed coatings was evaluated using a scanning electron microscope JEOL-JSM7001F, at an operating voltage of 20 kV.

The chemical composition of the coatings was determined using an X-ray energy dispersive spectrometer (EDS) analysis.

The particle size of the F 0.1 coating was studied using a Transmission Electron Microscope (TEM) (Hitachi H-8100-NA with an acceleration voltage of 200 kV). Before imaging, F 0.1 coating particles were detached from the titanium substrate and dispersed in ethanol. Then the suspension particles were placed on the carbon-coated copper grid and dried at room temperature.

Attenuated total reflectance (FTIR-ATR) spectroscopy using a Nicolet (Thermo Electron) was used to characterize the functional groups and chemical composition of

the HA, F 0.01, and F 0.1 coating over a range of 650–4000 cm^{-1} and a resolution of 8 cm^{-1} .

X-ray photoelectron spectroscopy (XPS; Kratos Axis Ultra HSA, Aluminum mono, $E_0 = 15 \text{ kV}$ (90W) 1 eV per step in a 300 $\mu\text{m} \times 700 \mu\text{m}$ area) was used for fluorine, calcium, and phosphorus content analysis at the surface of the F 0.1 coating (Figure 36).

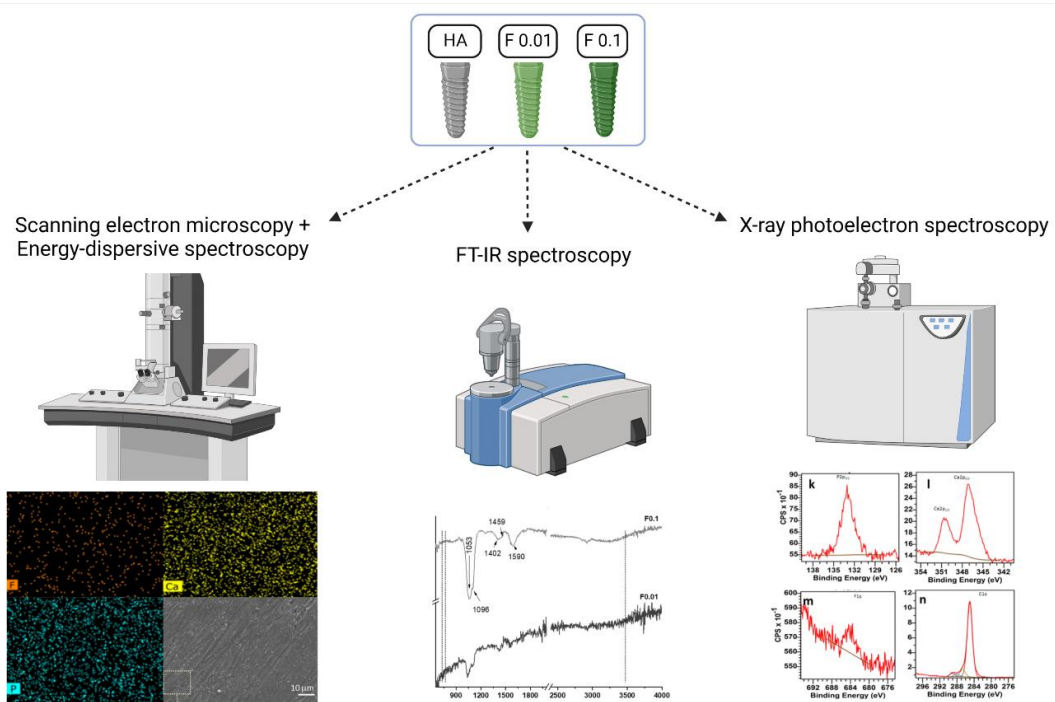


Figure 36 - Physical and chemical characterization schematization.

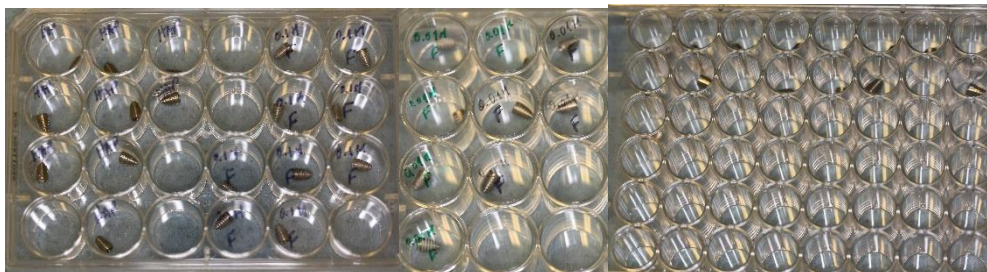


Figure 37 - Implant groups HA, F 0.1, and F 0.01 distribution in tissue culture plates.

3.2 – Biological characterization - In vitro response to osteoblastic cells

The biological response of the developed coatings was evaluated *in vitro* (Figure 38), with human bone marrow-derived stromal cell (BMSCs) cultures, in coated commercially pure titanium Grade 4 disks.

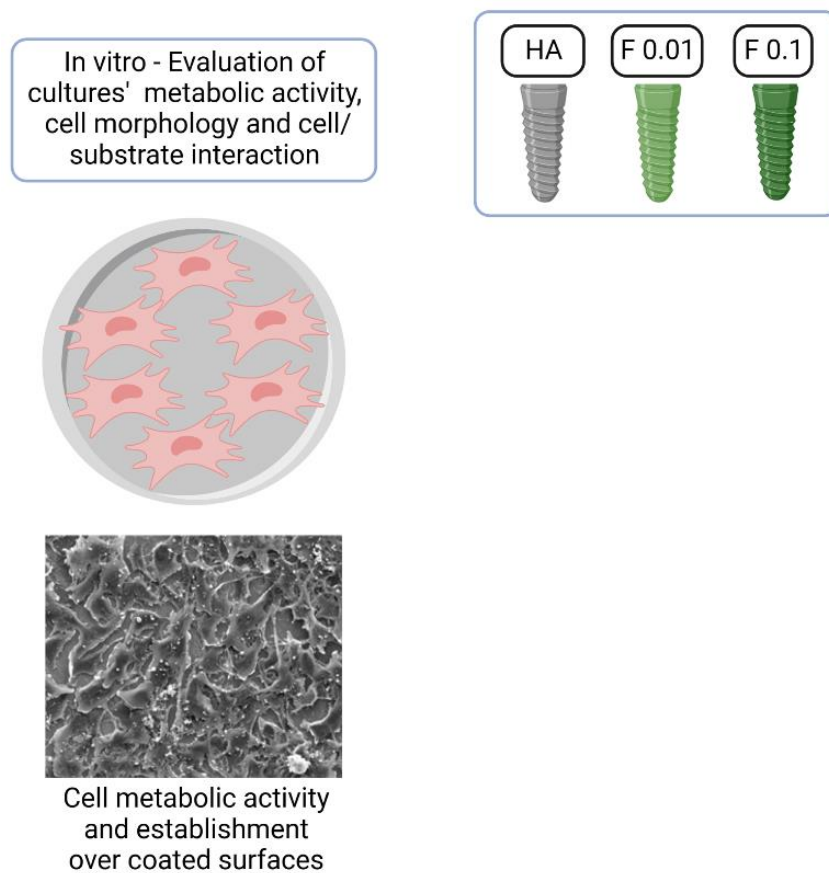


Figure 38 - Biological characterization schematization – *in vitro* assays.

BMSCs were commercially available and were obtained from a certified vendor (Lonza cat. number PT-2501). Cells were grown in alpha-minimum essential medium (α -MEM, Sigma) supplemented with 10% fetal bovine serum (FBS, Gibco), 50 μ g/mL ascorbic acid (Gibco), penicillin (10 units/mL)/streptomycin (2.5 μ g/mL) (P/S solution, Sciencell) and 2.5 μ g/mL fungizone (Gibco) – Basal medium. Cultures were grown up to around 70–80% confluence (\sim 10 days), at defined experimental conditions - 37 $^{\circ}$ C and

5% CO₂ in the air. At this time point, adherent cells were enzymatically released with a 0.04% trypsin/0.25% EDTA solution, and sub-cultured. Cells were characterized for the expression of relevant surface markers through flow cytometry and found to be broadly positive for CD 105, CD 146, and CD 90 – characteristic mesenchymal stromal cells markers; and negative for CD45 – a major hematopoietic marker, thus fulfilling the established criteria as mesenchymal stromal cells.

Cells from the fourth passage were used in the described experiment. Briefly, cells were cultured (5×10^4 cells/cm²) in osteogenic-inducing conditions – i.e., basal medium, as previously described further supplemented with 10 mM β -glycerophosphate and 10 nM dexamethasone, over the coated titanium disks' surface, with medium change twice a week, for a period up to 21 days. Cultures established over HA-coated titanium disks were used as control. Cell behavior was characterized as follows.

3.2.1. - Cell viability/metabolic activity

Cultures' viability/metabolic activity was estimated by the resazurin assay, at days 1, 3, 7, 10, 14, and 21 of the culture. Briefly, fresh culture medium supplemented with 10% resazurin was added, at each time point, to the growing cells, and cultures were subsequently incubated in the defined culture conditions for 3 h. Afterward, a volume of 100 μ L of the incubating medium was transferred to a 96-well plate and the fluorescence was quantified in a microplate reader (Synergy HT, BioTek - 535 nm excitation, and 590 nm emission wavelengths). The results were expressed in relative fluorescence units (RFU).

3.2.2 – Scanning electron microscopy (SEM) evaluation

For the SEM assessment, cultures were fixed with glutaraldehyde (1.5%) for 10 minutes, and were then washed with PBS, and maintained in a buffer solution (pH 7.3)

of 0.14 M sodium cacodylate until further processing. Samples were dehydrated in graded alcohols, critical-point dried, sputter-coated with a gold/palladium thin film, and observed in a scanning electron microscope equipped with X-ray energy dispersive spectroscopy (EDS) microanalysis capability (Quanta 400 FEG ESEM/EDAX Genesis X4M).

3.3 – Biological characterization - *In vivo* response to bone implantation

3.3.1 - Animals

In this study 8 male New Zealand white rabbits (*Oryctolagus cuniculus*) (Figure 39), 12 weeks old, weighing 2.9 ± 0.32 Kg were acquired from a certified vendor – Granja San Bernardo, Spain. All procedures were approved by the local Institutional Animal Care and Use Committee (IACUC), based on standard protocols, under national and European legislation for experimental animal research – European Directive 2010/63/EU. All procedures had the supporting recognition of the joint institutional committee for animal welfare (ORBEA-UTAD) and were carried out under project license (nº010532/2018) approved by the National Competent Authority for animal research - Directorate General of Food and Veterinary (DGAV, Lisbon, Portugal).



Figure 39 - New Zealand white rabbits (*Oryctolagus cuniculus*).

Animals were acclimatized for 3 weeks before any experimental manipulation, and were housed in environmentally enriched individual cages, in a temperature-, humidity-, and air renewal-controlled room, in a 12h light-dark cycle, in UTAD Animal Facilities. Animals were fed a standard diet (Mucedola 2RB15) and water *ad libitum* and

were monitored daily throughout the acclimatization and experimental period. All procedures were conducted in compliance with the ARRIVE - Animal Research: Reporting of In Vivo Experiments - guidelines (<https://arriveguidelines.org/>).

3.3.2 - Surgical procedure

Each animal received a total of 6 implants, three on the proximal left tibia and three on the proximal right tibia, which was randomly distributed (Figure 40). 4 rabbits were endorsed for the postoperative follow-up in one of the following groups: 4 and 8 weeks (4 animals per timepoint, 8 implants per experimental group; n=8, (Figure 41).

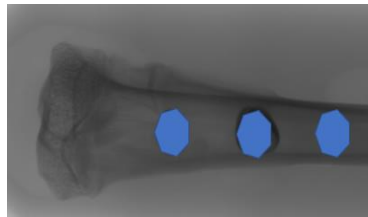


Figure 40 - Representation of the implant placement at the proximal tibia.

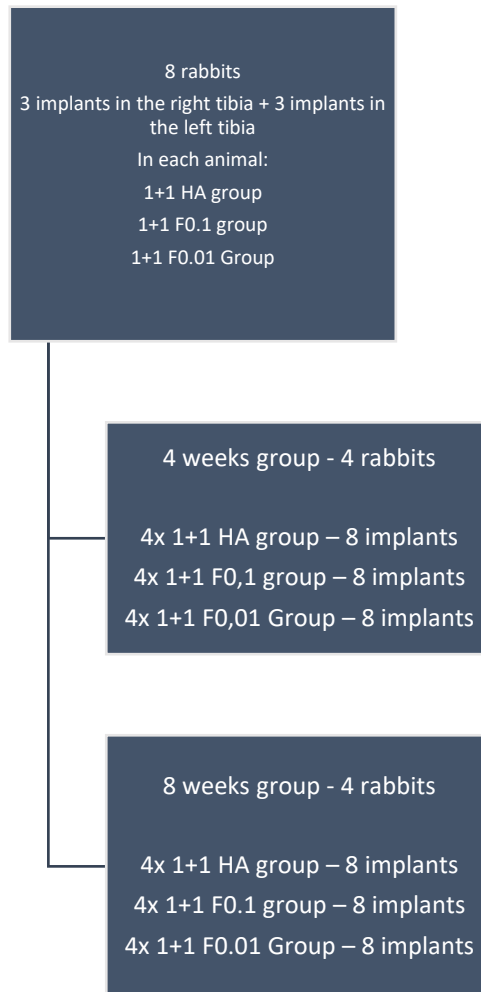


Figure 41 - Implant distribution within the in vivo experimental study.

Before the surgical implantation, animals were pre-medicated with intramuscular injections of 1 mg/kg midazolam. Buprenorphine (0.03 mg/kg), administered subcutaneously, was used for analgesia and continued for 5 days. General anesthesia was achieved upon the intraperitoneal administration of 25 mg/kg ketamine and 5 mg/Kg xylazine. Throughout the surgical procedure, sterile saline was administered at 10 mL/kg/h while animals were maintained on a heated surface and carbomer eye gel was administered to prevent ocular lesions. O₂ was administered by a facial mask throughout the surgical procedure (Figure 42).

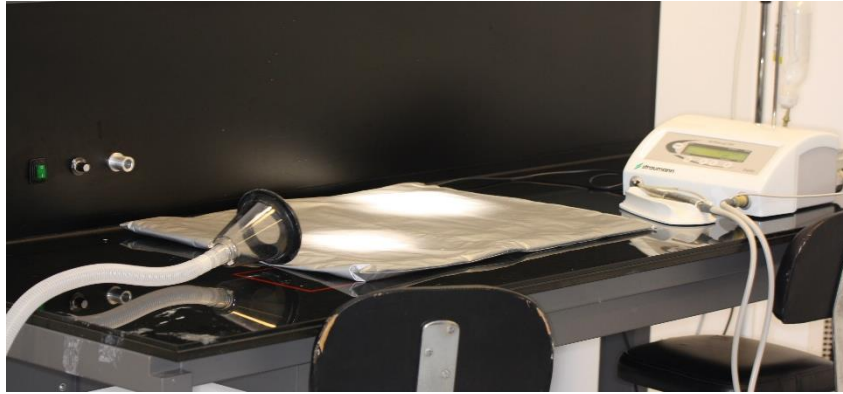


Figure 42 - Operation table featuring the implantology motor and the O₂ administration tube.

The following material was prepared for the surgical protocol (Figure 43):

- ✓ 48 Megagen Anyridge® implants with 4 x 7 in 3 groups of surface coatings (HA, F 0.1, F0.01)
- ✓ Carpul for local anesthetics
- ✓ Scalpel and number 15 blades
- ✓ Periosteal elevators
- ✓ Trays
- ✓ Implant handpiece motor from NSK® and serum
- ✓ Megagen® surgical kit
- ✓ Needle holder and scissors
- ✓ Absorbable sutures 4.0
- ✓ Gauze



Figure 43 - Implant Megagen® System surgical Kit and surgical instruments used.

Following the validation of the anesthetic plane, trichotomy was conducted on both legs that were aseptically prepared for surgery upon povidone iodine alcoholic solution disinfection (Figure 44).

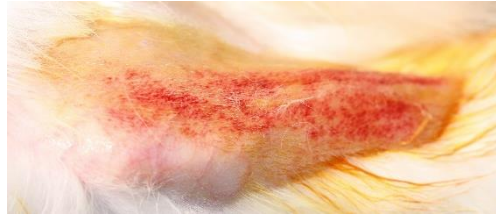


Figure 44 - Trichotomy for surgery.

Mepivacaine 3% (Scandinibsa, Inibsa) was infiltrated around the incision area and an anteromedial approach to the proximal tibia was conducted (Figure 45).



Figure 45 - Mepivacaine 3% infiltration.

Following, an approximately 4 cm full-thickness incision was conducted, and, upon careful periosteum elevation, with no release incisions, the tibial bone surface was exposed (Figure 46).

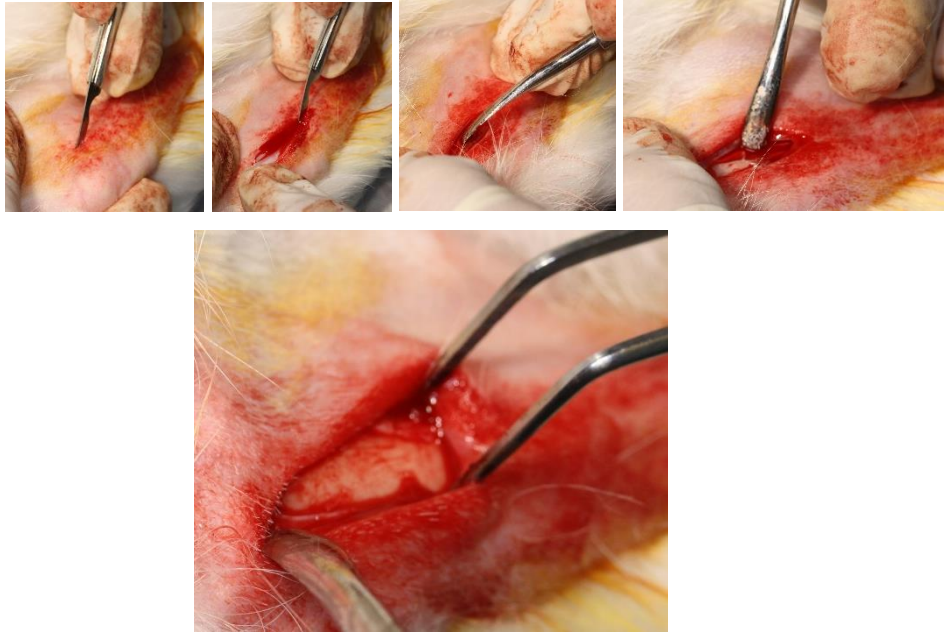


Figure 46 - Incision, full thickness flap elevation, and exposed bone surface from the surgical area.

Bone drilling protocol was established as recommended by the manufacturer – lance drill, followed by 2.0, 2.8, 3.2, and 3.8 mm in diameter drills, marked at 7 mm, with the recommended torque values for the Megagen® Anyridge® 4x7 implants. Implants were placed using the handpiece connector, at a 30 Nm torque, and with more than 1.5 mm in between. No cover screws were used, and the implants were completely submerged under soft tissue (Figure 47).

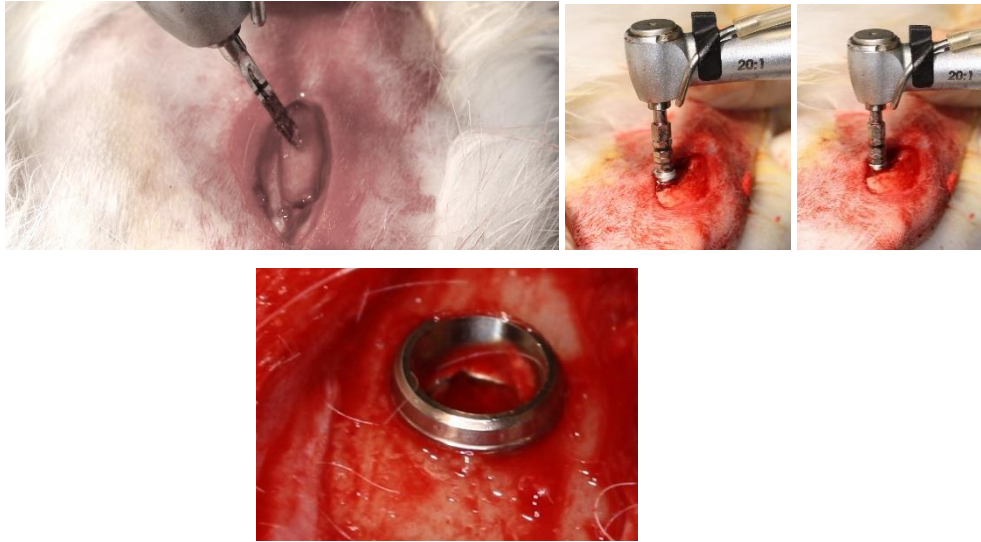


Figure 47 - Bone drilling protocol and implant placement examples.

The soft tissues were then closed in layers with absorbable sutures – 3 simple sutures for the periosteum closure, and 6-8 simple sutures for cutaneous suturing. A topical cleaning of the surgical site was then achieved with a povidone-iodine alcoholic solution, and the animals were then transported back for general anesthetic reversion and post-op medication (Figure 48).

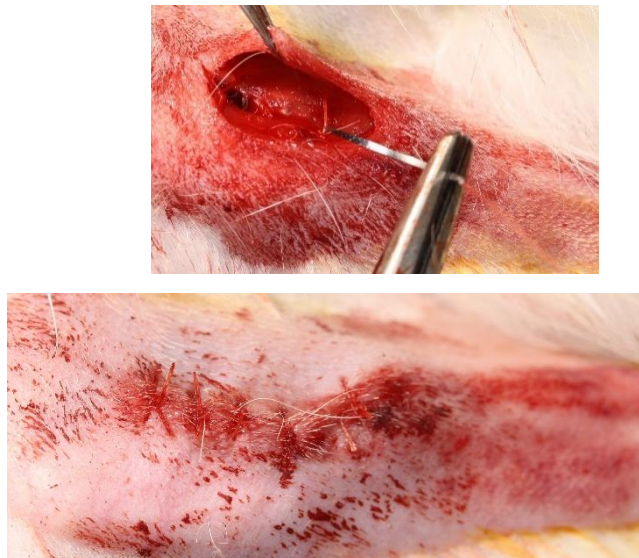


Figure 48 - Soft tissue suturing in layers.

During the postoperative recovery, animals were allowed to move freely and were routinely monitored for behavioral and physiological alterations. The biological response to the placed implants was evaluated through microtomography, focusing on the bone formation process in the vicinity of the implants. A representative scheme of the study overview is following presented (Figure 49).

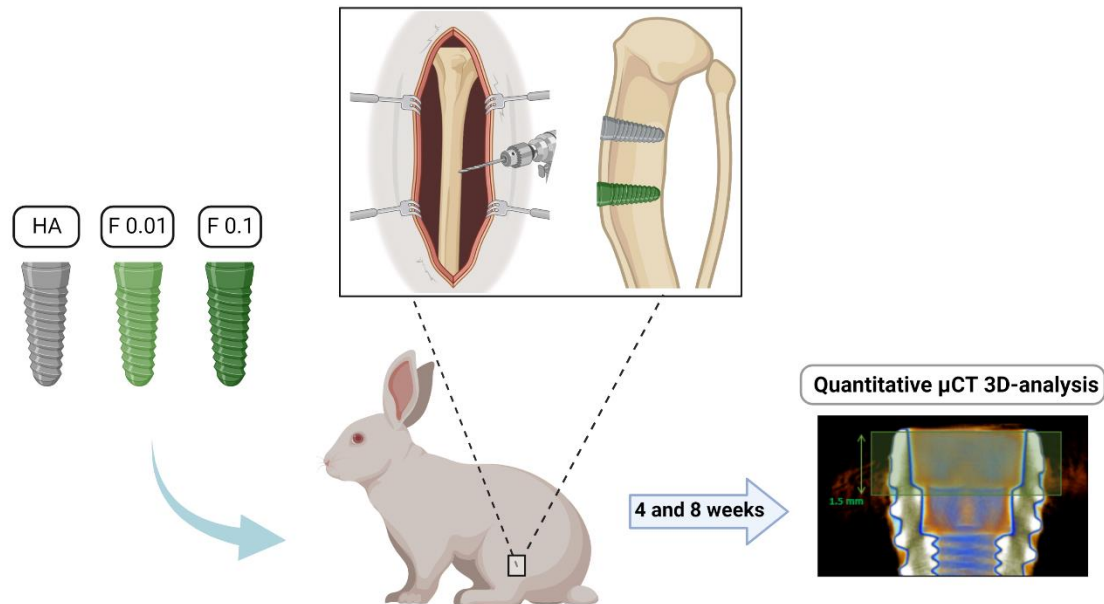


Figure 49 - Biological characterization schematization – in vivo assays.

3.3.3 – Microtomographic evaluation

At 4 and 8 weeks upon implantation, animals were euthanized. Tibiae were dissected, fixed in alcohol, and scanned using a Skyscan 1276 system (Bruker, Kontich, Belgium) at 100 kV, 200 uA, using an aluminum/copper filter and a resolution of 10 μm. The scans were performed with a 360° rotation, setting a rotation step of 0.2° and a framing averaging of eight.

The reconstruction of the obtained projection images was performed with the NRecon software (Bruker, version 1.7.4.2) with fixing parameters such as beam hardening (16%), ring artifact reduction (0), and minimum/maximum for CS to image conversion of 0.0 to 0.07. Subsequently, implants were aligned along the coronal axis

and isolated from each other using DataViewer software (Bruker, version 1.5.6.3). Three-dimensional images were obtained using CTVox software (Bruker, version 3.3.0).

Morphological analysis of the bone around implants was performed using the CTAnalyser software (Bruker, version 1.17.7.2) following the guidelines from Bruker. Briefly, an anatomical reference was selected in the upper portion of the implant, and a fixed height of 1.5 mm was set. Then, the implants were isolated from the bone and other anatomical structures by binary selection, and a ring of 20 pixels of thickness was drawn around the implant frame, to define the region of interest (ROI). Finally, the images were reloaded, and binary thresholding was set to isolate the implant and the bone from the rest of the anatomical structures. The defined bone inside the ROI was analyzed:

1. three-dimensionally:
 - a. Bone volume (BV),
 - b. bone volume fraction (BV/TV),
 - c. bone surface (BS).
2. as well as bi-dimensionally:
 - a. bone-to-implant contact, calculated as the percent intersection surface (TIS/TS) – the ratio between total intersection surface (TIS), and total surface (TS).

3.4 – Statistical analysis

Statistical analysis was conducted on the SPSS software (SPSS Statistics 27, Chicago, IL, USA). Quantitative data are expressed as mean \pm standard deviation (SD). Kruskal-Wallis nonparametric test was used and differences between groups were considered to be significant for $p < 0.05$.

IV. Results

"You control your destiny -- you don't need magic to do it. And there are no magical shortcuts to solving your problems."

Merida, Brave

4.1 – Coating preparation and characterization

Figure 50, Figure 51, and Figure 52 show representative images of scanning electron microscopy analysis reporting the surface morphology of HA-, F 0.01-, and F 0.1-coated titanium implants, respectively.

The HA coating presents a rod-like morphology (Figure 50), completely covering the surface of the TI substrate.

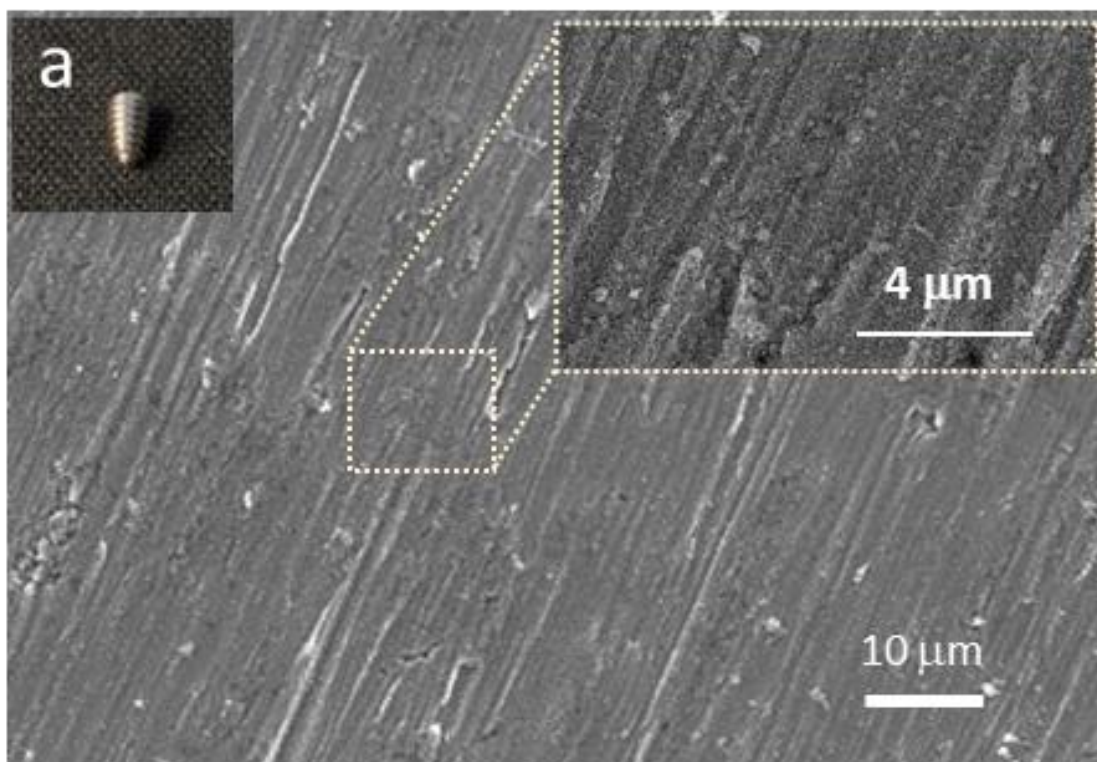


Figure 50 – Representative SEM images of the surface of the HA coatings obtained by the hydrothermal method (a). Inset corresponds to a high magnification area of the defined region.

On the other hand, F 0.01 reveals a uniform F-distributed coating with a “mud-like” morphology, completely covering the titanium surface, without evidence of porosity or discontinuities (Figure 51).

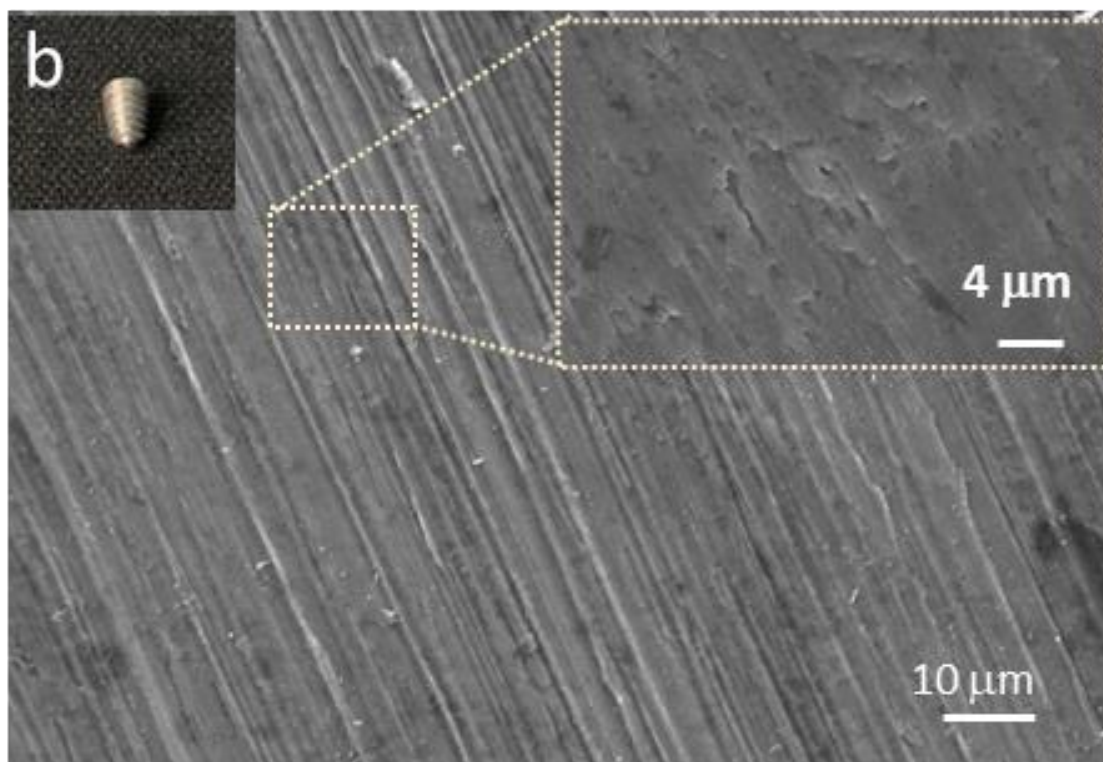


Figure 51 – Representative SEM images of the surfaces of the F 0.01 coatings obtained by the hydrothermal method (b). Inset corresponds to a high magnification area of the defined region.

Comparatively, a morphology change was observed on the surface of F 0.1 (Figure 52 and Figure 53), in which individual and aggregated F particles were observed in a homogeneous “dumbbell-like” morphology, further aligned parallelly to the

substrate surface. The average length of the “dumbbell-like” particles was determined by TEM and found to be within the range of 650 ± 20 nm by 250 ± 10 nm (inset Figure 53).

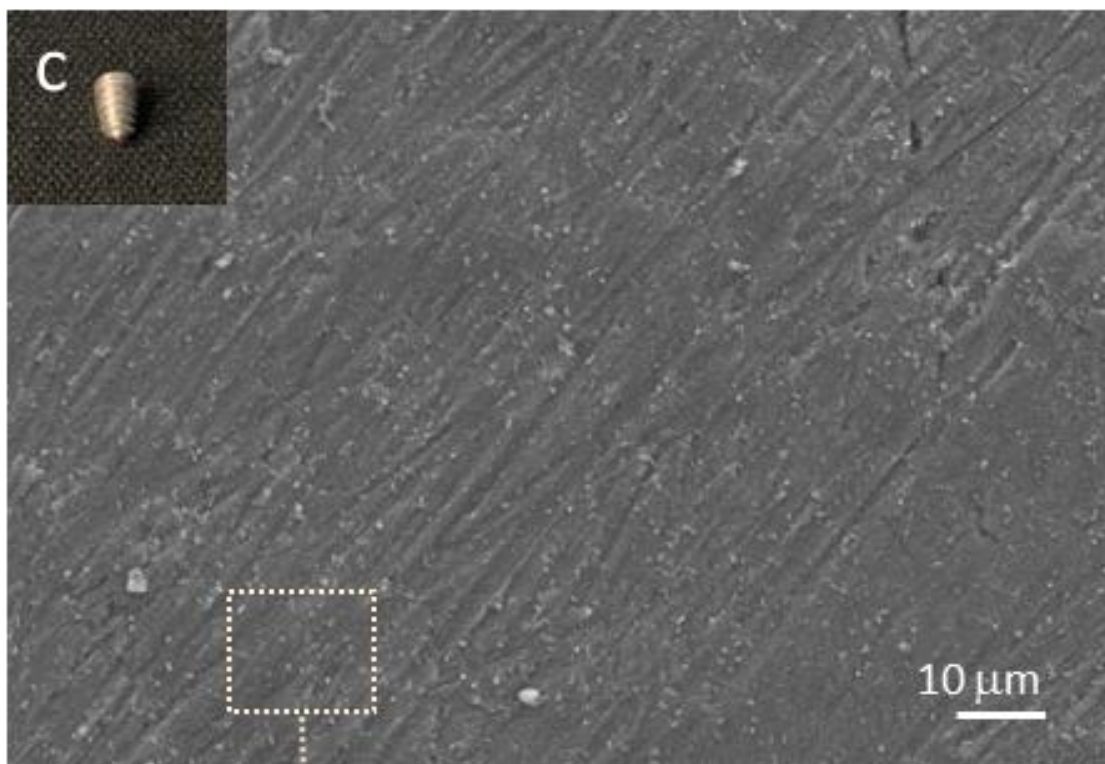


Figure 52 – Representative SEM images of the surfaces of the F 0.1 coatings obtained by the hydrothermal method (c).

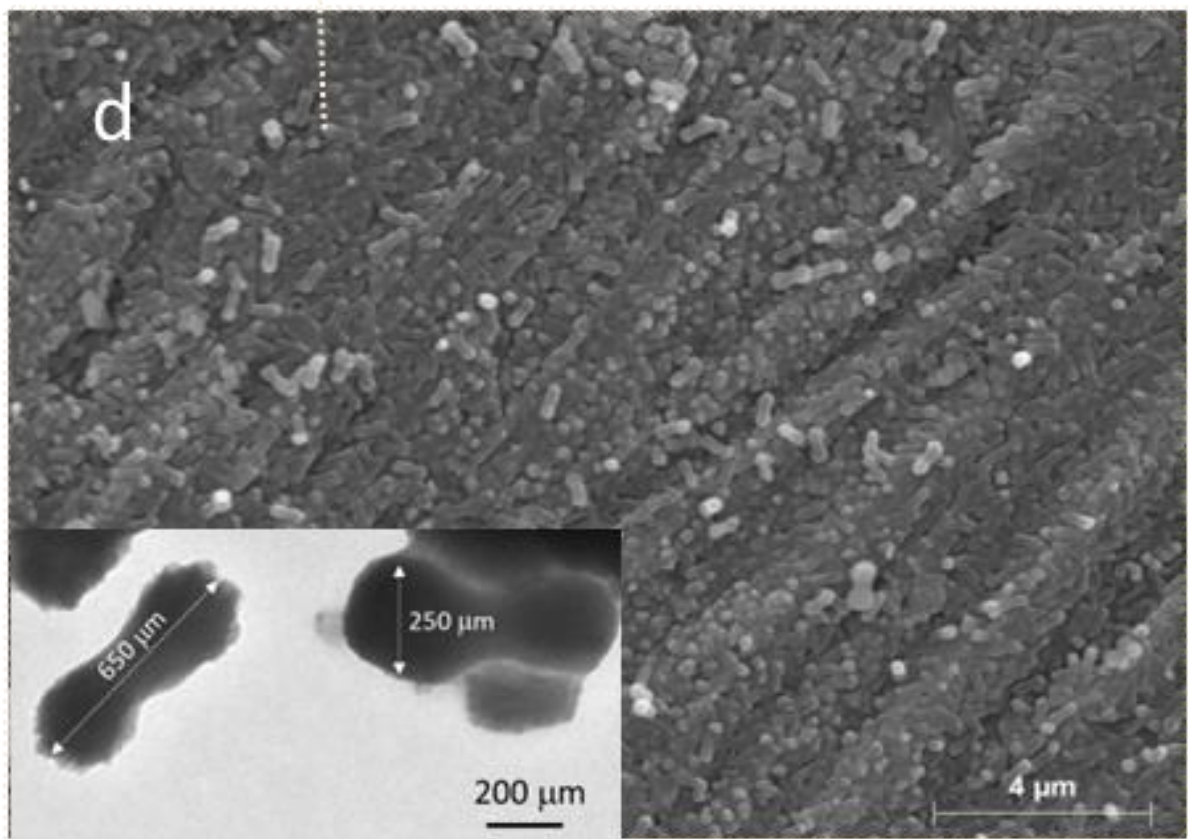


Figure 53 - Magnified SEM image of F 0.1 (corresponding to the square area in figure 52 (c)). Inset shows a representative TEM image of the F 0.1 coating particles, displaying representative measurements.

For a detailed elemental characterization, EDS mapping analyses were performed on the F 0.1 coating (Figure 54), and EDS analyses on F 0.01 and HA coatings.

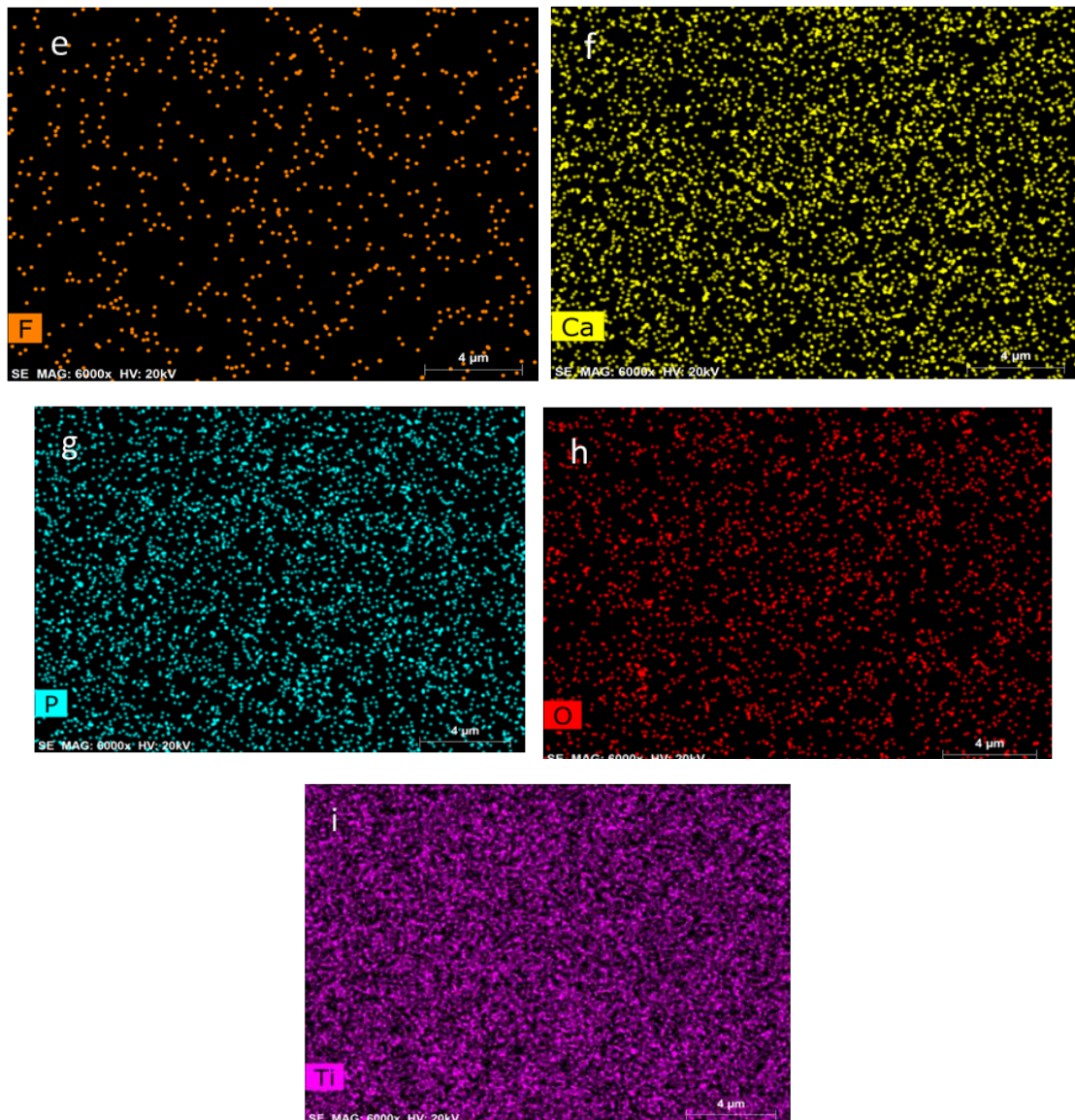


Figure 54 - EDS elemental mapping images for F (e), Ca (f), P (g), O (h), and Ti (i) of the F 0.1 coating surface.

The obtained results revealed that fluorine (F) (Figure 54e), calcium (Ca) (Figure 54f), phosphorus (P) (Figure 54g), oxygen (O) (Figure 54h), and titanium (Ti) (Figure 54i) elements were homogeneously distributed over the coated implant surface.

The relative fluoride content of each of the two coatings (F 0.01 and F 0.1), measured by EDS, revealed that the atomic percentage of fluorine (F) ions increase from 0.7% on the F 0.01 coating, to 5.08% on the F 0.1.

In addition, ATR-FTIR analyses were performed, to disclose F interactions within the coating surface (Figure 55). Absorption bands at 1053 and 1096 cm^{-1} assigned to stretching vibration of the phosphate groups were detected in the ATR-FTIR spectrum of F 0.01 and F 0.1 (Figure 55).

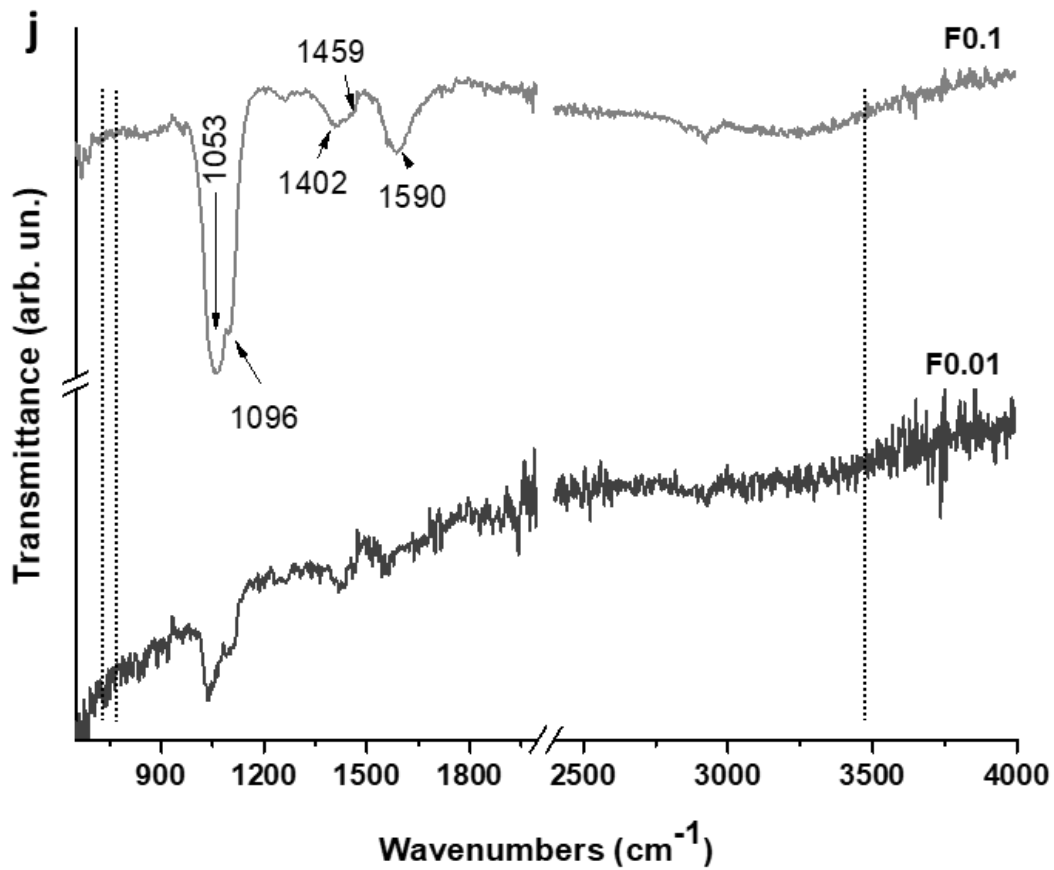


Figure 55 - ATR-FTIR spectra of the F 0.01 and F 0.1 coatings (j).

To validate the presence of the fingerprint peak of fluorapatite structure, XPS analyses were performed, and the results are shown in Figure 56.

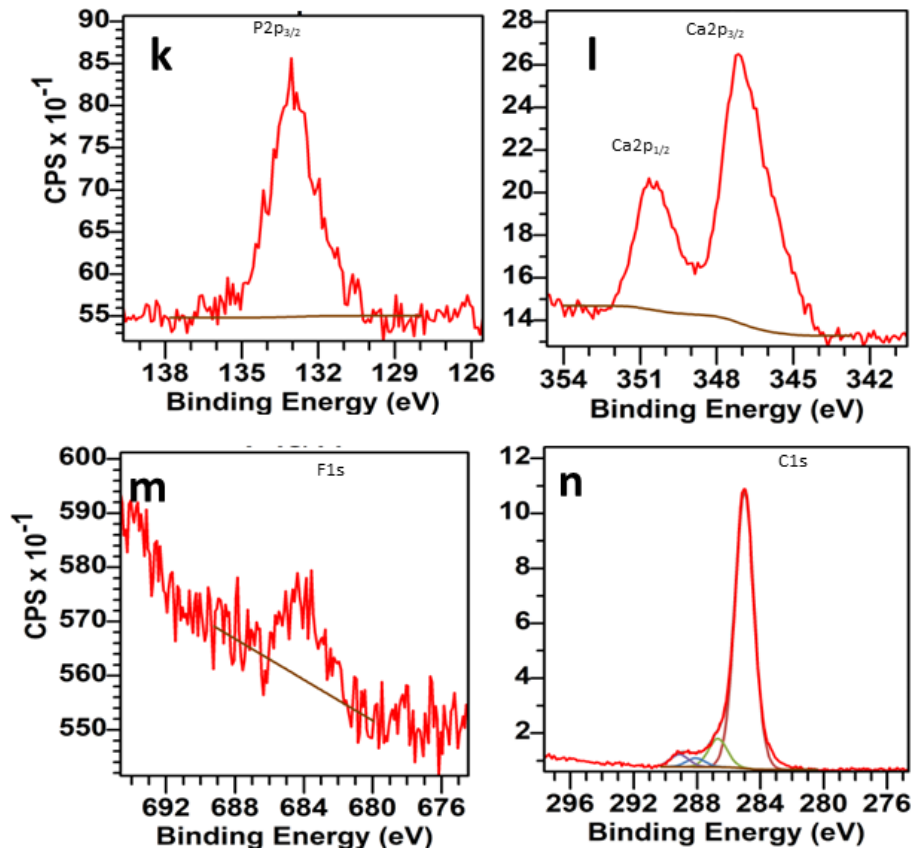


Figure 56 - XPS of the F 0.1 coating: (k) P 2p, (l) Ca 2p, (m) F 1s (n) C 1s.

4.2 – Biological evaluation

The biological characterization of the developed fluorapatite coatings was assayed *in vitro*, upon the assessment of osteogenic-induced human mesenchymal stromal cell cultures, and *in vivo*, upon the implantation of the developed constructs (coated implants) within an orthotopic translational experimental model - the rabbit's proximal tibia.

4.2.1 – *In vitro* evaluation - Human mesenchymal stromal cell response to the developed coatings

Assessment of the metabolic activity on day 1 revealed that all the materials allowed the adhesion of viable cells, with no significant differences between conditions.

The metabolic activity of the seeded cell populations increased throughout the culture period, up to 21 days, for all the assayed conditions. Comparatively, from day 7 onwards, F 0.01 and F 0.1 conditions presented significantly higher values than those of HA. Likewise, on day 14 and 21, F 0.1-coated substrates presented significantly higher resazurin reduction levels than those of F 0.01-coated substrates (Figure 57).

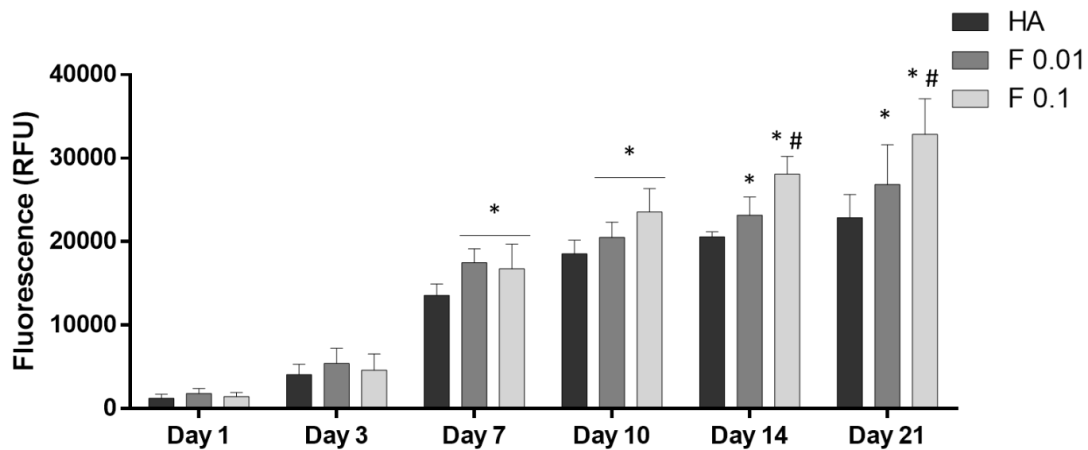


Figure 57 - Metabolic activity of human mesenchymal stromal cell cultures established over HA-, F 0.01-, and F 0.1-coated substrates for 21 days.

Scanning electron microscopy observation allowed to disclose the development and organization of the established cell culture, as well as the cell-substrate interactions. Low-magnification images of day 10 (Figure 58) revealed a thorough and organized cell layer covering the entire surface of the seeded materials. Comparatively, the structured cell layers appear to be more compact on F-containing substrates (F 0.01 and F 0.1), further evidencing some areas of detachment, that may elapse from the increased cellular density - in line with the increased metabolic activity data, attained on day 10 of culture.

Micrographs from day 21 (Figure 59) revealed a similar trend, with a higher cell density over both F 0.01 and F 0.1 coatings. High magnification images further allow the disclosure of the cell arrangement in a rich fibrillar matrix, in which mineralized deposits could be identified in close association with the cell layer. The deposits seem to be particularly abundant and more exuberant in the cultures grown over the F 0.1 coating.

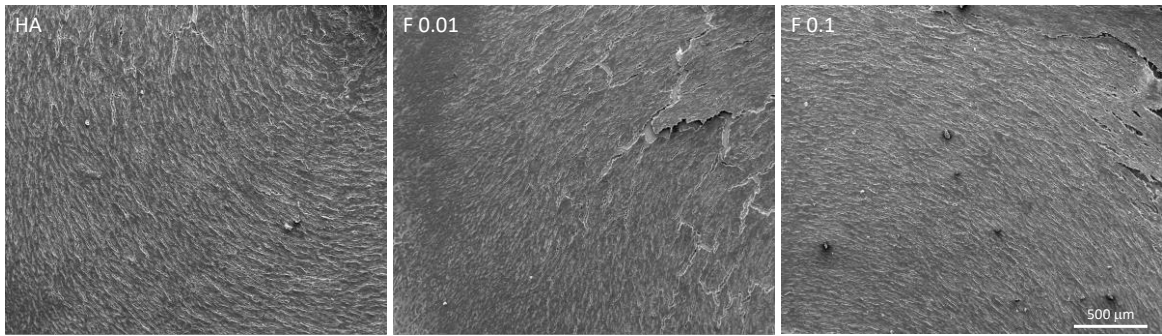


Figure 58 – Representative SEM micrographs of human mesenchymal stromal cell cultures established over HA-, F 0.01-, and F 0.1-coated substrates for 10 days.

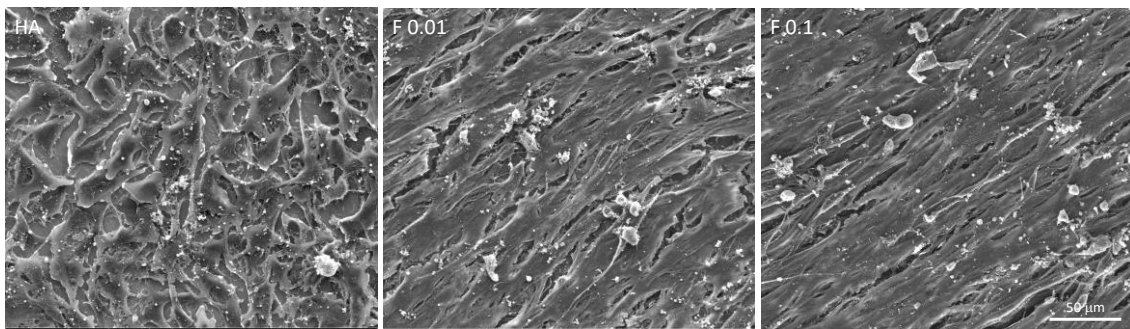


Figure 59 – Representative SEM micrographs of human mesenchymal stromal cell cultures established over HA-, F 0.01-, and F 0.1-coated substrates for 21 days.

4.2.2 - *In vivo* evaluation – Bone tissue response to the developed coatings, in a rabbit model

The biological response to the developed implant-coated constructs, upon orthotopic implantation in the rabbits' tibia, was characterized through microtomography (Figure 60 and Figure 61). This technique allowed the analysis of bone tissue 3D parameters - such as bone volume (BV), bone volume ratio (BV/TV); as well as 2D parameters such as bone surface (BS) and data regarding the direct interaction between the implant and the bone tissue, as the bone-to-implant contact (BIC).

To achieve high-quality histomorphometric data, proper data processing was conducted to minimize titanium-dependent imaging artifacts, following published information [121].

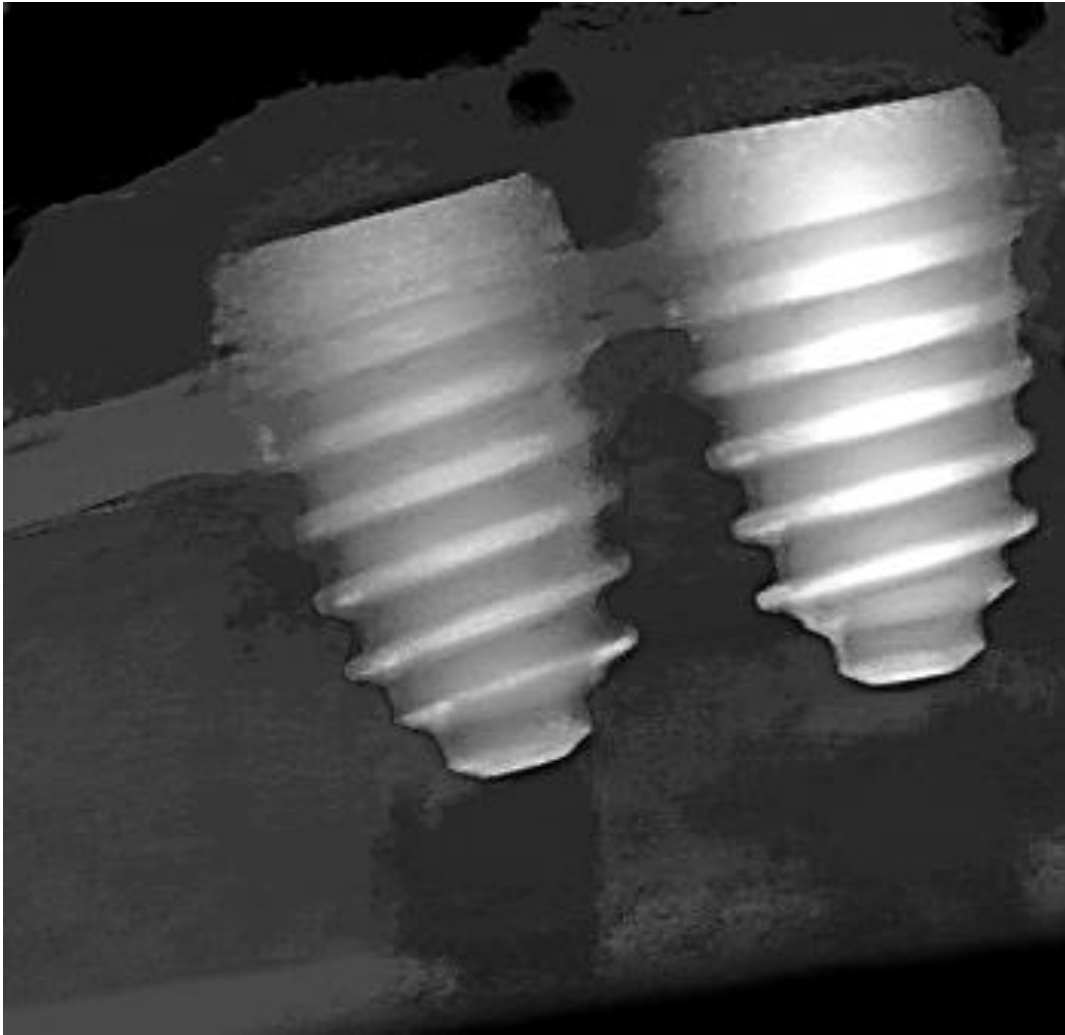


Figure 60 – Representative 3D microtomographic reconstruction of implants placed in the proximal tibia, on the 4 weeks' group.

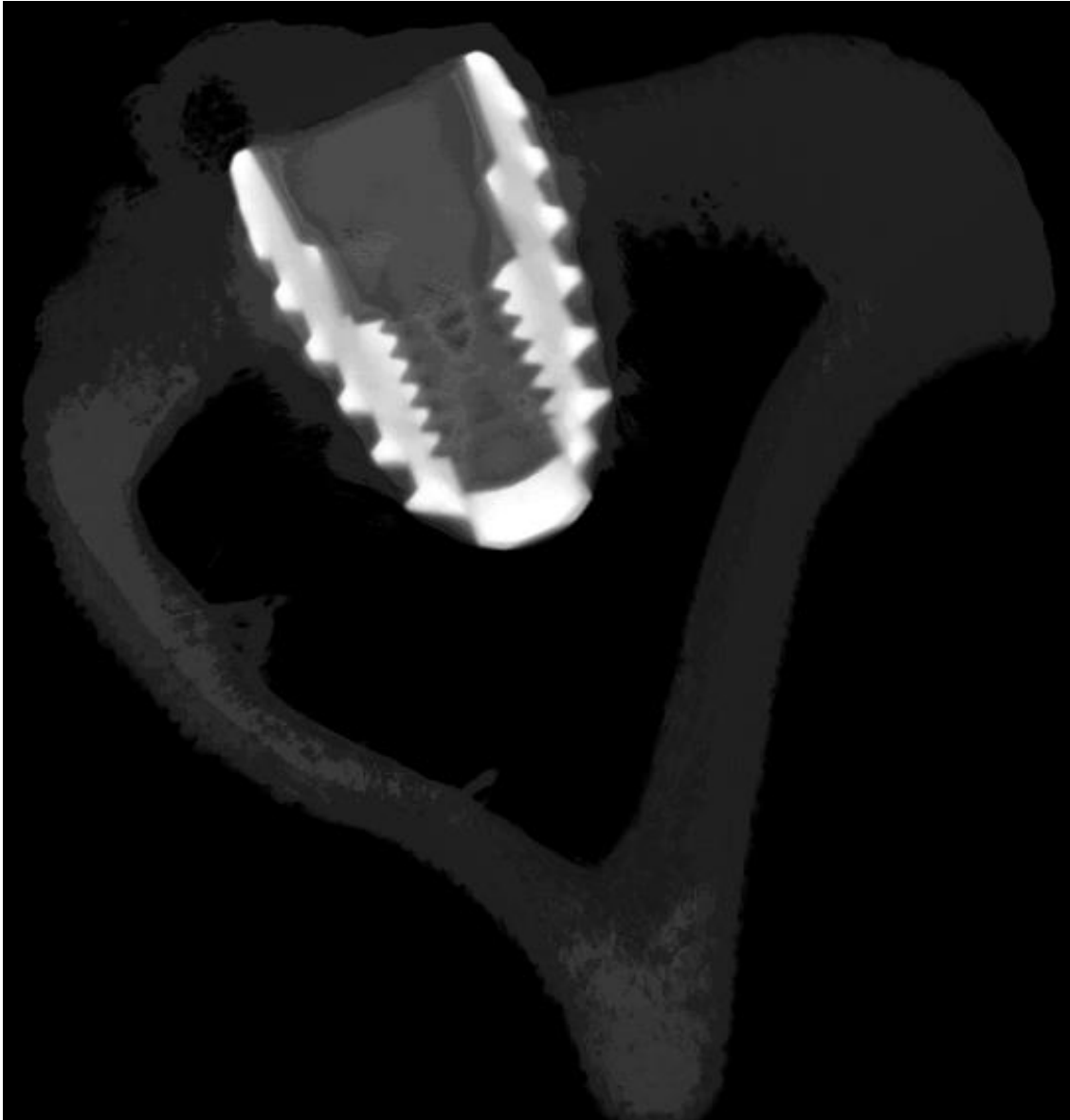


Figure 61 -- Representative microtomographic cross-section of an implant placed in the proximal tibia, on the 4 weeks' group, disclosing the bone-implant interface.

Biological outcomes were evaluated at two time points, 4 weeks, and 8 weeks.

All animals recovered adequately during the postoperative period without any complications. At euthanasia, no signs of clinical alterations (i.e., ulceration, inflammation, infection, or abnormal tissue formation) were disclosed within the surgical area, with implants remaining integrated *in situ*.

4 weeks

Sectional reconstructions of the microtomographic data revealed an established cortical bone structure at the coronal aspect of the implant, with newly formed bone tissue growing along the threads (Figure 62), for all the constructs' compositions.

Quantitative volumetric analysis (Figure 63) revealed, as compared to HA (control), a significantly higher BV for F 0.01 and F 0.1, with the latter being significantly higher than that of F 0.01. Also, F 0.1 presented a significantly higher BV/TV ratio, as compared to HA and F 0.01. In regards to BS, both fluorapatite compositions presented a significantly increased level, a trend similarly verified for the BIC analysis.

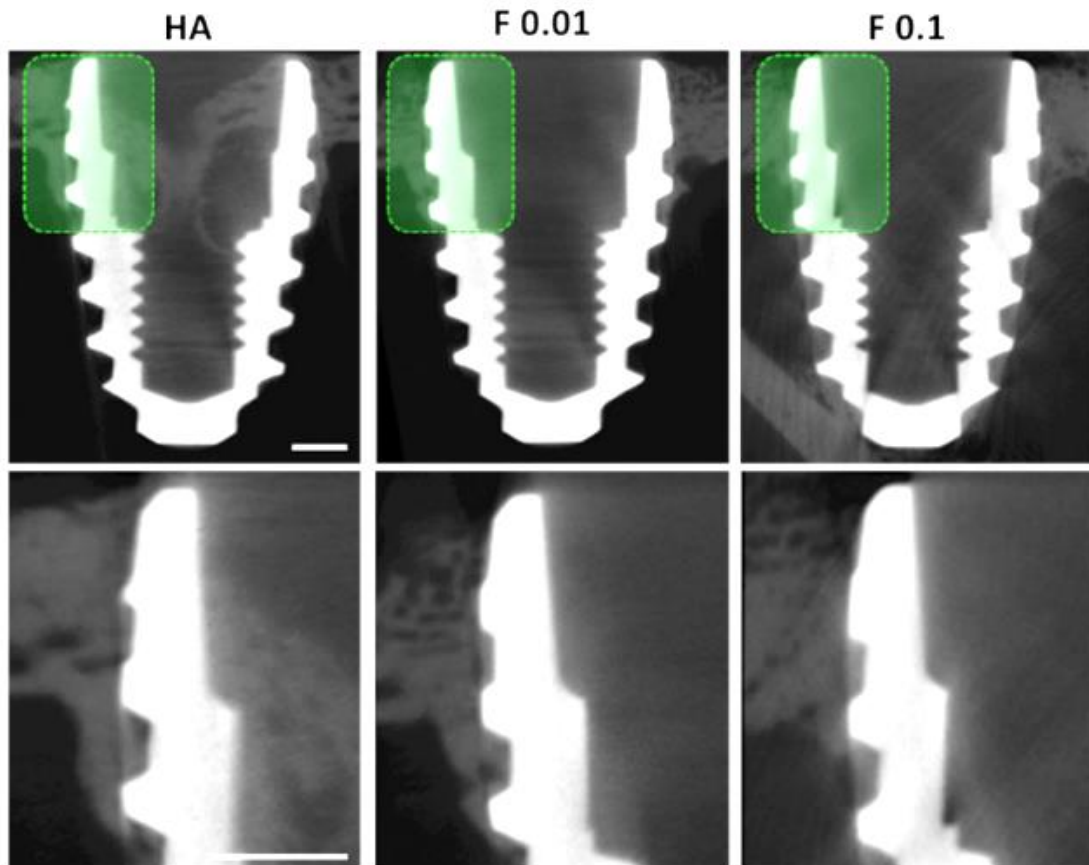


Figure 62 - Bi-dimensional microtomographic reconstructions of HA, F 0.01, and F 0.1 implants, at the 4 weeks' time point. Bottom images correspond to the inset areas of the top images. Scale bars correspond to 1 mm.

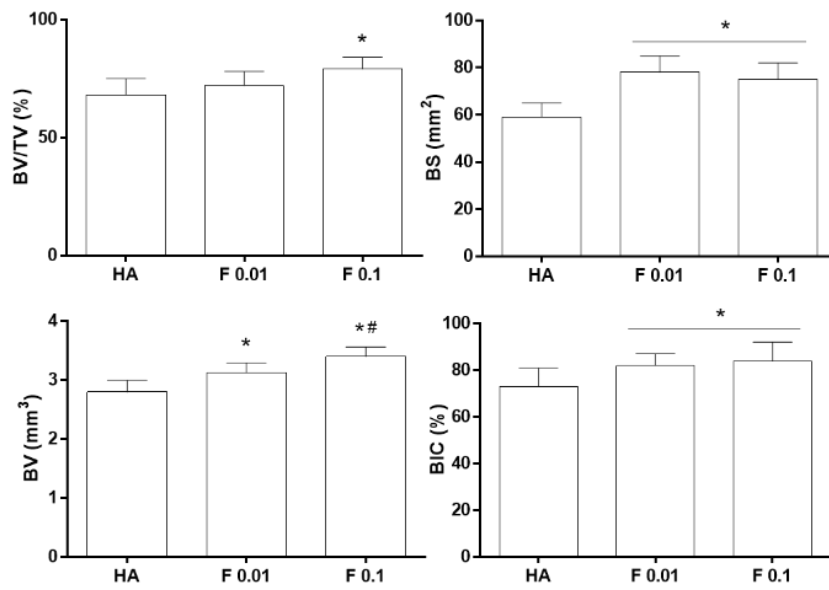


Figure 63 - Histomorphometric data of the coated constructs – HA, F 0.01, and F 0.1, at the 4 weeks' time point. $p < 0.05$; * significant different to control; # significant different to the other experimental group.

3D reconstructions (Figure 64) substantiate the attained morphometric findings, presenting an increased bone volume for fluorapatite-containing coatings, with augmented bone surface and, as well, an increased contact area with the implant.

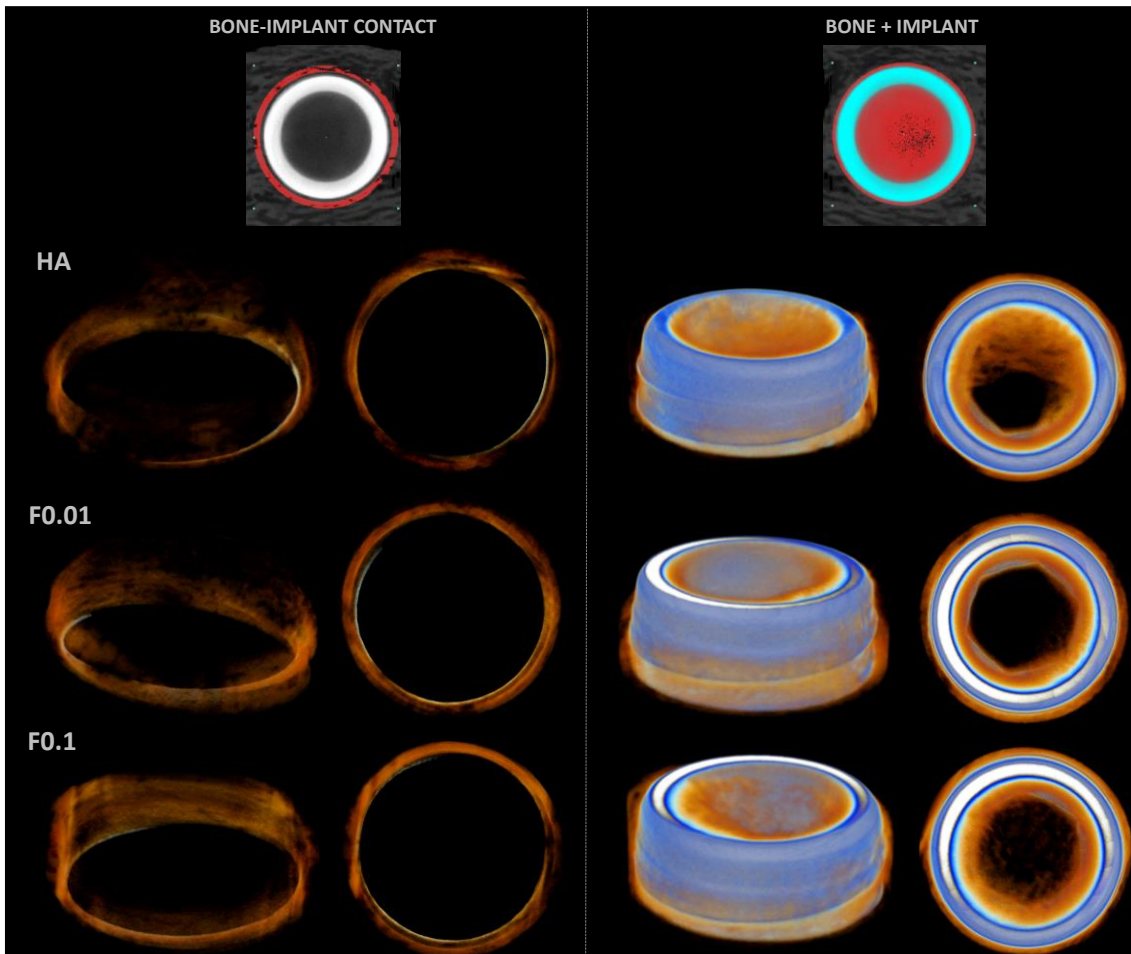


Figure 64 - Representative three-dimensional microtomographic reconstructions of the coated constructs – HA, F 0.01, and F 0.1, at the 4 weeks' time point.

8 weeks

A more advanced bone formation process was attained for all conditions, with increased bone levels at the most coronal region of the implants, extending apically along the implant surface (Figure 65).

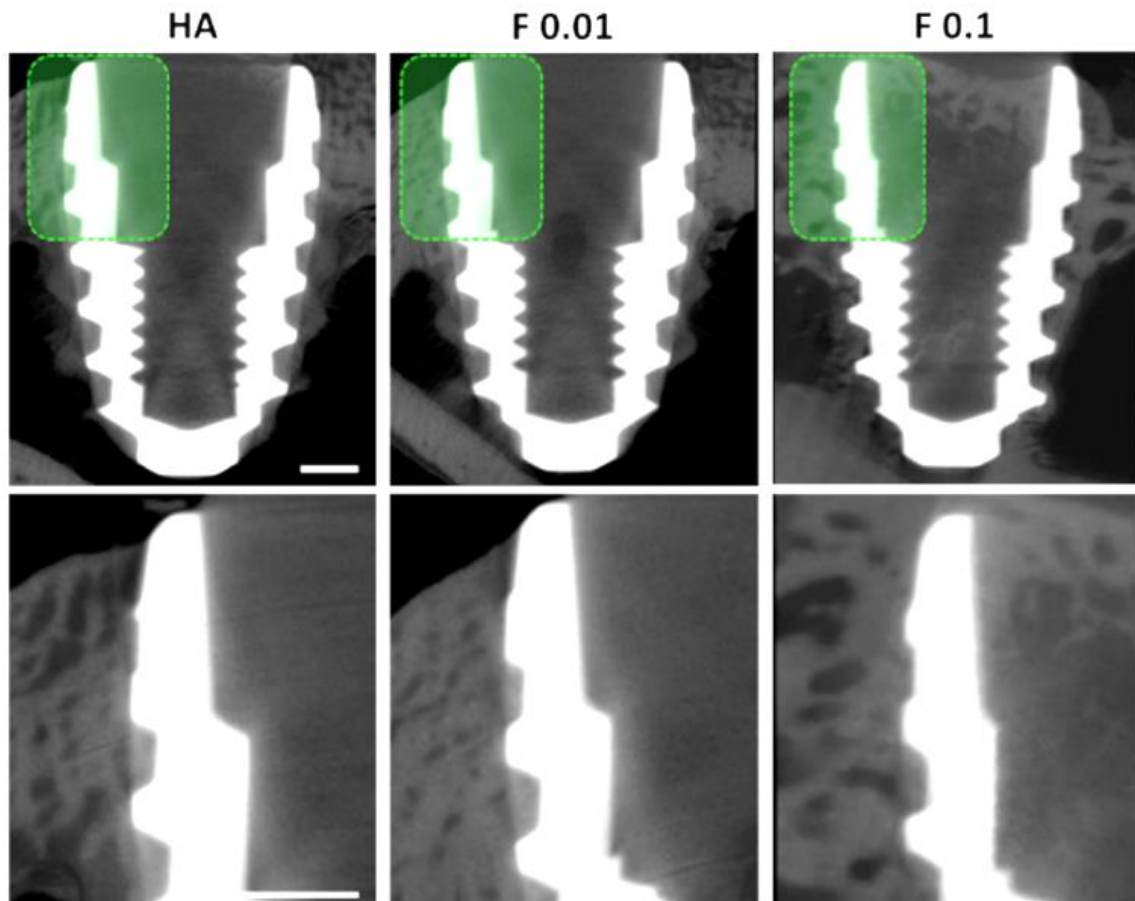


Figure 65 - Bi-dimensional microtomographic reconstructions of HA, F 0.01, and F 0.1 implants, at the 8 weeks' time point. Bottom images correspond to the inset areas of the top images. Scale bars correspond to 1 mm.

Morphometric data (Figure 66) revealed increased levels, as compared to data from the 4 weeks implantation time (Figure 63). Compared to HA, fluorapatite-containing coatings presented an increased BV and BS, and the F 0.1 formulation further presented an increased BV/TV. Also, the BIC was found to be significantly higher in both F 0.01 and F 0.1, despite the absence of differences between conditions.

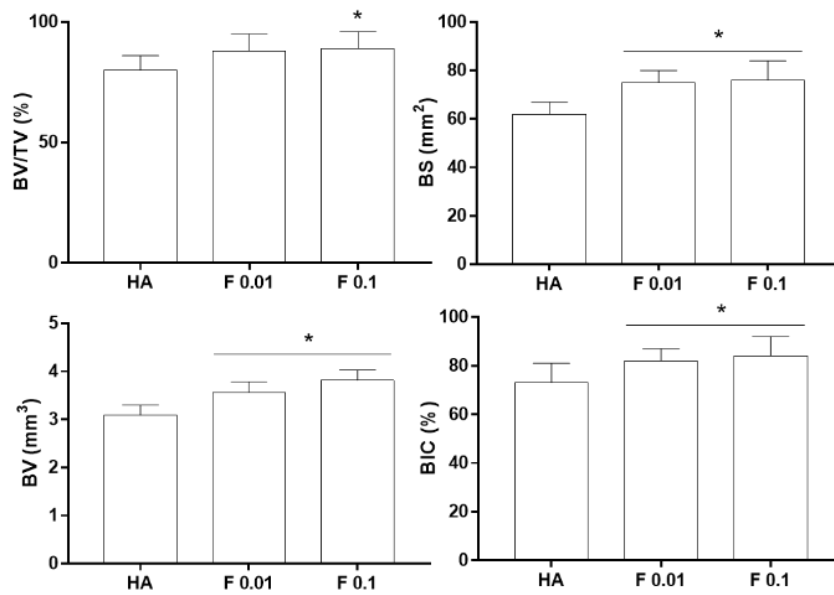


Figure 66 - Histomorphometric data of the coated constructs – HA, F 0.01, and F 0.1, at the 8 weeks time point. $p < 0.05$; * significant different to control.

The 3D reconstruction of the peri-implant regions at 8 weeks of healing (Figure 67) corroborates the described findings, with increased bone formation at the coronal region, particularly within fluorapatite coatings, suggesting an increased mineralized tissue volume and increased surficial intersection with the implant surface.

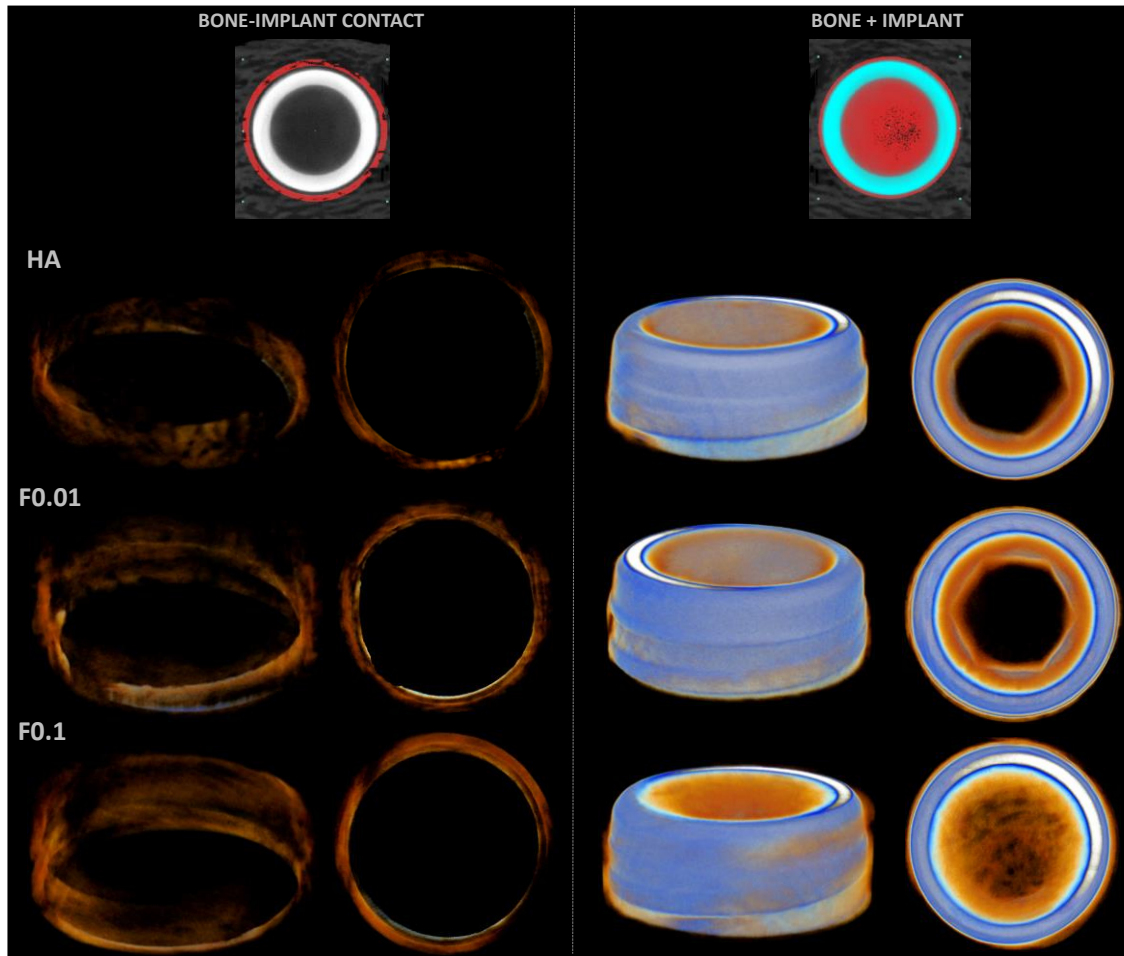


Figure 67 - Representative three-dimensional microtomographic reconstructions of the coated constructs – HA, F 0.01, and F 0.1, at the 8 weeks' time point.

V. *Discussion*

"Sometimes the right path is not the easiest one."

Grandmother Willow, Pocahontas

The influence of topographical characteristics on a micrometric and nanometric level, on the surface of dental implants, is of clear relevance for the modulation of cellular behavior and consequently, to the biological outcome [78, 122-124]. Investigations are still far from determining the most adequate and flawless implant surfaces, with the best selective bifunctionality and selectiveness for each specific tissue of the biological interface [122, 123]. Accordingly, manufacturing complex surfaces, with nanotopographies and stable homogeneous coatings is still a technical challenge [122], and this indicates the need for further investigations like the present one.

5.1 - Dental implants

The choice of dental implants used in this investigation was based on some criteria:

- Megagen Anyridge® is an extensively studied implant, with good clinical results, confirmed by literature [108, 125-127], and familiar to the author, which decreases the possibility of an error during the surgical protocol.
- It also uses the hydrothermal method for coating the titanium grade 4 implants, to achieve a calcium phosphate-coated surface [128]. This way the same method would be used for the surface treatment, knowing that it has been used with success in that implant macrotopography.
- Used implants are 7mm long by 4mm wide, which are suggested dimensions to be used in the implantation of the rabbit tibia [129].

5.2 - Coating methodology - the hydrothermal method

In this work, the hydrothermal method was used for coating dental implants. This method was chosen keeping in mind that it overcomes difficulties encountered in other methods, like plasma-sprayed, such as structural and phase discrepancies, thick depositions (30-100 μm), deposition of highly crystalline bioceramics, and non-uniform

coatings, which converge to reduce the bifunctionality and implant-surface coating interfacial strength [74, 93, 99]. The hydrothermal method is [73, 74, 100]:

- Simple;
- Scalable to larger mass production;
- Cost-effective;
- Environmentally friendly;
- Versatile;
- Produces a homogeneous coating on complex-shaped substrates like dental implants;
- Produces a well-defined composition coating;
- Produces a coating with crystallinity similar to the one of the bone tissue;

As mentioned before, a homogeneous coating over the implant also allows for a homogeneous and predictable biological response all around the implant surface [72]. Also, keeping a well-defined composition allows for determining specific concentrations of elements that are being studied, such as fluorine, further eliciting a predictable response. The crystallinity obtained by this method, being similar to the one of the bone tissue, is advantageous to maintain similar conditions on both sides of the interface, so that cell proliferation and bone formation develop within a familiar environment [72].

5.3 - Fluor and fluorapatite coating

As stated above and by previous studies, hydroxyapatite has limited bioactivity and its biological properties may be enhanced, particularly in dental implants' coating applications [78, 114, 130]. To achieve this, literature has shown that the addition of fluoride to the hydroxyapatite lattice is a way to [109]:

- induce bioactivity;
- increase the density of the bioceramic;
- reduce the solubility of the bioceramic.

Fluoride, therefore, seems to improve the biological response within the bone tissue through the ionic release, capable of increasing osteoblastic proliferation and differentiation [110, 111]. Fluoride may act on calcium phosphate coatings by direct substitution [131]. This and may lead to the promotion of human stem cell proliferation and differentiation, with higher levels of bone morphogenic protein-2 (BMP-2), RUNX2, and bone sialoprotein expression [131].

However, fluoride content needs to be precisely balanced within the materials' composition, as a high fluoride release may be cytotoxic to bone cells and ultimately impair the bone healing /regeneration process [110, 112]. The importance of a preliminary *in vitro* study, for biological validation, was a demand. It was enough to understand possibly toxic levels of fluor on living cells, safe doses, and its potential behavior on human tissue.

The toxic action of fluoride resides in the fact that fluoride ions act as enzymatic poisons, inhibiting enzyme activities and, ultimately, interrupting metabolic processes [132]. However, some enzymes (e.g., adenylyl cyclase, glycogen phosphorylase, and more) are stimulated by fluoride if present in millimolar concentrations [132]. Fluoride in humans probably will not reach concentrations used in laboratory studies with isolated cells/tissues, but there may be moments when fluoride ions reach microenvironments in which interferences may occur, especially at the active sites of certain enzymes [132]. In a more general and embracing look at the bone tissue, it is suggested that the effects of fluoride on bone quality depend on the balance between the favorable effects and undesirable effects, affected by daily doses and the duration of fluoride administration/release, and the amount of fluoride reaching the bone microenvironment [132]. Analyzing fluoride's impact on bone, it is shown that different effects are attained in different parts of the tissue [132]. Briefly, fluoride administration seems to increase the bone mineral density of trabecular bone (important for example, for weight bearing) and decrease the bone mineral density of cortical bone, the outside layer of the bone, important for resistance to torsional and sheer stress [132]. World Health Organization in 2002, indicated that for a total intake of 14 mg/day, there would be a risk of skeletal adverse effects [132]. Fluor is therefore likely to be associated to an increased risk of effects on the skeleton at total fluoride intakes above about 6 mg/day

[132]. According to this information, it is unlikely that the levels of fluor used on the implant coating would have toxic effects, either locally or systemically, and it is likely beneficial to biological responses at the molecular level [130].

In this study, the formation of fluorapatite via hydroxyl substitution was therefore evaluated, and two different morphologies with distinct fluoride concentrations were compared to a hydroxyapatite coating.

The solution used in the hydrothermal method contained several components, each with a specific function. The first element was citric acid used so that it could tailor the coating morphology – aiming to promote osteogenesis by the presence of its citrates, discussed in detail below [100]. The second element is calcium nitrate added to help adjust the pH of the solution, together with ammonia [100]. The pH should be kept at around 8 because, in a more acidic environment, the coating changes its characteristics [100]. The formation of a fluorapatite coating introduces calcium in the coating composition, so it also becomes a connection for the phosphate group and accelerates the osseointegration process [100]. For the production of a hydroxyapatite coating, the third added element is ammonium hydrophosphate, but for the fluorapatite coating, ammonium fluoride was the added component. This introduced fluoride ions to this process. The implants placed at the beginning of the process in the autoclave were washed with ethanol to remove any debris or the possibility of contamination particles, and then washed with water to remove the ethanol so that it does not react and originate oxide formations, that would *per se* react with the ions [100]. A preliminary study was performed previously, to adjust the conditions of the method [117].

5.4 - Coating preparation and characterization

SEM is the most used method for morphology characterization at micrometric levels, and it helps to identify the composition elements of the structures [59].

As seen in the results, Figure 50, Figure 51, and Figure 52 exhibit morphologies found for HA-, F 0.01-, and F 0.1-coated titanium implants, respectively. The HA coating presents a typical rod-like morphology, as described in the literature (Figure 50) [100]. F 0.01 reveals a uniformly F-distributed coating with a “mud-like” morphology, completely covering the titanium surface, without evidence of porosity or discontinuities (Figure 51). This homogeneity is important for stable characteristics throughout all implant surfaces, allowing the achievement of a similar biological outcome and response around the entire surface of the implant [72].

A morphology change was observed on the surface of F 0.1 (Figure 52) - individual and aggregated F particles were observed in a homogeneous “dumbbell-like” morphology, further aligned parallelly to the substrate surface (Figure 53). The average length of the “dumbbell-like” particles determined by TEM was around 650 ± 20 nm by 250 ± 10 nm (inset Figure 53). This observed morphology change can be attributed to a fractal growth of the fluorapatite particles (Figure 68), caused by the large dipolar field along the c axis of fluorapatite, provided by the presence of citrate ions in the precipitating medium [117, 118].

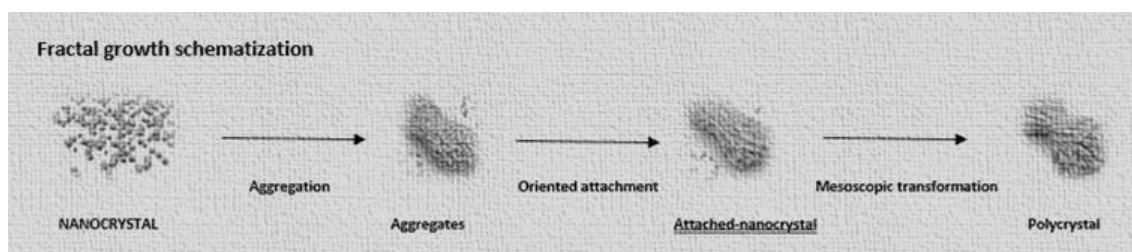


Figure 68 - Fractal growth schematization based on the information of Vidal et al and Wu et al [117, 118].

Considering the obtained results, it is reasonable to surmise that citrate molecules have a strong interaction with the fluorapatite particles' surface, and conditioned the final morphology of the coating. Moreover, it is known that fluoride ions have a higher affinity to occupy positions on the hydroxyapatite lattice in comparison to hydroxyl ions, which enhances thermodynamic stability and decreases the solubility and degradation of the coating. These modifications are expected to lead to more gradual

coating resorption, with the added reported benefit of increasing the differentiation behavior of osteoblastic cells and stimulating bone growth, when compared to HA coatings [109, 119, 133, 134].

To obtain a detailed elemental characterization, EDS mapping analyses were performed on the F 0.1 coating (Figure 54) and EDS analyses on F 0.01 and HA coating. As described in the results, fluorine (F) (Figure 54-e), calcium (Ca) (Figure 54-f), phosphorus (P) (Figure 54-g), oxygen (O) (Figure 54-h), and titanium (Ti) (Figure 54-i) were homogeneously distributed over the implant surface. The relative fluoride content of each of the two coatings (F 0.01 and F 0.1), measured by EDS, revealed that the atomic percentage of fluorine (F) ions increase from 0.7% in the F 0.01 coating to 5.08% in the F 0.1. This result indicates the successful incorporation of F into both hydroxyapatite coatings. In principle, fluoride ions should be incorporated through the ionic substitution of hydroxyl ions [135].

Based on the previous hypothesis, ATR-FTIR analyses were performed. This method is used to obtain the coating composition through the vibration of the several bands present in the coating.

Beforehand, it is important to note the main difference between absorption and adsorption - the first is a bulk material phenomenon, and what the surface absorbs, becomes part of the coating material [136, 137]. On the other hand, the adsorption phenomenon is the connection of molecules on the surface of the implant, and it refers to the external molecules that connect to the coating and may influence the biological response [136, 137]. In our study, there was no adsorption on the surface. The analysis was restricted to what was formed on the surface during the hydrothermal method.

The notable typical absorption bands at 1053 and 1096 cm^{-1} assigned to stretching vibration of the phosphate groups [117, 138] were detected in the ATR-FTIR spectrum of F 0.01 and F 0.1 (Figure 55). The absence of the characteristic hydroxyl bands at 632 cm^{-1} , 3571 cm^{-1} , and the presence of one additional band (due to the high concentration of fluorine at $\sim 740 \text{ cm}^{-1}$, usually attributed to the libration mode of the OH group connected with a fluorine ion by a hydrogen bond [109, 139]) suggests that the formed coating is composed by fluorapatite [115, 140, 141].

In addition, the absorption peaks at 1402 and 1590 cm^{-1} , and a small absorption peak at 1459 cm^{-1} , observed in the F 0.1 spectrum revealed the presence of carboxylate groups in the F coating, most probably coming from the citrate species [100]. In addition, according to ATR-FTIR results (Figure 55), the intensity of carboxylate and phosphates absorption peaks was increased by the F^- incorporation into the coating. In our previous results [100], it was found that only a weak band associated with carboxylic groups was observed on the HA coating, while for F-containing coatings, three bands were observed, which confirms that the coordination mode of the citrate species with the particles present in the titanium surface is dependent on the ionic composition of the precipitant medium. In this specific system, the presence of fluoride ions modifies the configuration of citrate species adsorbed, which could have a strong impact on the biological response [142]. Moreover, according to the literature, the presence of citrate in the precipitation medium is expected to enhance the substitution of OH^- by F^- , and accelerate the crystallization process [119].

To validate the presence of the fingerprint peak of the fluorapatite structure, XPS analyses were performed (Figure 56 k-n). XPS analysis is a chemical analysis to measure the connection energy between atoms.

It can be observed that all characteristic peaks of fluorapatite, P2p, and Ca2p, at 133.2 and 347.2 eV, respectively [143], were detected in the F 0.1 coating. Looking in detail, it can be observed one additional small peak at ~ 684.3 eV, belonging to F1s, indicates that F^- ions were incorporated into the fluorapatite lattice structure [144, 145].

The F/Ca ratio, calculated directly from the XPS data was $\text{F/Ca} = 0.182$. In stoichiometric fluorapatite $\text{Ca}_{10}(\text{PO}_4)_6\text{F}_2$ the F/Ca ratio should be, at maximum $2:10=0.2$. Considering the obtained ratio, it can be suggested that the produced fluorapatite is close to stoichiometry.

Furthermore, looking at the calculated Ca/P ratio (~ 1.83) it turns out that the ratio is higher than the stoichiometric value Ca/P ratio = 1.67 [144], which may be due to the presence of citrate species on the F-containing coatings. The presence of the citrate species was confirmed by the 3 fitted peaks, corresponding to C1s photoelectrons from carbon bonded to other carbon and/or hydrogen atoms, carbon

singly bonded to oxygen, and carbon in a carboxylate/carboxylic group [100]. Overall, from ATR-FTIR and XPS results, it can be confirmed that the developed F 0.1 coating is composed of fluorapatite.

One of the aims of using the fluorapatite was to try not to just have hydroxyapatite impregnated or loaded with fluor, but to have the fluorapatite on the coating. In some methods, the replacement is only partial [66]. To be able to achieve it, the OH group from the $\text{Ca}_5(\text{PO}_4)_3\text{OH}$ – hydroxyapatite – must be removed and replaced with fluor [100]. The way to validate this achievement can be accomplished with the analysis of the ATR-FTIR spectra of F 0.01 and F 0.1, as presented in Figure 55. If it was only partial, with fluor-doped hydroxyapatite, the band would appear near 3500 cm^{-1} [143]. Because this was not detected, the OH group has been eliminated.

Biological characterization

Cell culture models focus on the morphological aspect, growth capacity, and differentiation of cells on materials with various chemicals, compositions, and topography [124]. The importance of an *in vitro* study is, among other reasons, to determine if the fluor level to be used is safe and effective, and to acknowledge the biological response that it triggers [124]. Literature seems unclear as to the level of fluor that could become toxic. It usually reaches hand of *in vitro* studies to evaluate the cellular and tissue behavior and to complete the information of safety on animal studies, one rational approach would be trying to find the blood serum concentration of fluor that could indicate a potential risk for systemic effects [78]. Some *in vitro* studies addressed the fluor in percentages similar to that used in commercialized dental implants, with the atomic concentration of fluoride on titanium surface of around 0.45% - which is within the 0.3%–1% range of other studies in the same field [146]. At these concentrations, there is no toxicity [146-148].

Several *in vitro* studies have shown enhanced osteoblastic functionality with increased differentiation and osteogenesis [146, 149, 150]. Our results seem to be similar to the literature findings.

Regarding the *in vivo* study, the sample size was calculated based on the results of other similar studies, such as by Offermanns et al, and others [78, 114, 129], achieving a number of placed implants that would allow valid data to be compared between the 3 surfaces.

The biological characterization of the developed fluorapatite coatings was assayed in an *in vivo* translational model of the orthotopic implant placement, within the rabbit's proximal tibia. The animals chosen for this study were 8 12-month-old New Zealand White rabbits. These animals were chosen because the literature shows that for implant placements and osseointegration research, they are a common model and mimic submerged and unloaded healing conditions [78, 129]. They were 12-month-old, in adulthood, such as similar models used in literature, revealing skeletal maturity [78]. The rabbit has been a popular choice for the evaluation of biomaterials' biological response, reaching up to around one-third of the published literature on dental implant-related research [151]. Rabbits reach skeletal maturity at around 6 months of age, and given the fast bone turnover, they allow for an early evaluation of the bone tissue response [152].

In humans, to obtain and study osseointegration, the period of 3-6 months seems to be a necessary time [129]. In animal models, a shorter time is needed given the higher metabolic rate – 4 to 6 weeks, and authors usually evaluate 2, 4, 6, 8, and 12 weeks' time points to disclose distinct time points of the osseointegration process [129]. According to the increased metabolism in this animal model, it was determined that 4 weeks and 8 weeks would be good time points for the evaluation of the early osteointegration and process of bone formation in the early stages, according to the literature [78, 114, 129].

The rabbit tibia was used in this model, and because it is essentially a hollow bone, except for the upper and lower cortical plates and some minor trabecular structure, it could show a lack of bone apposition [129]. Even so, bone apposition was shown in this study, which demonstrated the high osteogenic capacity of the studied coatings.

Tibial implantation permits an adequate bone volume for the surgical placement of up to 3 clinically relevant implants per side, within the range of 3 to 4 mm diameter and length up to 10 mm, allowing the use of routine characterization techniques to access osseointegration [153, 154]. The thick cortical bone - broadly responsible for the primary fixation of the implants – also establishes a favorable environment for the early evaluation of the bone-to-implant interface [152].

The drilling protocol for implant placement followed the general protocol for Megagen Anyridge® implants, with copious irrigation at the surgical site with isotonic saline solution, to preclude thermal damage to the tissues [8]. Implants were also inserted with normal values of torque, using a handpiece and a manual wrench for final adjustments. Implants were placed at least 1.5mm apart, according to recognized standards [155, 156]. The implants are bone-level and were submerged, to be protected from the influence of the exterior environment because no cover screws nor abutments were available for placement [157].

In the past, other *in vivo* studies have shown that fluoride ions' incorporation yields osteoinduction at the implants' interface [78], increasing bone density, and leading to osteogenic cell proliferation [78]. Several *in vivo* studies found superior results for fluoride-modified implant surfaces, showing that this is a promising path for better osseointegration, and justifying our research [149, 158, 159].

In addition, there were no reported complications such as wound dehiscence, infection, or allergic reactions, disclosing these potential negative influences on the outcome results, including the 4 weeks and 8 weeks groups.

The biological response to the developed implant-coated constructs was characterized through microtomography. This technique allows a nondestructive 3D imaging and morphometric analysis of the bone tissue with a very high resolution. Attained datasets can be used to reconstruct the implant and neighboring bone tissue, further characterizing tissue parameters in a given region of interest [160-162]. This allows the feasible analysis of bone tissue 3D parameters, such as bone volume (BV), bone volume ratio (BV/TV), as well as 2D parameters such as bone surface (BS) and data regarding the direct interaction between the implant and the bone tissue, as the bone-

to-implant contact (BIC), given a proper data processing to minimize titanium-dependent imaging artifacts [121].

The 4 weeks group's microtomographic data, quantitative volumetric analysis, and 3D reconstructions, all revealed an increased bone volume, augmented bone surface, and an increased contact area with the implant for fluorapatite-containing surfaces, compared with HA, and in particular, within the F 0.1 group. This seems to indicate that fluor can accelerate bone formation, in comparison with hydroxyapatite, and it comes to terms with other published studies [14, 66, 78].

At 8 weeks, results showed a more advanced bone formation than the 4 weeks group. Data also revealed better outcomes for fluorapatite compositions than for HA, and F 0.1 had the most increased BV, BS, BV/TV, and BIC. This continues to show that the F 0.1 composition seems to induce an increased bone formation. It continues to corroborate with the literature about fluor presence in dental implant surfaces, and the possible advantages of achieving increased osseointegration, for faster clinical use [66, 78].

The biological assessment revealed the increased capability of fluorapatite coatings to enhance bone tissue formation in the vicinity of the implant and to increase the bone-to-implant contact, at both 4 and 8 weeks of implantation. F 0.1 coating was found to further induce bone tissue formation at the earliest time point, as compared to F 0.01, in line with the increased F content. Recently, fluoride-containing apatite coatings become a topic of interest in implantology-related research [163].

Hydroxyapatite has long been considered the bioceramic of choice for bone-related applications, given its biocompatible response, high affinity to the bone tissue, and ability to induce early osseointegration [164]. Clinical applicability has however been limited by the reported coating delamination and dubious long-term success [165], associated with the plasma spraying coating technique. The alternative coating strategy currently employed, the hydrothermal synthesis is expected to surpass these limitations given the ability to control crystal structure, crystal morphology, and grain purity of the coating nanoparticles, by adjusting the reaction conditions. In addition, the coating thickness can reach tens of nanometers and uniform coatings can be prepared on

complex surface shapes using the hydrothermal method. Furthermore, the prepared calcium phosphate-based coatings have high interfacial bonding strength and density, which can significantly improve the corrosion resistance of metallic substrates [166, 167].

In addition, F-containing apatite coatings have demonstrated an enhanced biological response and bioactivity, as compared to hydroxyapatite, within distinct preparation and deposition methodologies [168-170]. Higher thermal stability and mechanical properties have also been recognized within F-containing apatites [171, 172].

In the present study, F-containing surfaces enhanced bone formation and allowed an increased BIC, with F 0.1 coating allowing for an enhanced biological outcome. Previous *in vitro* studies reported an increased osteoblastic proliferation within distinct F-substituted apatites, as compared to non-substituted ones [134] - a process that may be associated with the ability of fluorine to act on relevant cell signaling pathways, as the Jun N-terminal kinase (JNK) and p38 MAPK [173]. Similarly, F-containing substrates were also found to enhance osteoblastic differentiation, thus upregulating the expression of osteogenesis-related markers such as alkaline phosphatase and osteocalcin [114, 131, 174]. Mechanistically, this process may relate to the upregulation of the Wnt signaling pathway via the fluoride-mediated GSK-3 β phosphorylation, or via BMP/Smad signaling, also modulated by fluoride [175, 176]. On the other hand, F was found to diminish the osteoclastic functionality – either directly through the downregulation of a major transcription factor, NFATc1 [177]; or indirectly, increasing the expression of the osteoprotegerin decoy receptor, inhibiting the osteoblast-mediated osteoclast differentiation [178]. This regulation – a decreased bone resorption conjoined to an increased bone formation, further verified within *in vivo* models [179], is expected to accelerate the early osseointegration process and consequently, the overall implant success rate.

One of the existing and more acknowledged implants with fluoride chemical surface treatment is the Osseospeed® surface, which is obtained with sandblasting and fluoridation [66, 130, 180]. *In vivo* tests show dioxide titanium with a negative charge, which facilitates the deposition of calcium ions on the surface, that have a high affinity

to the phosphate groups of many organic molecules (proteins, glycans, etc.) [66, 180]. Fluoride, given its high electronegativity, increases calcium ions sedimentation speed and also the density of the trabecular bone, by stimulating osteoblasts functional activity, as increasing alkaline phosphatase activity [180]. *In vitro*, bonds between calcium ions and groups of phosphate are shown to be strong, of the covalent type, if the surface itself is coated with fluoride ions which are released in the surrounding space following the establishment of the such bond [66, 180]. Although this surface and the ones studied by us, all take advantage of the presence of fluor, this fluoridation of OsseoSpeed® surface seems to be only impregnated with residual levels of fluoride on titanium dioxide [66, 130, 181]. The surfaces characterized in this study have been treated with fluor by hydroxyl substitution of hydroxyapatite, chemically incorporating fluor as one of the coating elements, and using specific concentrations of fluor, for understanding how different levels of the ion can affect the biological behavior of the implant.

Nevertheless, in addition to the reported beneficial effects on bone metabolism/regeneration, fluoride may also elicit detrimental effects on bone tissue dynamics, altering cellular functionality and inducing structural damage, as verified in bone fluorosis [182]. The major factor determining the fluoride-mediated biological outcomes seems to be the amount of bioavailable F⁻ within the microenvironment [183]. In accordance, both F 0.1 and F 0.01 formulations induced the osteogenic response, with the former outperforming the latter, demonstrating the adequacy of F levels in the coatings' composition [184].

Of additional relevance, the identified citrate species are further expected to tailor the biological outcomes. Citrate is a major component of the bone structure, distributed in two major pools: collagen-associated and HA-associated citrate [120]; and known to enhance the biomineralization process. Citrate also seems to play a chelating activity, binding to important ionic species such as Mg, Zn, and Ca, constituting a major ionic store in the bone tissue [185]. The exogenous citrate supplementation has been further found to facilitate osteogenesis and cellular commitment of precursor populations, favoring the metabolic changes - switch from aerobic glycolysis to oxidative phosphorylation, needed to meet the increased energetic requirements determined by

the osteogenic differentiation [142, 185, 186]. Citrate molecules may further indirectly induce the expression of osteogenic transcription factors (e.g., RUNX2 and downstream targets) by the stabilization of β -catenin [142, 187]. Accordingly, the presence of citrate species on the produced coatings is expected to synergize with F to improve the osteogenic response.

VI. *Conclusion*

"Even miracles Take a little time."

Fairy godmother, Cinderella

In the present work, innovative F-containing hydroxyapatite coatings were prepared by the hydrothermal method and deposited over commercial titanium implants with no previous surface treatment, aiming for enhanced osseointegration.

The physicochemical characterization validated the incorporation of F⁻ into the hydroxyapatite (HA) lattice through OH⁻ substitution with fluorapatite formation, further evidencing the presence of citrate species.

The *in vitro* biological evaluation revealed an increased cell proliferation and differentiation, as verified by the increased mineral deposition, on F-containing coatings.

The *in vivo* biological assessment of the developed constructs in a translational animal model revealed an enhanced bone formation process in the vicinity of the fluorapatite-coated implants, with increased bone-to-implant contact and bone formation, as compared to hydroxyapatite-coated implants.

The attained enhancement in osteogenesis is attributable to the conjoined modulatory activity of selected F⁻ and citrate levels within the produced coatings.

Accordingly, the production of fluorapatite coatings with citrate entails a promising approach for enhanced osteointegration in implant dentistry.

About the future

The long-term osseointegration of titanium implants is established and proven successful. New surface coating techniques may bring additional biological and chemical potential for dental implants. However, patient needs and biosafety must remain the main trendlines, guiding innovation and research and development processes. Knowledge from oral health professionals, and specific education with research, for example, is fundamental to understanding and choosing treatment tools.

The study presented some limitations, which can contribute to some future changes in the continuity of this investigation. In this way, adhesion forces were not measured, and therefore, the connection of the coating to the titanium could not be characterized. But, because of the nanometric level of the developed surface, it was found that:

- It does not present macro-fractures;
- It follows the surface topography and roughness of the implant;
- It accompanies the bendiness and micromovements of the implant.

The effect of coating composition on biofilm could also be evaluated. Expecting it to be the next stage in the following studies, to determine what the literature reveals as promising results regarding a potential F-mediated antibacterial activity, viewed within *in vitro* or *in vivo* studies.

Also, the removal torque for the osteointegrated implants was not evaluated. It could be beneficial to study the differences as in other studies, in which fluor-coated implants seem to present a higher removal torque, when compared to the control group, with no fluor on the coating.

Furthermore, it is also known that the fine-tuning of the surface properties determines specific cellular populations' functionality, allowing greater control over the molecular and cellular events that determine the establishment of the required interfaces. This could also be the next step in the investigation, getting into greater detail on the specificities of the F-containing coating characteristics.

Other research topics embrace the incorporation of antibiotics on calcium phosphate coatings. Antimicrobial agents may be impregnated into the coating and gain the possibility of the long-term controlled release of the drug, preventing postsurgical infection complications, and eventually lowering the implant loss rate. Growth factors can also be incorporated into coatings, and this is a very promising option, according to literature, to further enhance early osteointegration and healing.

In memoriam



Professor Doutor António Faria Gomes

*“Laughter is timeless,
imagination has no age,
and dreams are forever”
Walt Disney*

References

1. <https://www.worldometers.info>. Worldometer. 2020.
2. Census, U.S. <https://www.census.gov/>. 2020.
3. data, O.w.i. <https://ourworldindata.org/age-structure>. 2020.
4. Aging, N.I.o. <https://www.nia.nih.gov/>. 2020.
5. Lamster, I.B., et al., *The aging mouth: differentiating normal aging from disease*. Periodontol 2000, 2016. **72**(1): p. 96-107.
6. Gomez-de Diego, R., et al., *Indications and contraindications of dental implants in medically compromised patients: update*. Med Oral Patol Oral Cir Bucal, 2014. **19**(5): p. e483-9.
7. Kingston, I.K.D., *Oral Rehabilitation: A Case-Based Approach*. 1st ed. 2012: Wiley-Blackwell.
8. Lindhe, J. and N.P. Lang, *Tratado De Periodontia Clínica E Implantologia Oral*. 2018: GUANABARA.
9. Emami, E., et al., *The impact of edentulism on oral and general health*. Int J Dent, 2013. **2013**: p. 498305.
10. www.pexels.com/. Available from: <https://www.pexels.com/pt-br/foto/cuidado-dental-cuidado-dentario-odontologia-higiene-6627603>.
11. www.stockfreeimages.com. Available from: <https://www.stockfreeimages.com/p1/dental-bridge.html>.
12. ALARA. Available from: <https://www.cdc.gov/nceh/radiation/alara.html>.
13. *Megagen*.
14. Junker, R., et al., *Effects of implant surface coatings and composition on bone integration: a systematic review*. Clin Oral Implants Res, 2009. **20 Suppl 4**: p. 185-206.
15. Esposito, M., Y. Ardebili, and H.V. Worthington, *Interventions for replacing missing teeth: different types of dental implants*. Cochrane Database Syst Rev, 2014(7): p. CD003815.
16. Branemark, P.I., et al., *Intra-osseous anchorage of dental prostheses. I. Experimental studies*. Scand J Plast Reconstr Surg, 1969. **3**(2): p. 81-100.
17. Branemark, P.I., et al., *Osseointegrated titanium fixtures in the treatment of edentulousness*. Biomaterials, 1983. **4**(1): p. 25-8.
18. Tsukiboshi, M., *Autotransplantation of teeth*. 2001: Quintessence books ed.
19. www.ancient-origins.net/.
20. Linkow, L.I., *The blade vent--a new dimension in endosseous implantology*. Dent Concepts, 1968. **11**(2): p. 3-12.
21. Plamer, R.S., BJ; Howe, LC; Palmer, P.J., *Implants in Clinical Dentistry*. 2006: Informa Healthcare. 273.
22. Abi-Aad, H., et al., *Immediate vs conventional loading of variable-thread tapered implants supporting three- to four-unit fixed partial dentures in the posterior maxilla: 1-year interim results of a split-mouth randomised controlled trial*. Eur J Oral Implantol, 2018. **11**(3): p. 337-350.
23. Blaschke, C. and D.R. Schwass, *The socket-shield technique: a critical literature review*. Int J Implant Dent, 2020. **6**(1): p. 52.
24. Ogawa, T., et al., *Effectiveness of the socket shield technique in dental implant: A systematic review*. J Prosthodont Res, 2022. **66**(1): p. 12-18.
25. Gluckman, H., M. Salama, and J. Du Toit, *A retrospective evaluation of 128 socket-shield cases in the esthetic zone and posterior sites: Partial extraction therapy with up to 4 years follow-up*. Clin Implant Dent Relat Res, 2018. **20**(2): p. 122-129.

26. Cumbo, C., et al., *Implant platform switching concept: a literature review*. Eur Rev Med Pharmacol Sci, 2013. **17**(3): p. 392-7.
27. Choi, J.W., et al., *Load-Bearing Capacity and Retention of Newly Developed Micro-Locking Implant Prosthetic System: An In Vitro Pilot Study*. Materials (Basel), 2018. **11**(4).
28. Ramanauskaite, A., K. Becker, and F. Schwarz, *Clinical characteristics of peri-implant mucositis and peri-implantitis*. Clin Oral Implants Res, 2018. **29**(6): p. 551-556.
29. Schwarz, F., et al., *Peri-implantitis*. J Periodontol, 2018. **89 Suppl 1**: p. S267-S290.
30. Dreyer, H., et al., *Epidemiology and risk factors of peri-implantitis: A systematic review*. J Periodontal Res, 2018. **53**(5): p. 657-681.
31. Chrcanovic, B.R., T. Albrektsson, and A. Wennerberg, *Reasons for failures of oral implants*. J Oral Rehabil, 2014. **41**(6): p. 443-76.
32. Schnitman, P.A. and L.B. Shulman, *Recommendations of the consensus development conference on dental implants*. J Am Dent Assoc, 1979. **98**(3): p. 373-7.
33. Raikar, S., et al., *Factors Affecting the Survival Rate of Dental Implants: A Retrospective Study*. J Int Soc Prev Community Dent, 2017. **7**(6): p. 351-355.
34. Cochran, D.L., *A comparison of endosseous dental implant surfaces*. J Periodontol, 1999. **70**(12): p. 1523-39.
35. Ramanauskaite, A., et al., *Effect of history of periodontitis on implant success: meta-analysis and systematic review*. Implant Dent, 2014. **23**(6): p. 687-96.
36. Marrone, A., et al., *Prevalence and risk factors for peri-implant disease in Belgian adults*. Clin Oral Implants Res, 2013. **24**(8): p. 934-40.
37. Jiang, B.Q., et al., *A clinical study on the effectiveness of implant supported dental restoration in patients with chronic periodontal diseases*. Int J Oral Maxillofac Surg, 2013. **42**(2): p. 256-9.
38. Casado, P.L., et al., *History of chronic periodontitis is a high risk indicator for peri-implant disease*. Braz Dent J, 2013. **24**(2): p. 136-41.
39. Levin, L., et al., *Periodontal disease as a risk for dental implant failure over time: a long-term historical cohort study*. J Clin Periodontol, 2011. **38**(8): p. 732-7.
40. Karoussis, I.K., et al., *Long-term implant prognosis in patients with and without a history of chronic periodontitis: a 10-year prospective cohort study of the ITI Dental Implant System*. Clin Oral Implants Res, 2003. **14**(3): p. 329-39.
41. Rocuzzo, M., et al., *Ten-year results of a three-arm prospective cohort study on implants in periodontally compromised patients. Part 1: implant loss and radiographic bone loss*. Clin Oral Implants Res, 2010. **21**(5): p. 490-6.
42. Jemt, T., et al., *A retrospective study on 1592 consecutively performed operations in one private referral clinic. Part II: Peri-implantitis and implant failures*. Clin Implant Dent Relat Res, 2017. **19**(3): p. 413-422.
43. Derks, J. and C. Tomasi, *Peri-implant health and disease. A systematic review of current epidemiology*. J Clin Periodontol, 2015. **42 Suppl 16**: p. S158-71.
44. Rocuzzo, M., et al., *Clinical outcomes of peri-implantitis treatment and supportive care: A systematic review*. Clin Oral Implants Res, 2018. **29 Suppl 16**: p. 331-350.
45. Albrektsson, T., et al., *"Peri-Implantitis": A Complication of a Foreign Body or a Man-Made "Disease". Facts and Fiction*. Clin Implant Dent Relat Res, 2016. **18**(4): p. 840-9.
46. Ichim, P.I., et al., *Design optimization of a radial functionally graded dental implant*. J Biomed Mater Res B Appl Biomater, 2016. **104**(1): p. 58-66.
47. De Bruyn, H., et al., *Implant surface roughness and patient factors on long-term peri-implant bone loss*. Periodontol 2000, 2017. **73**(1): p. 218-227.
48. Berglundh, T., et al., *De novo alveolar bone formation adjacent to endosseous implants*. Clin Oral Implants Res, 2003. **14**(3): p. 251-62.
49. Bornstein, M.M., et al., *Cone beam computed tomography in implant dentistry: a systematic review focusing on guidelines, indications, and radiation dose risks*. Int J Oral Maxillofac Implants, 2014. **29 Suppl**: p. 55-77.

50. Yamada, M. and H. Egusa, *Current bone substitutes for implant dentistry*. J Prosthodont Res, 2018. **62**(2): p. 152-161.
51. Zhang, Y., et al., *Dental Implant Nano-Engineering: Advances, Limitations and Future Directions*. Nanomaterials (Basel), 2021. **11**(10).
52. Esposito, M., et al., *Failure patterns of four osseointegrated oral implant systems*. J Mater Sci Mater Med, 1997. **8**(12): p. 843-7.
53. Esposito, M., et al., *Biological factors contributing to failures of osseointegrated oral implants. (II). Etiopathogenesis*. Eur J Oral Sci, 1998. **106**(3): p. 721-64.
54. www.istockphoto.com/.
55. Reissmann, D.R., P. Poxleitner, and G. Heydecke, *Location, intensity, and experience of pain after intra-oral versus extra-oral bone graft harvesting for dental implants*. J Dent, 2018. **79**: p. 102-106.
56. Paolone, M.G. and R. Kaitsas, *Orthodontic-periodontal interactions: Orthodontic extrusion in interdisciplinary regenerative treatments*. Int Orthod, 2018. **16**(2): p. 217-245.
57. Thoma, D.S., et al., *Effects of soft tissue augmentation procedures on peri-implant health or disease: A systematic review and meta-analysis*. Clin Oral Implants Res, 2018. **29 Suppl 15**: p. 32-49.
58. Liu, X., et al., *Binary titanium alloys as dental implant materials-a review*. Regen Biomater, 2017. **4**(5): p. 315-323.
59. Dohan Ehrenfest, D.M., et al., *Classification of osseointegrated implant surfaces: materials, chemistry and topography*. Trends Biotechnol, 2010. **28**(4): p. 198-206.
60. Zhang, L.C., L, *A Review on Biomedical Titanium Alloys: Recent Progress and Prospect*. . Adv. Eng. Mater, 2019. **21**.
61. Kaur, M.S., K, *Review on titanium and titanium based alloys as biomaterials for orthopaedic applications*. . Mater. Sci. Eng. C., 2019. **102**: p. 844-862.
62. Kim, K.T., et al., *General review of titanium toxicity*. Int J Implant Dent, 2019. **5**(1): p. 10.
63. Mombelli, A., D. Hashim, and N. Cionca, *What is the impact of titanium particles and biocorrosion on implant survival and complications? A critical review*. Clin Oral Implants Res, 2018. **29 Suppl 18**: p. 37-53.
64. Smeets, R., et al., *Definition, etiology, prevention and treatment of peri-implantitis--a review*. Head Face Med, 2014. **10**: p. 34.
65. Wennerberg, A., T. Albrektsson, and R. Jimbo, *Implant Surfaces and their Biological and Clinical Impact*, ed. A. Wennerberg. 2015: Springer.
66. Smeets, R., et al., *Impact of Dental Implant Surface Modifications on Osseointegration*. Biomed Res Int, 2016. **2016**: p. 6285620.
67. El Hassanin, A., et al., *Effect of Implant Surface Roughness and Macro- and Micro-Structural Composition on Wear and Metal Particles Released*. Materials (Basel), 2021. **14**(22).
68. Albrektsson, T. and A. Wennerberg, *On osseointegration in relation to implant surfaces*. Clin Implant Dent Relat Res, 2019. **21 Suppl 1**: p. 4-7.
69. Buser, D., et al., *Interface shear strength of titanium implants with a sandblasted and acid-etched surface: a biomechanical study in the maxilla of miniature pigs*. J Biomed Mater Res, 1999. **45**(2): p. 75-83.
70. Le Guehennec, L., et al., *Surface treatments of titanium dental implants for rapid osseointegration*. Dent Mater, 2007. **23**(7): p. 844-54.
71. Rosa, M.B., et al., *The influence of surface treatment on the implant roughness pattern*. J Appl Oral Sci, 2012. **20**(5): p. 550-5.
72. Kunrath, M.F., et al., *Innovative surfaces and alloys for dental implants: What about biointerface-safety concerns?* Dent Mater, 2021. **37**(10): p. 1447-1462.
73. Kien, P., T. Quan, and L. Tuyet Anh, *Coating Characteristic of Hydroxyapatite on Titanium Substrates via Hydrothermal Treatment*. Coatings, 2021. **11**(10): p. 1226-1226.

74. Moloodi, A., et al., *Evaluation of fluorohydroxyapatite/strontium coating on titanium implants fabricated by hydrothermal treatment*. Progress in Biomaterials, 2021. **10**(3): p. 185-194.
75. Abraham, C.M., *A brief historical perspective on dental implants, their surface coatings and treatments*. Open Dent J, 2014. **8**: p. 50-5.
76. Nishimoto, S.K., et al., *The effect of titanium surface roughening on protein absorption, cell attachment, and cell spreading*. Int J Oral Maxillofac Implants, 2008. **23**(4): p. 675-80.
77. Cochran, D.L., et al., *Bone response to unloaded and loaded titanium implants with a sandblasted and acid-etched surface: a histometric study in the canine mandible*. J Biomed Mater Res, 1998. **40**(1): p. 1-11.
78. Offermanns, V., et al., *Comparing the effect of strontium-functionalized and fluoride-modified surfaces on early osseointegration*. J Periodontol, 2018. **89**(8): p. 940-948.
79. Yeo, I.S., *Reality of dental implant surface modification: a short literature review*. Open Biomed Eng J, 2014. **8**: p. 114-9.
80. Gonshor, A., G. Goveia, and E. Sotirakis, *A prospective, multicenter, 4-year study of the ACE Surgical resorbable blast media implant*. J Oral Implantol, 2003. **29**(4): p. 174-80.
81. O'Brien, G.R., A. Gonshor, and A. Balfour, *A 6-year prospective study of 620 stress-diversion surface (SDS) dental implants*. J Oral Implantol, 2004. **30**(6): p. 350-7.
82. Peleg, M., A.K. Garg, and Z. Mazor, *Predictability of simultaneous implant placement in the severely atrophic posterior maxilla: A 9-year longitudinal experience study of 2132 implants placed into 731 human sinus grafts*. Int J Oral Maxillofac Implants, 2006. **21**(1): p. 94-102.
83. Ormianer, Z. and A. Palti, *Long-term clinical evaluation of tapered multi-threaded implants: results and influences of potential risk factors*. J Oral Implantol, 2006. **32**(6): p. 300-7.
84. Degidi, M., et al., *Comparative analysis of immediate functional loading and immediate nonfunctional loading to traditional healing periods: a 5-year follow-up of 550 dental implants*. Clin Implant Dent Relat Res, 2009. **11**(4): p. 257-66.
85. Akoglu, B., et al., *Five-year treatment outcomes with three brands of implants supporting mandibular overdentures*. Int J Oral Maxillofac Implants, 2011. **26**(1): p. 188-94.
86. Ormianer, Z. and A. Palti, *Retrospective clinical evaluation of tapered screw-vent implants: results after up to eight years of clinical function*. J Oral Implantol, 2008. **34**(3): p. 150-60.
87. Ormianer, Z., et al., *Retrospective clinical evaluation of tapered implants: 10-year follow-up of delayed and immediate placement of maxillary implants*. Implant Dent, 2012. **21**(4): p. 350-6.
88. Ozkan, Y., B. Akoglu, and Y. Kulak-Ozkan, *Five-year treatment outcomes with four types of implants in the posterior maxilla and mandible in partially edentulous patients: a retrospective study*. Int J Oral Maxillofac Implants, 2011. **26**(3): p. 639-47.
89. Esposito, M., et al., *The role of implant surface modifications, shape and material on the success of osseointegrated dental implants. A Cochrane systematic review*. Eur J Prosthodont Restor Dent, 2005. **13**(1): p. 15-31.
90. Palmquist, A., et al., *Titanium oral implants: surface characteristics, interface biology and clinical outcome*. J R Soc Interface, 2010. **7 Suppl 5**: p. S515-27.
91. Jokstad, A., et al., *Quality of dental implants*. Int Dent J, 2003. **53**(6 Suppl 2): p. 409-43.
92. Matos, G.R.M., *Surface Roughness of Dental Implant and Osseointegration*. J Maxillofac Oral Surg, 2021. **20**(1): p. 1-4.
93. Vahabzadeh, S., et al., *Phase stability and biological property evaluation of plasma sprayed hydroxyapatite coatings for orthopedic and dental applications*. Acta Biomaterialia, 2015. **17**: p. 47-55.

94. Lazzara, R.J., et al., *A human histologic analysis of osseotite and machined surfaces using implants with 2 opposing surfaces*. Int J Periodontics Restorative Dent, 1999. **19**(2): p. 117-29.
95. Zetterqvist, L., et al., *A prospective, multicenter, randomized-controlled 5-year study of hybrid and fully etched implants for the incidence of peri-implantitis*. J Periodontol, 2010. **81**(4): p. 493-501.
96. Park, J.Y. and J.E. Davies, *Red blood cell and platelet interactions with titanium implant surfaces*. Clin Oral Implants Res, 2000. **11**(6): p. 530-9.
97. Cochran, D.L., et al., *The use of reduced healing times on ITI implants with a sandblasted and acid-etched (SLA) surface: early results from clinical trials on ITI SLA implants*. Clin Oral Implants Res, 2002. **13**(2): p. 144-53.
98. Wennerberg, A. and T. Albrektsson, *On implant surfaces: a review of current knowledge and opinions*. Int J Oral Maxillofac Implants, 2010. **25**(1): p. 63-74.
99. Mohseni, E., E. Zalnezhad, and A.R. Bushroa, *Comparative investigation on the adhesion of hydroxyapatite coating on Ti-6Al-4V implant: A review paper*. International Journal of Adhesion and Adhesives, 2014. **48**: p. 238-257.
100. Arrés, M., et al., *Surface and mechanical properties of a nanostructured citrate hydroxyapatite coating on pure titanium*. Journal of the Mechanical Behavior of Biomedical Materials, 2020. **108**: p. 103794-103794.
101. Best, S., et al., *The dependence of osteoblastic response on variations in the chemical composition and physical properties of hydroxyapatite*. J Mater Sci Mater Med, 1997. **8**(2): p. 97-103.
102. [www.pubchem.ncbi.nlm.nih.gov/compound/Hydroxyapatite](https://pubchem.ncbi.nlm.nih.gov/compound/Hydroxyapatite). Available from: <https://pubchem.ncbi.nlm.nih.gov/compound/Hydroxyapatite>.
103. Misch, C.E. and F. Dietsch, *Bone-grafting materials in implant dentistry*. Implant Dent, 1993. **2**(3): p. 158-67.
104. Novaes, A.B., Jr., et al., *Histomorphometric analysis of the bone-implant contact obtained with 4 different implant surface treatments placed side by side in the dog mandible*. Int J Oral Maxillofac Implants, 2002. **17**(3): p. 377-83.
105. Kasemo, B. and J. Lausmaa, *Biomaterial and implant surfaces: on the role of cleanliness, contamination, and preparation procedures*. J Biomed Mater Res, 1988. **22**(A2 Suppl): p. 145-58.
106. Zechner, W., et al., *Osseous healing characteristics of three different implant types*. Clin Oral Implants Res, 2003. **14**(2): p. 150-7.
107. Schupbach, P. and R. Glauser, *The defense architecture of the human periimplant mucosa: a histological study*. J Prosthet Dent, 2007. **97**(6 Suppl): p. S15-25.
108. Park, J.W., K.B. Park, and J.Y. Suh, *Effects of calcium ion incorporation on bone healing of Ti6Al4V alloy implants in rabbit tibiae*. Biomaterials, 2007. **28**(22): p. 3306-13.
109. Borkowski, L., et al., *Fluorapatite ceramics for bone tissue regeneration: Synthesis, characterization and assessment of biomedical potential*. Materials Science and Engineering: C, 2020. **116**: p. 111211-111211.
110. Li, Z., et al., *Effects of fluoridation of porcine hydroxyapatite on osteoblastic activity of human MG63 cells*. Science and Technology of Advanced Materials, 2015. **16**(3): p. 035006-035006.
111. Mansoorianfar, M., et al., *Surface modification of orthopedic implants by optimized fluorine-substituted hydroxyapatite coating: Enhancing corrosion behavior and cell function*. Ceramics International, 2020. **46**(2): p. 2139-2146.
112. Rezaee, T., M.L. Boussein, and L. Karim, *Increasing fluoride content deteriorates rat bone mechanical properties*. Bone, 2020. **136**: p. 115369-115369.
113. Ellingsen, J.E., *Surface configurations of dental implants*. Periodontol 2000, 1998. **17**: p. 36-46.

114. Berglundh, T., et al., *Bone healing at implants with a fluoride-modified surface: an experimental study in dogs*. Clin Oral Implants Res, 2007. **18**(2): p. 147-52.
115. Alhilou, A., et al., *Physicochemical and Antibacterial Characterization of a Novel Fluorapatite Coating*. ACS Omega, 2016. **1**(2): p. 264-276.
116. Campillo-Funollet, M.L., P; Reparaz, S; Valente, M., *On the assessment of hydroxyapatite fluoridation by means of Raman scattering*. The Journal of Chemical Physics, 2010. **132**(24): p. 244501.
117. Vidal, C., et al., *Fabrication of a biodegradable and cytocompatible magnesium/nanohydroxyapatite/fluorapatite composite by upward friction stir processing for biomedical applications*. Journal of the Mechanical Behavior of Biomedical Materials, 2022. **129**: p. 105137-105137.
118. Wu, Y.-J., Y.-H. Tseng, and J.C.C. Chan, *Morphology Control of Fluorapatite Crystallites by Citrate Ions*. Crystal Growth & Design, 2010. **10**(10): p. 4240-4242.
119. Degli Esposti, L., et al., *Combined Effect of Citrate and Fluoride Ions on Hydroxyapatite Nanoparticles*. Crystal Growth & Design, 2020. **20**(5): p. 3163-3172.
120. Costello, L.C., et al., *The status of citrate in the hydroxyapatite/collagen complex of bone; and its role in bone formation*. journal of Regenerative Medicine and Tissue Engineering, 2014. **3**(1): p. 4-4.
121. Liu, Y., et al., *3D X-ray micro-computed tomography imaging for the microarchitecture evaluation of porous metallic implants and scaffolds*. Micron, 2021. **142**: p. 102994-102994.
122. Rupp, F., et al., *Surface characteristics of dental implants: A review*. Dent Mater, 2018. **34**(1): p. 40-57.
123. Mendonca, G., et al., *Advancing dental implant surface technology--from micron- to nanotopography*. Biomaterials, 2008. **29**(28): p. 3822-35.
124. Novaes, A.B., Jr., et al., *Influence of implant surfaces on osseointegration*. Braz Dent J, 2010. **21**(6): p. 471-81.
125. Esposito, M., et al., *Dental implants with internal versus external connections: 5-year post-loading results from a pragmatic multicenter randomised controlled trial*. Eur J Oral Implantol, 2016. **9 Suppl 1**(2): p. 129-41.
126. Bechara, S., et al., *Short (6-mm) dental implants versus sinus floor elevation and placement of longer (≥ 10 -mm) dental implants: a randomized controlled trial with a 3-year follow-up*. Clin Oral Implants Res, 2017. **28**(9): p. 1097-1107.
127. Mangano, C., et al., *Immediate Loading of Single Implants: A 2-Year Prospective Multicenter Study*. Int J Periodontics Restorative Dent, 2017. **37**(1): p. 69-78.
128. Mangano, F.G., et al., *Early bone formation around immediately loaded implants with nanostructured calcium-incorporated and machined surface: a randomized, controlled histologic and histomorphometric study in the human posterior maxilla*. Clin Oral Investig, 2017. **21**(8): p. 2603-2611.
129. Dhaliwal, J.S., et al., *Osseointegration of standard and mini dental implants: a histomorphometric comparison*. Int J Implant Dent, 2017. **3**(1): p. 15.
130. Xuereb, M., J. Camilleri, and N.J. Attard, *Systematic review of current dental implant coating materials and novel coating techniques*. Int J Prosthodont, 2015. **28**(1): p. 51-9.
131. Al Mugeiren, O.M. and M.A. Baseer, *Dental Implant Bioactive Surface Modifiers: An Update*. J Int Soc Prev Community Dent, 2019. **9**(1): p. 1-4.
132. Anna Strunecká, J.P., Paul Connett, *Fluorine in medicine* Journal of Applied Biomedicine, 2004(2): p. 141-150.
133. Bhadang, K.A. and K.A. Gross, *Influence of fluorapatite on the properties of thermally sprayed hydroxyapatite coatings*. Biomaterials, 2004. **25**(20): p. 4935-4945.
134. Qu, H. and M. Wei, *The effect of fluoride contents in fluoridated hydroxyapatite on osteoblast behavior*. Acta Biomaterialia, 2006. **2**(1): p. 113-119.

135. Jha, L.J., et al., *Preparation and characterization of fluoride-substituted apatites*. Journal of materials science. Materials in medicine, 1997. **8**(4): p. 185-91.
136. Rabe, M., D. Verdes, and S. Seeger, *Understanding protein adsorption phenomena at solid surfaces*. Adv Colloid Interface Sci, 2011. **162**(1-2): p. 87-106.
137. Matsumoto, T., et al., *Effects of Surface Modification on Adsorption Behavior of Cell and Protein on Titanium Surface by Using Quartz Crystal Microbalance System*. Materials (Basel), 2020. **14**(1).
138. Caligari Conti, M., et al., *Optimisation of fluorapatite coating synthesis applied to a biodegradable substrate*. Surface Engineering, 2019. **35**(3): p. 255-265.
139. Bulina, N.V., et al., *Structure and thermal stability of fluorhydroxyapatite and fluorapatite obtained by mechanochemical method*. Journal of Solid State Chemistry, 2020. **282**: p. 121076-121076.
140. Slimen, J.B., et al., *Sintering of Potassium Doped Hydroxy-Fluorapatite Bioceramics*. Coatings, 2021. **11**(7): p. 858-858.
141. Wei, M., et al., *Synthesis and characterization of hydroxyapatite, fluoride-substituted hydroxyapatite and fluorapatite*. Journal of materials science. Materials in medicine, 2003. **14**(4): p. 311-20.
142. Fernandes, M.H., et al., *Citrate zinc hydroxyapatite nanorods with enhanced cytocompatibility and osteogenesis for bone regeneration*. Materials Science and Engineering: C, 2020. **115**: p. 111147-111147.
143. Deng, L., et al., *The surface regulation of calcite for defluoridation by fluorapatite-induced crystallization*. Journal of Water Process Engineering, 2021. **41**: p. 102082-102082.
144. Joseph Nathanael, A., et al., *Influence of fluorine substitution on the morphology and structure of hydroxyapatite nanocrystals prepared by hydrothermal method*. Materials Chemistry and Physics, 2013. **137**(3): p. 967-976.
145. Sun, J., et al., *Comparative study of hydroxyapatite, fluor-hydroxyapatite and Si-substituted hydroxyapatite nanoparticles on osteogenic, osteoclastic and antibacterial ability*. RSC Advances, 2019. **9**(28): p. 16106-16118.
146. Li, J.Y., et al., *Effect of Fluoride-Modified Titanium Surface on Early Adhesion of Irradiated Osteoblasts*. Biomed Res Int, 2015. **2015**: p. 219752.
147. Guo, J., et al., *The effect of hydrofluoric acid treatment of TiO₂ grit blasted titanium implants on adherent osteoblast gene expression in vitro and in vivo*. Biomaterials, 2007. **28**(36): p. 5418-25.
148. Kang, B.S., et al., *XPS, AES and SEM analysis of recent dental implants*. Acta Biomater, 2009. **5**(6): p. 2222-9.
149. Ellingsen, J.E., et al., *Improved retention and bone-to-implant contact with fluoride-modified titanium implants*. Int J Oral Maxillofac Implants, 2004. **19**(5): p. 659-66.
150. Wang, X.J., et al., *Effects of fluoride-ion-implanted titanium surface on the cytocompatibility in vitro and osseointegration in vivo for dental implant applications*. Colloids Surf B Biointerfaces, 2015. **136**: p. 752-60.
151. Blanc-Sylvestre, N., et al., *Pre-Clinical Models in Implant Dentistry: Past, Present, Future*. Biomedicines, 2021. **9**(11): p. 1538-1538.
152. Stübinger, S. and M. Dard, *The Rabbit as Experimental Model for Research in Implant Dentistry and Related Tissue Regeneration*. Journal of Investigative Surgery, 2013. **26**(5): p. 266-282.
153. Shin, D., et al., *Peripheral quantitative computer tomographic, histomorphometric, and removal torque analyses of two different non-coated implants in a rabbit model*. Clinical Oral Implants Research, 2011. **22**(3): p. 242-250.
154. Seong, W.-J., et al., *Comparison of Push-In versus Pull-Out Tests on Bone-Implant Interfaces of Rabbit Tibia Dental Implant Healing Model*. Clinical Implant Dentistry and Related Research, 2013. **15**(3): p. 460-469.

155. Danza, M., et al., *Distance between implants has a potential impact of crestal bone resorption*. Saudi Dent J, 2011. **23**(3): p. 129-33.
156. Ramanauskaite, A., A. Rocuzzo, and F. Schwarz, *A systematic review on the influence of the horizontal distance between two adjacent implants inserted in the anterior maxilla on the inter-implant mucosa fill*. Clin Oral Implants Res, 2018. **29 Suppl 15**: p. 62-70.
157. Abrahamsson, I., et al., *Peri-implant tissues at submerged and non-submerged titanium implants*. J Clin Periodontol, 1999. **26**(9): p. 600-7.
158. Abrahamsson, I., J.P. Albouy, and T. Berglundh, *Healing at fluoride-modified implants placed in wide marginal defects: an experimental study in dogs*. Clin Oral Implants Res, 2008. **19**(2): p. 153-9.
159. Dasmah, A., et al., *Integration of fluoridated implants in onlay autogenous bone grafts - an experimental study in the rabbit tibia*. J Craniomaxillofac Surg, 2014. **42**(6): p. 796-800.
160. Garbieri, T.F., et al., *The Embryonic Chick Femur Organotypic Model as a Tool to Analyze the Angiotensin II Axis on Bone Tissue*. Pharmaceuticals (Basel), 2021. **14**(5).
161. Francisco, I., et al., *From Blood to Bone-The Osteogenic Activity of L-PRF Membranes on the Ex Vivo Embryonic Chick Femur Development Model*. Materials (Basel), 2021. **14**(24).
162. Araujo, R., et al., *A new ex vivo model of the bone tissue response to the hyperglycemic environment - The embryonic chicken femur organotypic culture in high glucose conditions*. Bone, 2022. **158**: p. 116355.
163. Pajor, K., L. Pajchel, and J. Kolmas, *Hydroxyapatite and Fluorapatite in Conservative Dentistry and Oral Implantology—A Review*. Materials, 2019. **12**(17): p. 2683-2683.
164. Kattimani, V.S., S. Kondaka, and K.P. Lingamaneni, *Hydroxyapatite—Past, Present, and Future in Bone Regeneration*. Bone and Tissue Regeneration Insights, 2016. **7**: p. BTRI.S36138-BTRI.S36138.
165. Alsabeeha, N.H.M., S. Ma, and M.A. Atieh, *Hydroxyapatite-coated oral implants: a systematic review and meta-analysis*. The International journal of oral & maxillofacial implants. **27**(5): p. 1123-30.
166. Yang, S., et al., *Hydrothermal treatment of Ti surface to enhance the formation of low crystalline hydroxyl carbonate apatite*. Biomaterials Research, 2015. **19**(1): p. 4-4.
167. Lo, Y.-S., et al., *Direct growth of structurally controllable hydroxyapatite coating on Ti-6Al-4V through a rapid hydrothermal synthesis*. Applied Surface Science, 2021. **556**: p. 149672-149672.
168. Bhang, K.A., et al., *Biological responses of human osteoblasts and osteoclasts to flame-sprayed coatings of hydroxyapatite and fluorapatite blends*. Acta Biomaterialia, 2010. **6**(4): p. 1575-1583.
169. Tredwin, C.J., et al., *Hydroxyapatite, fluor-hydroxyapatite and fluorapatite produced via the sol-gel method: dissolution behaviour and biological properties after crystallisation*. Journal of Materials Science: Materials in Medicine, 2014. **25**(1): p. 47-53.
170. Kim, H.-W., H.-E. Kim, and J.C. Knowles, *Fluor-hydroxyapatite sol-gel coating on titanium substrate for hard tissue implants*. Biomaterials, 2004. **25**(17): p. 3351-3358.
171. Gross, K.A. and L.M. Rodríguez-Lorenzo, *Sintered hydroxyfluorapatites. Part I: Sintering ability of precipitated solid solution powders*. Biomaterials, 2004. **25**(7-8): p. 1375-1384.
172. Gao, Y., N. Karpukhina, and R.V. Law, *Phase segregation in hydroxyfluorapatite solid solution at high temperatures studied by combined XRD/solid state NMR*. RSC Advances, 2016. **6**(105): p. 103782-103790.
173. Everett, E.T., *Fluoride's Effects on the Formation of Teeth and Bones, and the Influence of Genetics*. Journal of Dental Research, 2011. **90**(5): p. 552-560.
174. Wang, Y., et al., *Osteoblastic cell response on fluoridated hydroxyapatite coatings*. Acta Biomaterialia, 2007. **3**(2): p. 191-197.
175. Pan, L., et al., *Fluoride promotes osteoblastic differentiation through canonical Wnt/ β -catenin signaling pathway*. Toxicology Letters, 2014. **225**(1): p. 34-42.

176. Huo, L., et al., *Flouride Promotes Viability and Differentiation of Osteoblast-Like Saos-2 Cells Via BMP/Smads Signaling Pathway*. *Biological Trace Element Research*, 2013. **155**(1): p. 142-149.
177. Pei, J., et al., *Fluoride decreased osteoclastic bone resorption through the inhibition of NFATc1 gene expression*. *Environmental Toxicology*, 2014. **29**(5): p. 588-595.
178. Liu, X.-l., et al., *Role of inhibition of osteogenesis function by Sema4D/Plexin-B1 signaling pathway in skeletal fluorosis in vitro*. *Journal of Huazhong University of Science and Technology [Medical Sciences]*, 2015. **35**(5): p. 712-715.
179. Zipkin, I., S. Bernick, and J. Menczel, *A MORPHOLOGICAL STUDY OF THE EFFECT OF FLUORIDE ON THE PERIODONTIUM OF THE HYDROCORTISONE-TREATED RAT*. *Periodontics*. **3**: p. 111-4.
180. Rocci, M., et al., *Comparing the TiOblast and Osseospeed surfaces. Histomorphometric and histological analysis in humans*. *Oral Implantol (Rome)*, 2008. **1**(1): p. 34-42.
181. Dohan Ehrenfest, D.M., et al., *Identification card and codification of the chemical and morphological characteristics of 14 dental implant surfaces*. *J Oral Implantol*, 2011. **37**(5): p. 525-42.
182. Cook, F.J., et al., *Non-endemic skeletal fluorosis: Causes and associated secondary hyperparathyroidism (case report and literature review)*. *Bone*, 2021. **145**: p. 115839-115839.
183. Wu, S., et al., *Sodium Fluoride under Dose Range of 2.4–24 μ M, a Promising Osteoimmunomodulatory Agent for Vascularized Bone Formation*. *ACS Biomaterials Science & Engineering*, 2019. **5**(2): p. 817-830.
184. Nagendra, A.H., B. Bose, and S. Shenoy P, *Recent advances in cellular effects of fluoride: an update on its signalling pathway and targeted therapeutic approaches*. *Molecular Biology Reports*, 2021. **48**(7): p. 5661-5673.
185. Morganti, C., et al., *Citrate Mediates Crosstalk between Mitochondria and the Nucleus to Promote Human Mesenchymal Stem Cell In Vitro Osteogenesis*. *Cells*, 2020. **9**(4): p. 1034-1034.
186. Ma, C., et al., *Citrate-based materials fuel human stem cells by metabonegenic regulation*. *Proceedings of the National Academy of Sciences*, 2018. **115**(50).
187. Shares, B.H., et al., *Active mitochondria support osteogenic differentiation by stimulating β -catenin acetylation*. *Journal of Biological Chemistry*, 2018. **293**(41): p. 16019-16027.

Attachment 1

MEGAGEN PORTUGAL <megagenportugal@gmail.com>
To: Eduardo Santiago <eduardoasantiago@gmail.com>

Wed, Nov 30, 2022 at 10:26 AM

Bom dia Dr. Eduardo,

Como está?

Já recebemos resposta da MegaGen:

"I got the approval for using pictures :)

Please let him know to reveal the source when he uses the photos."

Atentamente,

Pedro Carneiro



Attachment II

All images used were either:

- obtained on opensource images databases
- provided and authorized by Megagen® (attachment 1)
- from my personal database of images

FACULDADE DE MEDICINA DENTÁRIA

